

## SYNTHESIS, STRUCTURE AND ELECTROCHEMICAL CHARACTERIZATION OF HOMO- AND HETERODINUCLEAR COPPER COMPLEXES WITH COMPARTMENTAL LIGANDS

PIERO ZANELLO

*Dipartimento di Chimica dell'Università, Pian Dei Mantellini 44, 53100 Siena (Italy)*

SERGIO TAMBURINI and PIETRO ALESSANDRO VIGATO

*Istituto di Chimica e Tecnologia dei Radioelementi, C.N.R., Corso Stati Uniti 4,  
35100 Padova (Italy)*

GIAN ANTONIO MAZZOCCHIN

*Dipartimento di Spettroscopia, Elettrochimica e Chimica-Fisica dell'Università, Dorsoduro 2137,  
30123 Venezia (Italy)*

(Received 15 November 1985)

### CONTENTS

A. Introduction	166
B. Synthesis, structure and magnetic properties	167
(i) Complexes derived from keto precursors	169
(ii) Complexes with macrocyclic ligands	174
(iii) Complexes with acyclic side-off ligands	184
(iv) Complexes with acyclic end-off ligands	195
(v) Complexes with polypodal ligands	211
C. Redox properties in natural and synthetic compounds	225
D. Electrochemistry of dinuclear complexes with sites having the same donor set	226
(i) Adjacent $O_2-O_2-O_2$ donor set	226
(ii) Adjacent $N_2-O_2-N_2$ donor set	230
(iii) Adjacent $S_2-O_2-S_2$ donor set	238
(iv) Adjacent $NS-O_2-SN$ donor set	239
(v) Adjacent $NO-O_2-ON$ donor set	240
(vi) Adjacent $N_2-Cl_2-N_2$ donor set	242
(vii) Adjacent $N_3-O_2-N_3$ and $N_2S-O_2-SN_2$ donor sets	243
(viii) Adjacent $N_3-O_3-N_3$ donor set	244
(ix) Adjacent $NON-O-NON$ donor set	245
(x) Adjacent $NSN-O-NSN$ donor set	247
(xi) Adjacent $N_2-O-N_2$ donor set	247
(xii) Remote $N_4$ donor sets	249
(xiii) Remote $N_2O_2$ donor sets	250
(xiv) Remote $N_2S_2$ donor sets	255
(xv) Remote $N_3O$ donor sets	256

(xvi) Remote $O_2O_2$ donor sets . . . . .	256
(xvii) Remote $N_3$ donor sets . . . . .	257
(xviii) Remote $NS_2Cl_2$ , $N_3S_2$ and $N_2S_2O$ donor sets . . . . .	259
(xix) Remote $N_2$ donor sets . . . . .	260
E. Electrochemistry of binuclear complexes with sites having different donor atom sets . . . . .	261
(i) Adjacent $N_2-O_2-O_2$ donor sets . . . . .	261
(ii) Adjacent $N_2-O_2-Cl_2$ donor sets . . . . .	264
(iii) Adjacent $N_2Y-O_2-O_2$ ( $Y = N, P$ ) donor sets . . . . .	265
(iv) Adjacent $N_2S-O_2-O_2$ donor sets . . . . .	266
(v) $N_3$ remote-linked to $N_2S_2$ donor sets . . . . .	267
F. Conclusions . . . . .	267
References . . . . .	268

## A. INTRODUCTION

The recent growth of studies on multimetallic compounds comes from the areas of homogeneous catalysis, magnetic exchange between paramagnetic centres, and bioinorganic chemistry [1–5].

There are many multi-metal center proteins and enzymes in nature; prominent among these are many with homo- and heterodinuclear metal centres [6]. A magnetic interaction between the two metal ions is often essential for their biological function. Examples are the active sites in the “blue” multicopper oxidase, ceruloplasmin and the dioxygen binding sites in the hemocyanin respiratory proteins and tyrosinase, a mixed function oxidase [7–11]. An imidazole-bridged copper–zinc pair forms the active site of one type of superoxide dismutase [12–14].

Molecular systems having two (or more) redox active centres in close proximity, capable of cooperative interactions, are also of interest in relation to their potential as catalysts for non-biological substrate oxidation [15].

Considerable effort has thus been directed in recent years towards the synthesis of ligands capable of holding two metal ions, either the same or different, at separations ( $\approx 2.5$ – $6.0$  Å) which are subject to control by appropriate modification of the molecular topology. Attention to the metal . . . metal separation and the number, nature and disposition of the donor atoms allows the study of those physical and chemical properties which may depend on the binuclearity of the system [16].

In particular the possibility is offered for the binding and activation of small substrate molecules and ions between the metal centres and the investigation of structural and physicochemical host–guest relationships [16].

Hence, synthetic binuclear complexes can serve as suitable models for the natural binuclear metal centres when they mimic some physical or chemical

property of the protein site and thereby provide an improved understanding of the biological analogue [1-5].

Studies on these models have concentrated on magnetic susceptibility, redox properties, optical and electron paramagnetic resonance spectral parameters.

## B. SYNTHESIS, STRUCTURE AND MAGNETIC PROPERTIES

In 1970 the term binucleating ligands was introduced for a series of polydentate ligands capable of simultaneously securing two metal ions [17,18]. The complexes were prepared with the aim of binding and activating small molecules such as oxygen, carbon monoxide, carbon dioxide, or particular bonds, e.g. C-H, for the subsequent formation of organic substrates of biological or industrial relevance.

Since 1970 there has been a continuous increase in the synthesis of binucleating ligands and related complexes, and many reviews have been published on this subject [1-5].

The complexes obtained by these ligands have recently been divided into two general classes [16]:

(a) Complexes with metals sharing at least one donor atom of ligands containing adjacent sites in which the central donor atom provide a bridge. The ligands providing these complexes have collectively been termed compartmental ligands [1-5].

(b) Complexes in which the donor atoms are not shared. These complexes thus derive from ligands having isolated (or remote) donor sets.

The present review deals with homo- and heterodinuclear copper(II) complexes derived from compartmental ligands. Analogous complexes with other metal ions as well as the related mononuclear copper(II) analogues will

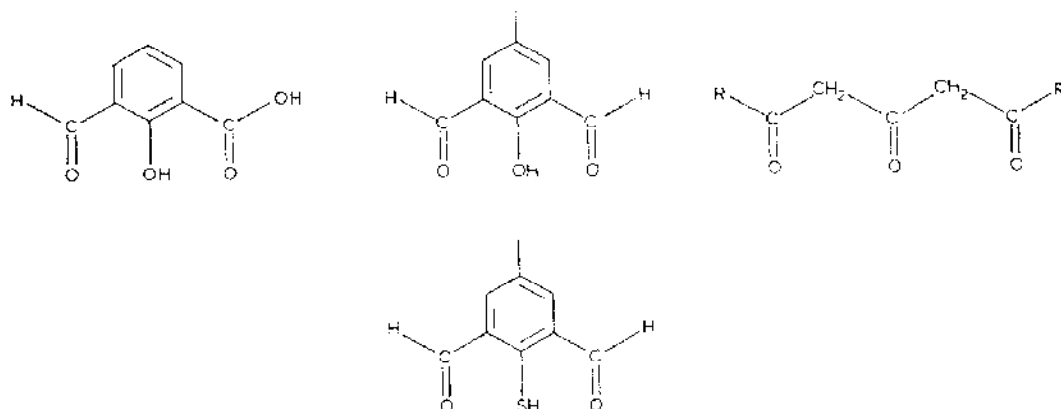


Fig. 1. Keto-precursors for the preparation of binucleating ligands.

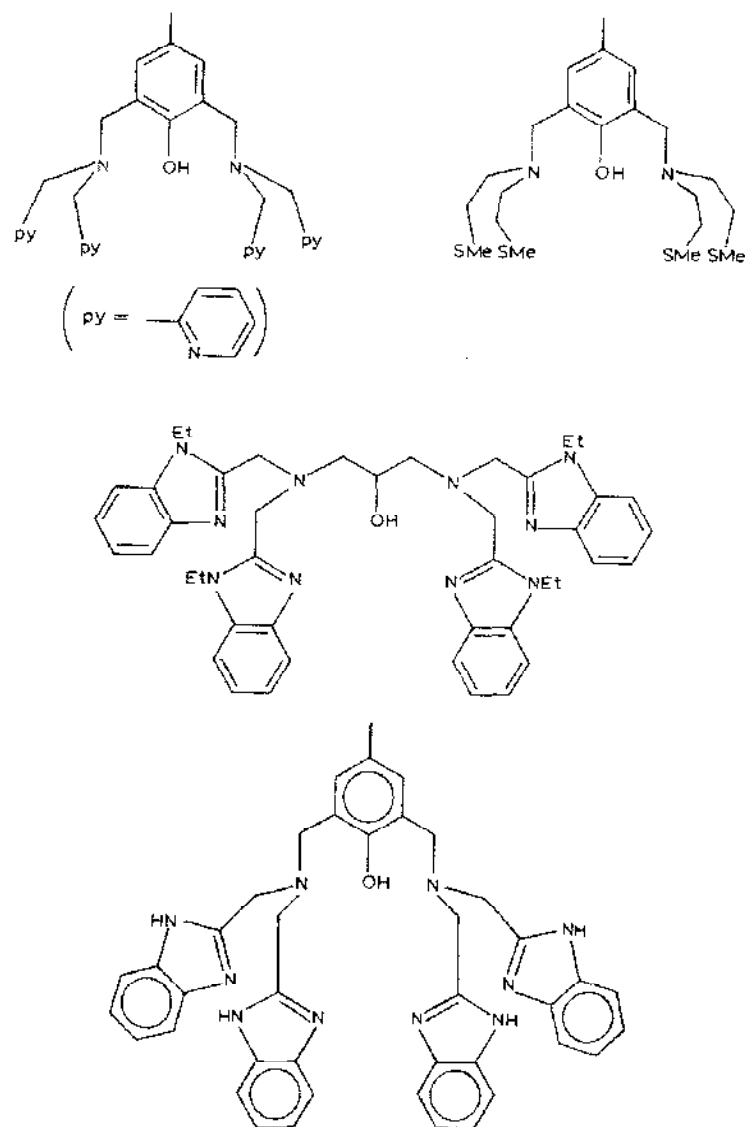
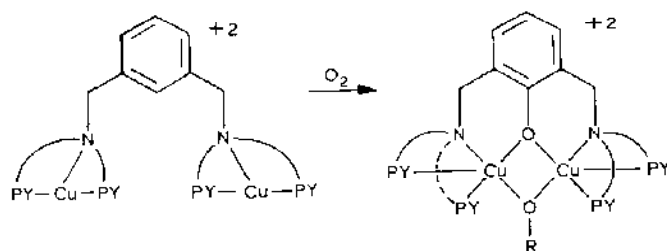


Fig. 2. Polypodal ligands containing a potentially binucleating phenoxy or alkoxy group.

be reported only when necessary for a better understanding of the properties of the dinuclear copper(II) complexes.

The compartmental ligands are predominantly Schiff bases (or the analogous compounds where the C=N bonds have been reduced to CH-NH), derived from 2,6-disubstituted phenols, thiophenols, 1,3,5-triketones,  $\beta$ -keto-phenol, keto-acids or diamino alcohols (Fig. 1) and polyamines.

More recently a new series of compounds, classifiable as compartmental ligands (termed polypodal ligands) [16] (Fig. 2) have also been prepared by reaction of copper(I) complexes with remote ligands and oxygen as shown in Scheme 1.

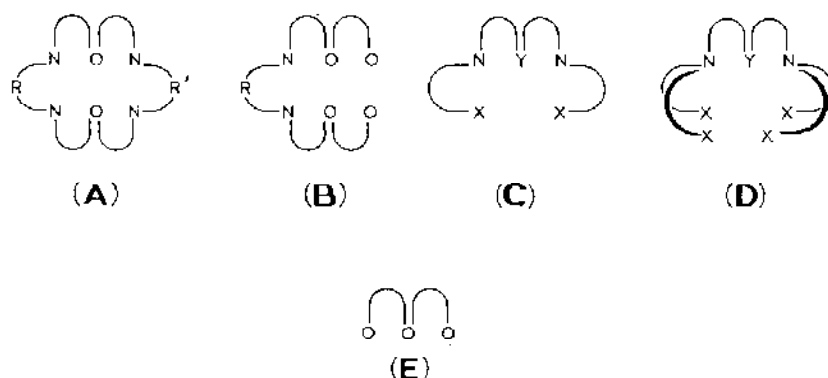


Scheme 1.

In all these compartmental ligands the central phenolic, alcoholic, thiophenolic, or keto-oxygen atom acts as a bridging donor atom.

Basically four types of ligand, in addition to the keto-precursors **E**, have been considered for the classification of the complexes examined in the present review. Type **A** are macrocycles, derived from “2 + 2” condensation polyamines, type **B** are side-off acyclic ligands in which a “2 + 1” condensation occurs, type **C** are end-off acyclic ligands in which a “1 + 2” condensation occurs (in the related metal complexes, Y provides an endogenous bridge; a further exogenous bridge may be provided by a mono- or bidentate anion), type **D** are polypodal ligands. The chains R and R' can contain additional donor atoms (NH, S, O, PPh, etc.) producing a multiplicity of different compartments.

Finally several copper(II) compounds, containing remote donor sets or ligands close to those examined in the present paper, have been considered and briefly reviewed in comparison with the copper(II) complexes with compartmental ligands.



#### (i) Complexes derived from keto precursors

Transition metal compounds derived from 1,3,5-triketones (Fig. 3a), [19,20] and from 4-substituted-2,6-diformyl-phenols or 4-substituted-2,6-diacetyl-phenols (Fig. 3b), [21] have been synthesized.

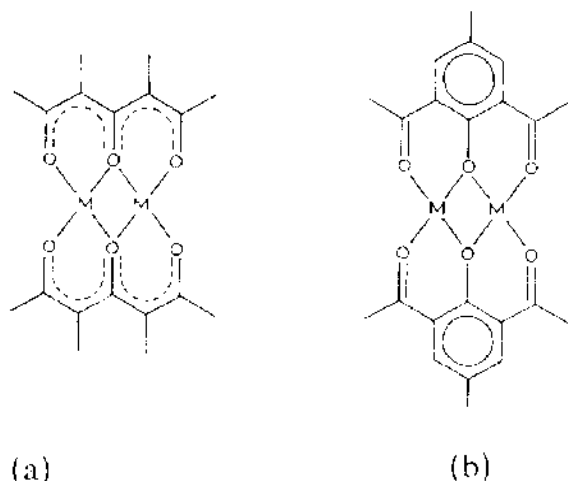
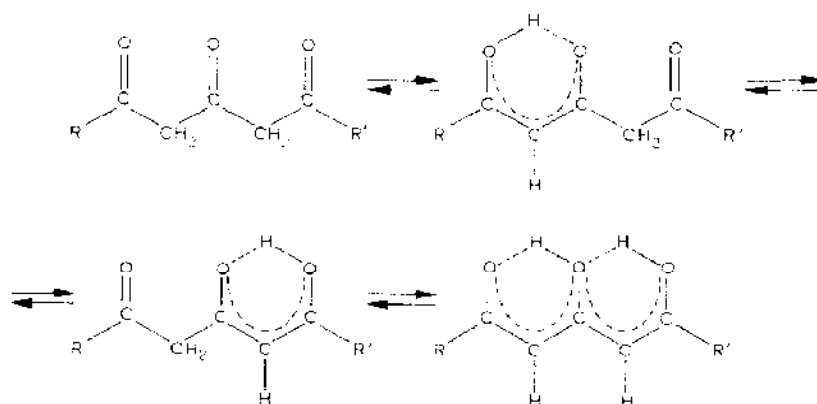


Fig. 3. The binuclear structure of complexes derived from (a) 1,3,5-triketones and (b) from 2,6-diformyl- or 2,6-diacetylphenols.

$\beta,\delta$ -Triketones can exhibit triketo, monoenol and bisenol forms in their tautomeric equilibria as shown in Scheme 2 [22–26] and can thus act as bidentate or terdentate ligands to form metal chelate complexes.



Scheme 2.

With *d* transition metal ions, the formation of binuclear species is relatively easy and only by employing particular experimental conditions (low temperature, etc.) can mononuclear species be obtained. These become binuclear, for instance, on heating in pyridine.

In the binuclear copper complex with 2,4,6-heptanetrione [27] (Fig. 4) the coordination geometry is square pyramidal, the four oxygen atoms attached to each copper atom being coplanar.

Analogously with 1,5-bis(*p*-methoxyphenyl)-1,3,5-pentane-trione, copper (II) forms the binuclear complex [28] shown in Fig. 5.

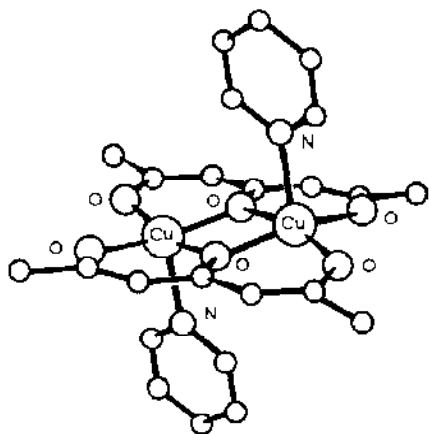


Fig. 4. The molecular structure of bis(2,4,6-heptanetrionato)dipyridine dicopper(II). Reprinted with permission from ref. 27.

The structure consists of discrete molecules in which each copper atom is bound to four ketonic oxygen atoms of two triketones and one axial pyridine. Each copper atom is thus five coordinate in an approximate square-pyramidal arrangement. This  $d^9-d^9$  complex exhibits strong intramolecular antiferromagnetism ( $-2J = 825 \text{ cm}^{-1}$ ) resulting in nearly diamagnetic behaviour at room temperature. These results are in contrast to the structurally related  $d^1-d^1$  vanadyl(IV) binuclear complex in which the value of  $-2J$  is  $160 \text{ cm}^{-1}$  [28].

In the copper complex, an exchange mechanism is operating through the  $\sigma$ -orbital system of the four-membered  $\text{Cu}_2\text{O}_2$  ring. Although the ring is not strictly planar, the exchange is almost strong enough to completely spin pair the electrons. In the vanadyl(IV) analogue the unpaired electron is not in a

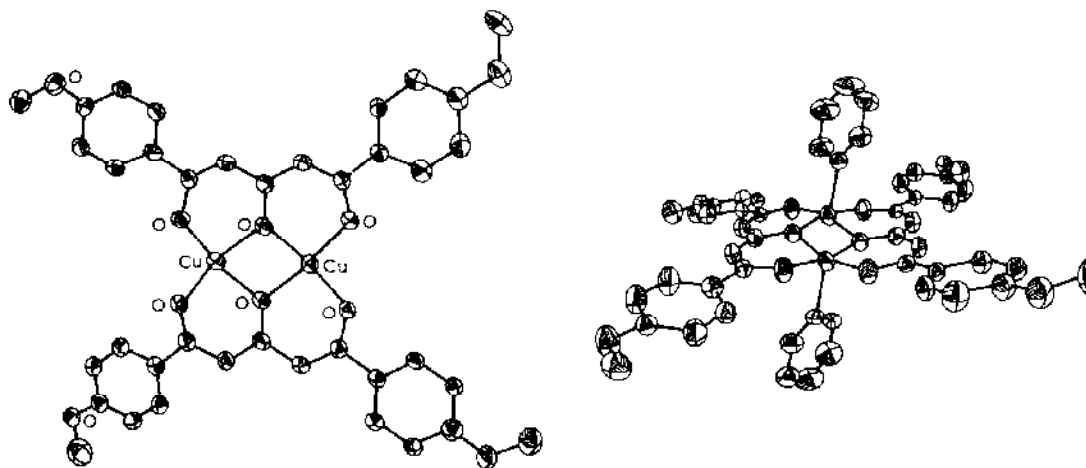


Fig. 5. The molecular structure of 1,5-bis(*p*-methoxyphenyl)-1,3,5-pentanetrionato-bis(pyridine) dicopper(II). Reprinted with permission from ref. 28. Copyright 1986 American Chemical Society.

$\sigma$ -symmetry orbital. It was suggested it lies in the  $d_{xy}$  orbital, and hence a direct metal-metal interaction was considered since  $d_{xy}$  is directed between the bridging oxygen [28]. Thus one would expect a weak exchange. Another superexchange mechanism involving the bridging oxygen and metal orbitals (i.e. electron excitation into orbitals of appropriate symmetry followed by exchange in these excited states) was considered to be less convincing [28].

The unit cell of the complex bis(benzoylacetylacetonato)bispyridine dicopper(II) [29] (Fig. 6) is composed by four centrosymmetric binuclear molecules with each of the two copper atoms coordinated to four ketonic oxygen atoms and one nitrogen from a pyridine molecule. The coordinated pyridine ligands are on opposite sides of the molecular plane precluding any dimerization. Such dimerization does occur, however, with the copper(II) complex of 2,5-bis(trifluoroacetyl)cyclopentanone [29]. This complex crystallizes as a dimer in which pairs of binuclear units related by inversion centers are weakly interacting.

The molecular unit is, as usual, composed of two copper atoms coordinated to four equatorial ketonic oxygen atoms and to an axial water oxygen. The sixth coordination site is occupied by a ketonic oxygen of the symmetry-related molecule at a distance of 3.01 Å (Fig. 7). The coordination sphere

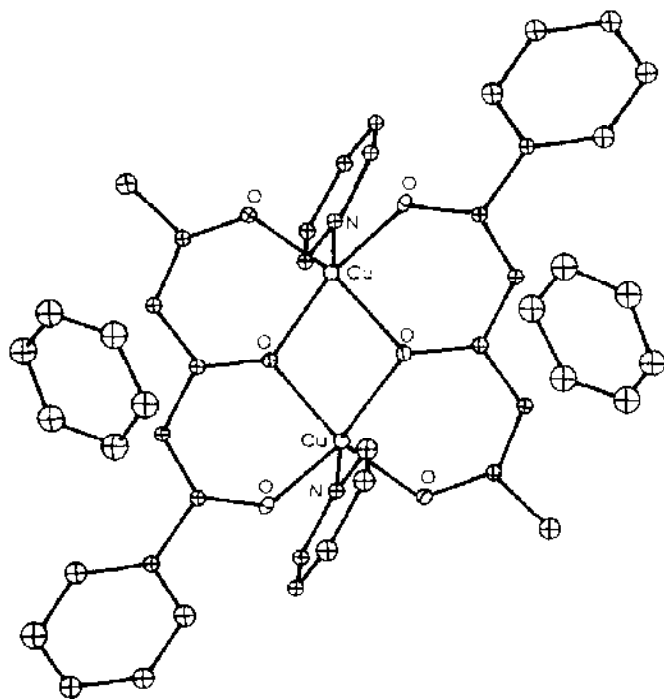


Fig. 6. The structure of bis(benzoylacetylacetonato)-bis-pyridine dicopper(II). Reprinted with permission from ref. 29. Copyright 1986 American Chemical Society.



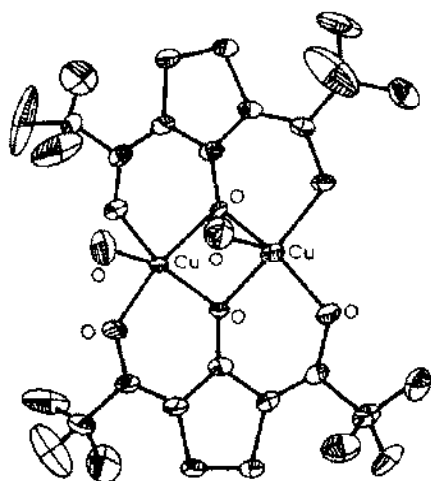


Fig. 7. The structure of bis[2,5-bis(trifluoroacetyl)cyclopentanone] diaquo dicopper(II). Reprinted with permission from ref. 29. Copyright 1986 American Chemical Society.

of the copper atoms is made up of distorted octahedra with the two coordinated water molecules on the same side of the plane described by the two copper atoms and two triketonates [29].

A pentacoordinated binuclear copper(II) complex has been obtained from the fluorinated ligand 1,1,1,7,7,7-hexafluoro-2,4,6-heptanetrione [30]; in this complex the apical position is occupied by a methanol molecule and four equatorial ketonic oxygens complete the coordination sphere (Fig. 8).

The structural parameters, which are important in the superexchange

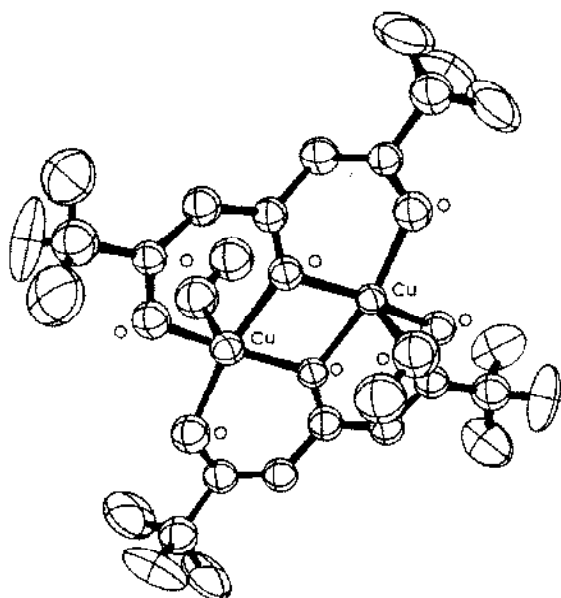
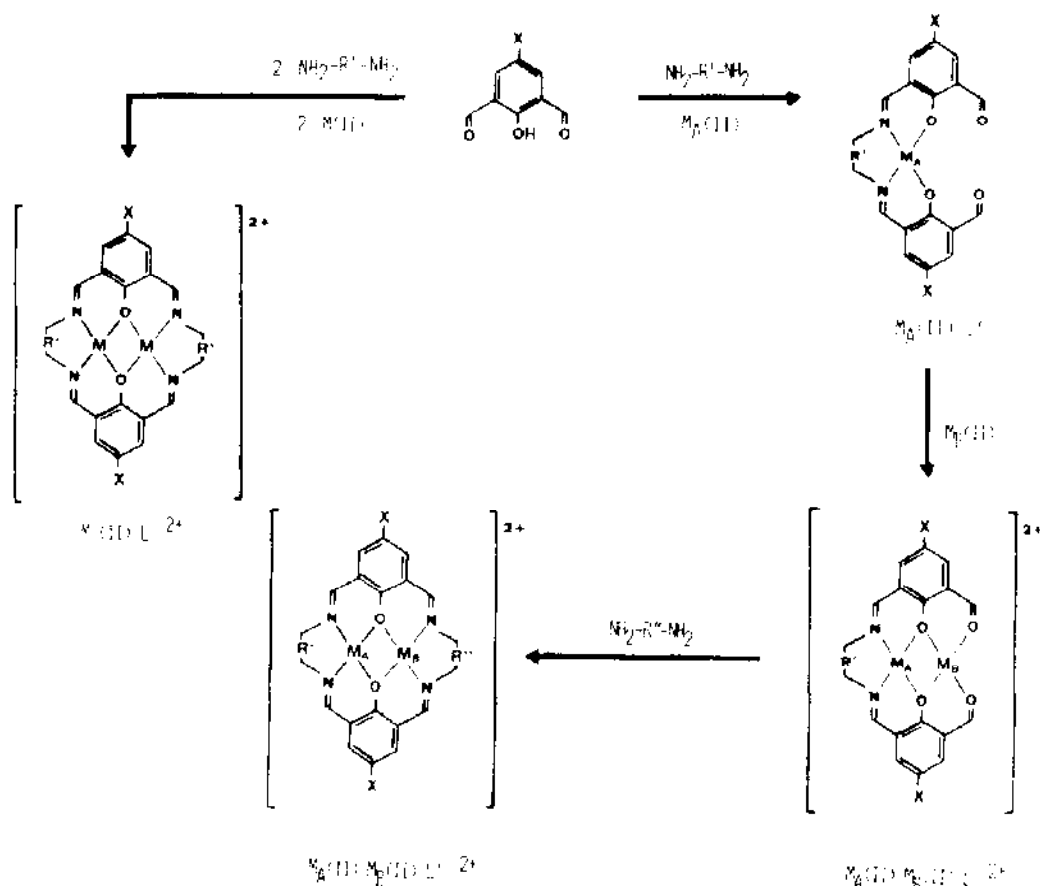


Fig. 8. The structure of bis(1,1,1,7,7,7-hexafluoro-2,4,6-heptanetrionato)dimethanol dicopper(II). Reprinted with permission from ref. 30. Copyright 1986 American Chemical Society.

interaction are essentially constant in bis(1,3,5-triketonato)dicopper(II) complexes; consequently the magnetic properties of these complexes show strong antiferromagnetic exchange, with no EPR signals at room temperature and often diamagnetism [30]. Therefore changes of substituent group produce a small perturbation on a very large exchange interaction.

### (ii) Complexes with macrocyclic ligands

Many studies deal with the preparation of binuclear complexes with symmetric or asymmetric cyclic ligands. Homodinuclear complexes can be synthesized utilizing a template synthesis [31], by reaction of the appropriate polyamine, 2,6-diformyl-4-substituted phenols (or 2,6-diacetyl-4-substituted phenols) in the presence of metal salts in alcoholic solution. For the heterodinuclear complexes, step by step reactions were employed. These syntheses are carried out according to Scheme 3.



Scheme 3.

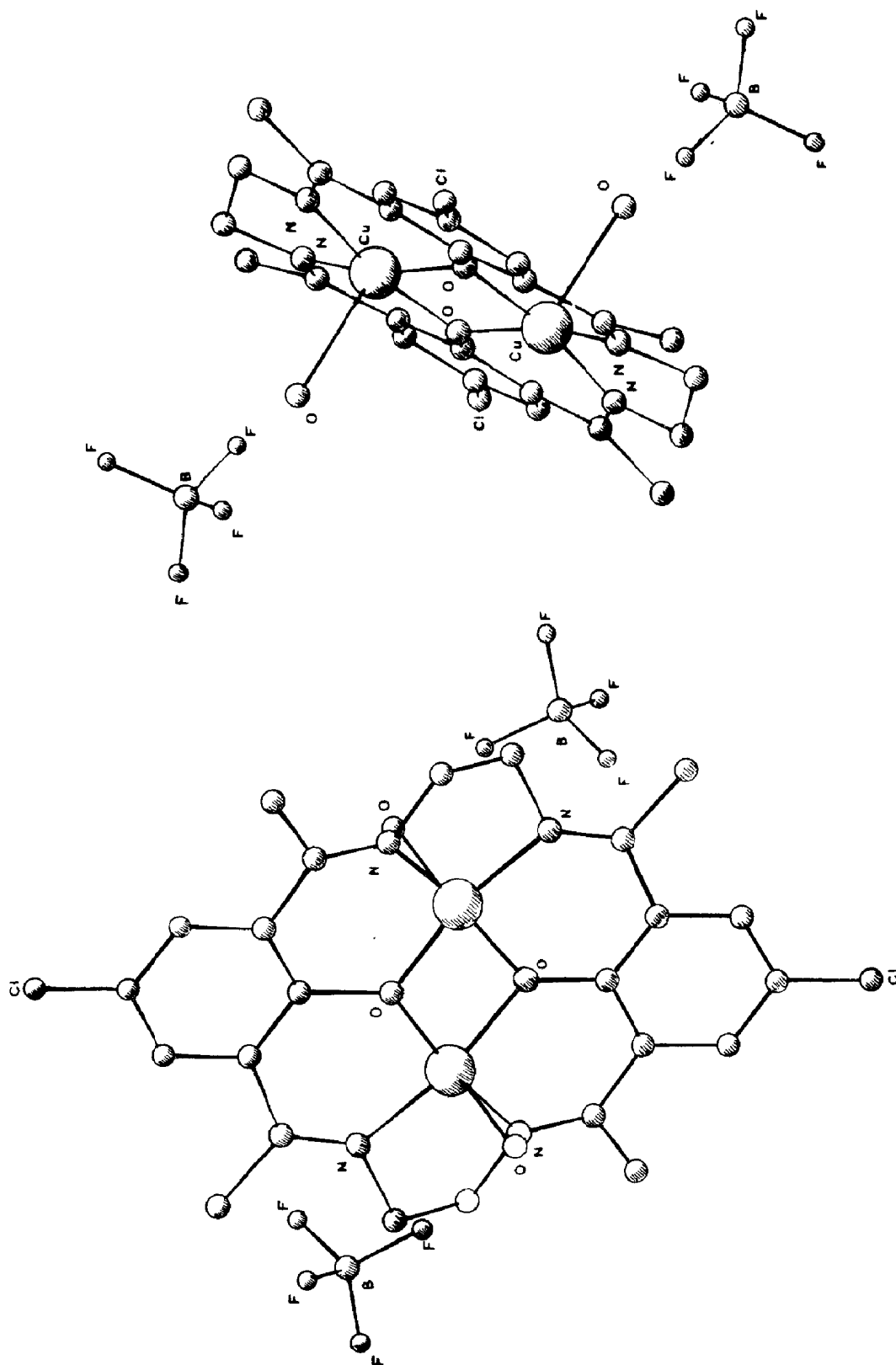


Fig. 9. Two views of the tetrafluoroborate copper(II) complex with the macrocycle obtained by condensation of 4-methyl-2,6-diformylphenol and 1,2-diaminoethane.

Recently the X-ray structure of the dinuclear copper(II) complex derived from 4-methyl-2,6-diacetylphenol and 1,2-diaminoethane in the presence of an equimolar amount of the metal template  $\text{Cu}(\text{BF}_4)_2 \cdot 6\text{H}_2\text{O}$  was de-

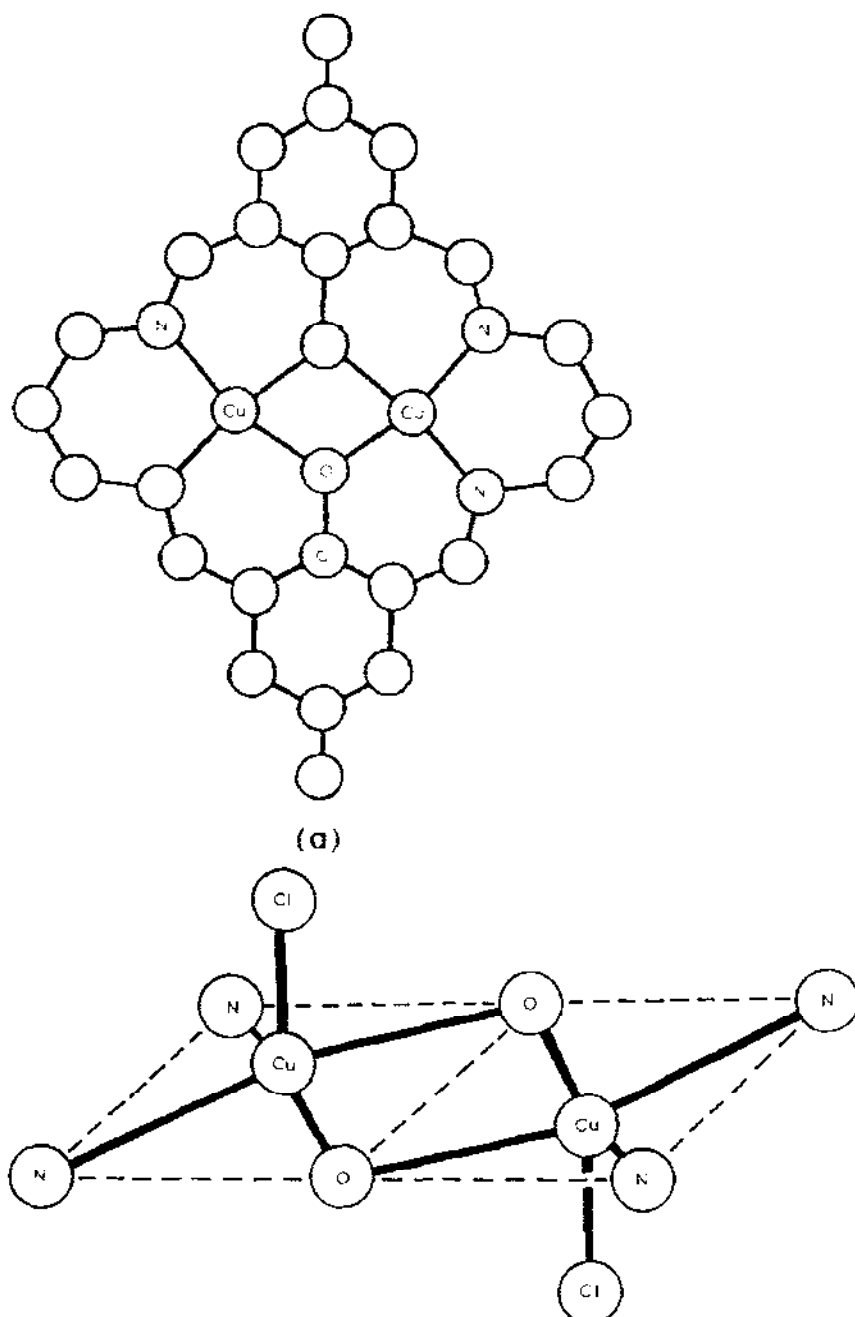


Fig. 10. The binuclear structure of  $\text{Cu}_2(\text{L}_3)(\text{Cl})_2 \cdot 6\text{H}_2\text{O}$  (a)  $\text{H}_2\text{L}_3$  is the macrocycle obtained by condensation of 4-methyl-2,6-diformylphenol and 1,3-diaminopropane. The chlorine atoms have been omitted for clarity. (b) Representation of the geometry around the binuclear core of the complex. Reprinted with permission from ref. 33.

terminated [32] and is shown in Fig. 9. The unit cell contains one dinuclear cation and two  $\text{BF}_4^-$  anions. The cation forms a centrosymmetric dinuclear complex in the crystal. The copper atoms are five coordinate in a square pyramidal configuration; four donor atoms of the macrocyclic ligand occupy the equatorial coordination sites and a water molecule is coordinated in the fifth apical position.

The crystal structure of the dinuclear copper(II) complex obtained by condensation of 4-methyl-2,6-diformylphenol and 1,3-diaminopropane in the presence of  $\text{CuCl}_2 \cdot 2\text{H}_2\text{O}$  (Fig. 10) shows two identical copper sites [33] with the two chlorine atoms in the apical positions on opposite sides of the plane defined by the donor set.

A similar coordination geometry was found for the cobalt(II) bromide analogue [34]. In this complex (Fig. 11) the central metal ions are further out of the macrocyclic plane ( $0.30 \text{ \AA}$ ) than is the copper(II) ion ( $0.21 \text{ \AA}$ ).

The magnetic properties of the above pentacoordinated square pyramidal complexes  $\text{M}_2\text{LX}_2$  ( $\text{X} = \text{Cl}, \text{Br}$ ;  $\text{M} = \text{Cu(II)}, \text{Ni(II)}, \text{Co(II)}, \text{Fe(II)}$  and  $\text{Mn(II)}$ ;  $\text{H}_2\text{L}$  = macrocyclic ligand) were investigated in the temperature range  $4.2\text{--}300 \text{ K}$  [35]. Strong antiferromagnetic exchange is present in the dinuclear copper(II) complex ( $J = -294 \text{ cm}^{-1}$ ); the net antiferromagnetic interaction decreases monotonically in the series  $\text{Cu(II)}$  ( $J = -294 \text{ cm}^{-1}$ ),  $\text{Ni(II)}$  ( $J = -27 \text{ cm}^{-1}$ ),  $\text{Co(II)}$  ( $J = -9.3 \text{ cm}^{-1}$ ) and  $\text{Fe(II)}$  ( $J = -4.2 \text{ cm}^{-1}$ ) and finally becomes a net ferromagnetic exchange interaction with the  $\text{Mn(II)}$  complex ( $J = +0.2 \text{ cm}^{-1}$ ) [35]. This  $J$  value variation across the series can be attributed to the changing number of unpaired electrons and associated pathways and to an increasing metal–ligand distance from copper(II) to manganese(II).

The dinuclear copper(II) complex prepared by condensing 1,3-diaminopropane with 2,6-diformyl-4-methylphenol and  $\text{Cu}(\text{ClO}_4)_2 \cdot 6\text{H}_2\text{O}$  has been reduced electrochemically, under an inert atmosphere, to the mixed copper(II)–copper(I) and the copper(I)–copper(I) complexes in two separate one-electron processes (vide postea) [if a CO atmosphere is used, the dinuclear  $[\text{Cu}^{\text{II}}\text{Cu}^{\text{II}}\text{L}_a]^{2+}$  can be reduced stepwise to  $[\text{Cu}^{\text{II}}\text{Cu}^{\text{I}}\text{L}_a\text{CO}]^+$  and

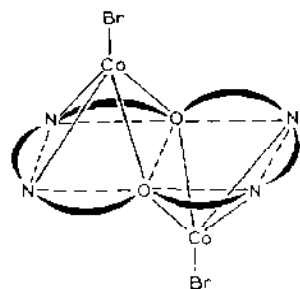
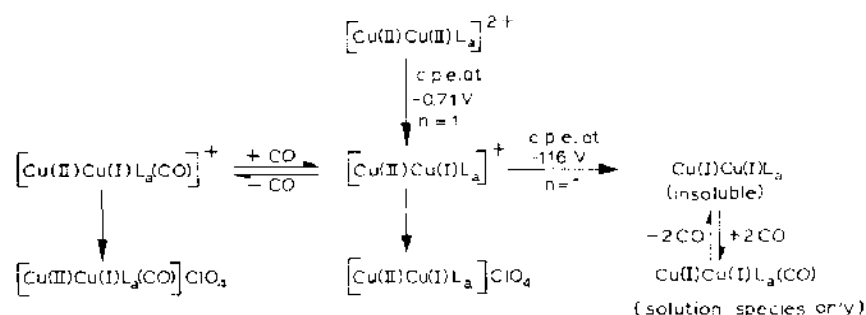


Fig. 11. A schematic representation of dicobalt(II) dibromide complex.



Scheme 4.

$\text{Cu}^{\text{I}}\text{Cu}^{\text{I}}\text{L}_a(\text{CO})_2$ ). The final  $\text{Cu}^{\text{I}}\text{Cu}^{\text{I}}\text{L}_a$  product is essentially insoluble in  $\text{CHCl}_3$ ,  $\text{CH}_2\text{Cl}_2$  and  $\text{CH}_3\text{OH}$  as shown in Scheme 4 [36,37]. The IR spectra of these compounds indicate that the macrocyclic ligand is intact and unreduced in the new compounds.

The magnetic moment values for  $[\text{Cu}^{\text{II}}\text{Cu}^{\text{I}}\text{L}_a](\text{ClO}_4)$  (1.81 B.M.) and  $[\text{Cu}^{\text{II}}\text{Cu}^{\text{I}}\text{L}_a(\text{CO})]\text{ClO}_4$  (1.94 B.M.) are typical of magnetically dilute  $\text{Cu(II)}$  complexes. These results contrast with the  $\mu_{\text{eff}}$  for  $[\text{Cu}^{\text{II}}\text{Cu}^{\text{II}}\text{L}_a](\text{ClO}_4)_2 \cdot 2\text{H}_2\text{O}$  (0.60 B.M.) which indicates quite strong coupling between the copper(II) centers.  $\text{Cu}^{\text{I}}\text{Cu}^{\text{I}}\text{L}$  is diamagnetic.

The extent of interaction between the metal centers in the ground state of the mixed valent complexes has been studied. For the carbonyl complex  $[\text{Cu}^{\text{II}}\text{Cu}^{\text{I}}\text{L}_a(\text{CO})]^+$  the observation of the localized odd electron at both high and low temperatures indicates that thermal electron transfer is either prevented entirely or is too slow to be observed on the EPR time scale at either temperature. The binding of CO to the  $\text{Cu(I)}$  site would be expected to markedly alter the energy differences between  $\text{Cu(I)}$  and  $\text{Cu(II)}$  perhaps to an extent which makes facile electron transfer not feasible. Based on its spectral properties  $[\text{Cu}^{\text{II}}\text{Cu}^{\text{I}}\text{L}_a(\text{CO})]\text{ClO}_4$  behaves as though it contains non-interacting metal centers. Electrochemical measurements (vide postea) on  $[\text{Cu}^{\text{II}}\text{Cu}^{\text{I}}\text{L}_a]^+$  indicate a fairly strong interaction. The complex  $[\text{Cu}^{\text{II}}\text{Cu}^{\text{I}}\text{L}_a](\text{ClO}_4)$  also displays evidence of the interaction between the two copper ions in its electronic and EPR spectra. The room temperature EPR spectra have been interpreted in terms of intramolecular electron transfer between copper ions at a rate which is rapid compared to the relatively slow resonance experiment. In frozen media that exchange is stopped or is too slow to be monitored. At room temperature  $[\text{Cu}^{\text{II}}\text{Cu}^{\text{I}}\text{L}_a]^+$  exhibits an isotropic seven-line solution EPR spectrum while an anisotropic pattern was observed in frozen solutions (77 K) with four lines for  $g_{\parallel}$  and unresolved  $g_{\perp}$ . Variable-temperature experiments show coalescence at about 200 K suggesting an intramolecular electron transfer rate of about  $1.7 \times 10^{10} \text{ s}^{-1}$  at 298 K. Electronic absorption spectral measurements in  $\text{CH}_2\text{Cl}_2$  revealed at

least two bands for  $[\text{Cu}^{\text{II}}\text{Cu}^{\text{I}}\text{L}_a]\text{ClO}_4$  at 1700 and 1200 nm, not present in the  $[\text{Cu}^{\text{II}}\text{Cu}^{\text{II}}\text{L}_a](\text{ClO}_4)_2 \cdot 2\text{H}_2\text{O}$ ,  $\text{Cu}^{\text{I}}\text{Cu}^{\text{I}}\text{L}_a$  or in the carbonyl derivatives. These bands have been attributed to intramolecular electron transfer processes [37].

The structure of the  $[\text{Cu}^{\text{II}}\text{Cu}^{\text{I}}\text{L}_a]\text{ClO}_4$  complex reveals distinct copper coordination sites in the solid state. Within the crystal, the flat cations are parallel and are arranged in slipped stacks with two alternating kinds of overlap. The intermolecular distance between the best planes through the four nitrogen atoms is 3.37 Å in both cases (Fig. 12).

The dinuclear cation is essentially planar; the two four-coordinated copper atoms Cu(1) and Cu(2) are each bonded to two imine nitrogen atoms and share the two bridging phenolate oxygens. The coordination about Cu(1) is square planar. The second copper is disordered over two sites with 35% in the Cu(2a) site and 65% in the Cu(2b) site. Cu(2b) is displaced 0.15 Å from the best plane of the two oxygen and two nitrogen ligands towards an aromatic ring carbon of an adjacent molecule. Cu(2a) is displaced 0.65 Å from the two-coordinated nitrogen and oxygen atoms towards the same aromatic ring carbon of an adjacent molecule. The overall geometry of Cu(2a) is square pyramidal, owing to Cu(2a)–C interaction (Cu(2a)–C distance = 2.55 Å). In the solid state this complex has been described [38] in terms of localized valence states, with one divalent (Cu(1)) and two types of monovalent copper ion (Cu(2a) and Cu(2b)).

The complex with methyl groups on the imminium carbons, [39] has an EPR spectrum exhibiting a four-line copper hyperfine pattern at room temperature in solution; in this complex the unpaired electron is localized on one copper ion on the EPR timescale.

The series of mixed-valence dinuclear copper(II)–copper(I) complexes 1–7, of Fig. 13, has been prepared [40] to study systematically the factors affecting intramolecular electron transfer.

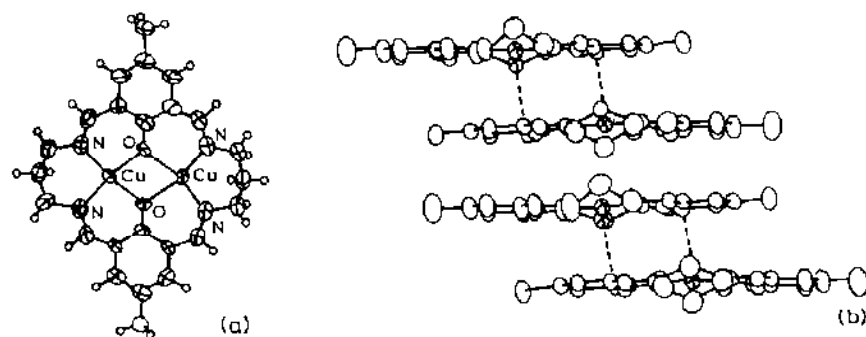


Fig. 12. (a) The structure of mixed-valent  $\text{Cu}^{\text{II}}\text{Cu}^{\text{I}}$  cation and (b) stacking interactions of the cations. Reprinted with permission from ref. 38. Copyright 1986 American Chemical Society.

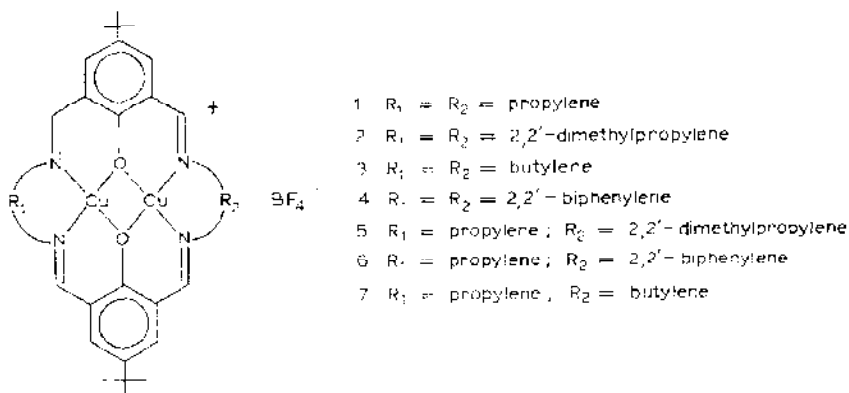


Fig. 13. Binuclear copper(II)-copper(I) complexes 1-7.

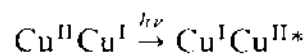
Chemical reduction of the dinuclear copper(II) complexes with sodium dithionite was used to obtain the mixed-valence complexes. These complexes precipitate, in methanol, as  $\text{BF}_4^-$  salts, immediately upon addition of the dithionite solutions.

In solutions at room temperature complexes 1-3 and 5 show an isotropic pattern with seven copper hyperfine lines. For these an average copper hyperfine splitting of  $37\text{--}41 \times 10^{-4} \text{ cm}^{-1}$  was found. Four line hyperfine patterns have been found for the other three complexes with an average copper hyperfine splitting of  $64\text{--}82 \times 10^{-4} \text{ cm}^{-1}$ , characteristic of the single unpaired electron localized on one copper center.

In a frozen (105 K) acetone:toluene (3:2) glass the unpaired electron in each of the seven complexes is localized on one of the two copper ions on the EPR timescale. It was suggested that in the complexes 6 and 7 the unpaired electron is localized on the propylene copper site.

The transformation temperature from a delocalized to a localized situation was estimated to be 200 K for 1, 230 K for 2 and 5 and 250 K for 3 (complexes 2 and 5 tend to dimerize at low temperature in solution). The temperature dependencies of the EPR spectra for complexes 4, 6 and 7 have been examined from room temperature up to 390 K. There were no signs of either mixed-valence species converting from EPR localized to EPR delocalized as the temperature of the acetone solution was increased to 390 K.

For all the above  $\text{Cu}^{\text{II}}\text{Cu}^{\text{I}}$  complexes the intervalence electron transfer transition

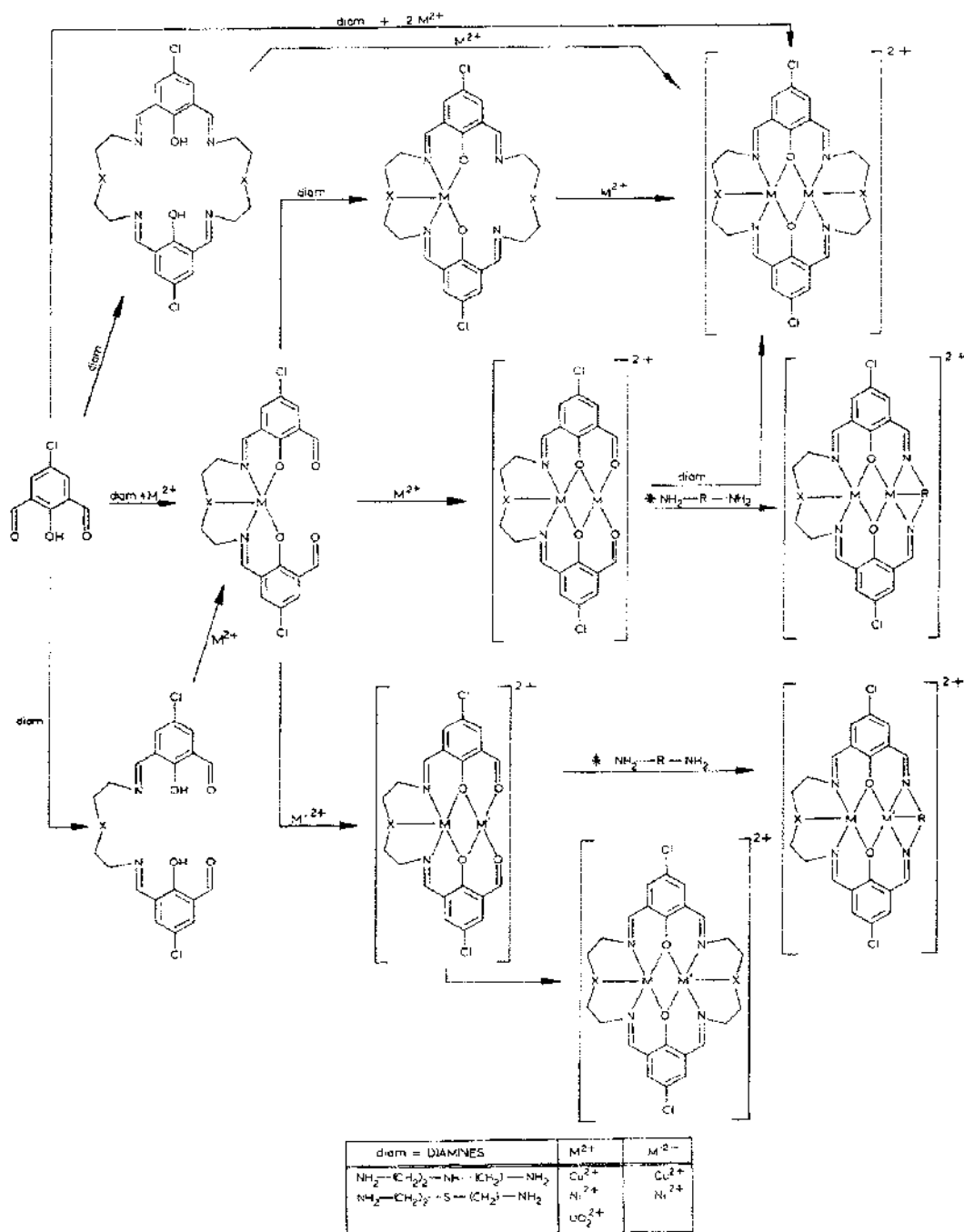


(the product is a vibrationally excited state), is seen as a particularly characteristic feature generally present in the near-IR region of the electronic absorption spectrum [40]. There is a general agreement with EPR



results; the weakest band was observed for the complexes where the electron is most localized.

By condensation of 2,6-diformyl-4-chlorophenol and the polyamines

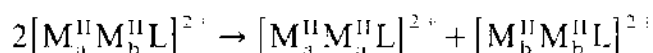


Scheme 5.

$\text{NH}_2-(\text{CH}_2)_2-\text{X}-(\text{CH}_2)_2-\text{NH}_2$  ( $\text{X} = \text{NH}, \text{S}$ ) or  $\text{NH}_2-(\text{CH}_2)_2-\text{NH}_2$  a series of acyclic and cyclic (symmetric or asymmetric) ligands have been synthesized [41,42]. By reaction of these preformed ligands, or of the keto- and amino-precursors in the presence of copper(II) (but also nickel(II) or uranyl(VI)) acetate, the complexes of Scheme 5 have been obtained.

In the symmetric cyclic mononuclear complexes, the metal ion occupies one of the two identical compartments; obviously the change by one coordination site to the other does not involve any variation in the physicochemical properties of the complex. The difference in the coordination ability of the two compartments in the asymmetric cyclic ligands is not always so high as to make one chamber selective for a particular metal ion. Consequently in the related mononuclear complexes it becomes easy for the central metal ion to change the coordination chamber, this depending on the physicochemical properties of the organic site and of the metal ion.

The preparation of heterodinuclear  $[\text{M}_a(\text{II})\text{M}_b(\text{II})\text{L}]^{2+}$  complexes with acyclic and cyclic ligands ( $\text{H}_2\text{L}$ ) was not always completely successful. The two chambers are not selective enough to prevent an exchange of coordination site of the metal ions; as a consequence scrambling of the type



can be observed.

This difficulty was overcome employing, in some cases, the following procedure: the addition of  $\text{M}_b^{\text{II}}$  salts to suspensions of  $\text{M}_a^{\text{II}}\text{L}$  in methanol resulted in the rapid complexation of  $\text{M}_b^{\text{II}}$  to the vacant  $\text{O}_2\text{O}_2$  site (for the acyclic complexes) and, for the preparation of the cyclic complex, by the subsequent addition of the polyamine.

Provided that the time in solution was short and the temperature was apparently too low to surmount the activation barrier for dissociation, little scrambling was observed.

2,6-Diacetylpyridine and 1,3-diamino-2-hydroxypropane lead, in methanol and in the presence of  $\text{Ba}(\text{NCS})_2$  or  $\text{Ba}(\text{ClO}_4)_2$ , to the corresponding barium complexes containing the compartmental macrocycle ( $\text{H}_2\text{L}_b$ ) (Fig. 14) [43,44].

Transmetallation with  $\text{Ba}(\text{H}_2\text{L}_b)\text{ClO}_4 \cdot 2\text{H}_2\text{O}$ , using copper(II) perchlorate in alcoholic solution, provides the dinuclear copper(II) complex  $[\text{Cu}_2(\text{HL}_b)(\text{ClO}_4)_3]$ .

The presence of an OH stretch at  $3475 \text{ cm}^{-1}$  and  $\nu(\text{C}=\text{N})$  at  $1650 \text{ cm}^{-1}$ , the very low magnetic moment ( $0.6 \mu_B$  per copper(II) atom) and the absence of EPR signals in the solid state and in acetonitrile solution at room temperature have been assumed proof of an oxo-bridged homodinuclear dicopper(II) unit [43,45].

The structure of the solvate  $[\text{Cu}_2(\text{HL}_b)(\text{CH}_3\text{CN})(\text{H}_2\text{O})(\text{ClO}_4)_3]$ , shown in

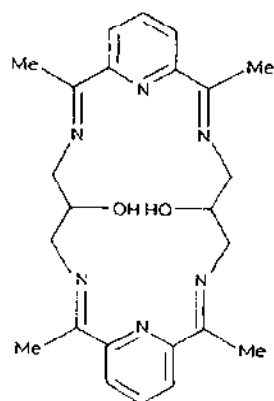


Fig. 14. Macrocycle derived from 2,6-diacetylpyridine and 1,3-diamine-2-hydroxypropane ( $H_2L_b$ ).

Fig. 15, grown from acetonitrile, [44] confirms the above suggestion. Each copper of the dinuclear cation has approximately square pyramidal geometry, being coordinated to three ligand nitrogen atoms, the bridging alkoxide and axial solvate molecule, acetonitrile for one copper and water for the other. The axial bonds are considerably longer than those in the square plane. The  $Cu \cdots Cu$  distance is 3.642 Å and the  $Cu-O-Cu$  angle is  $135.5^\circ$  (Fig. 15).

A new dinucleating ligand, resulting from the condensation of 2 mol of 2,2',2''-triaminotriethylamine and 3 mol of 2,6-diformyl-4-methylphenol has been reported together with a series of homo- and heterodinuclear complexes ( $Cu_2$ ,  $Fe_2$ ,  $Co_2$ ,  $Mn_2$ ,  $CoFe$ ,  $MnFe$ ) [46] (Fig. 16). The binucleating

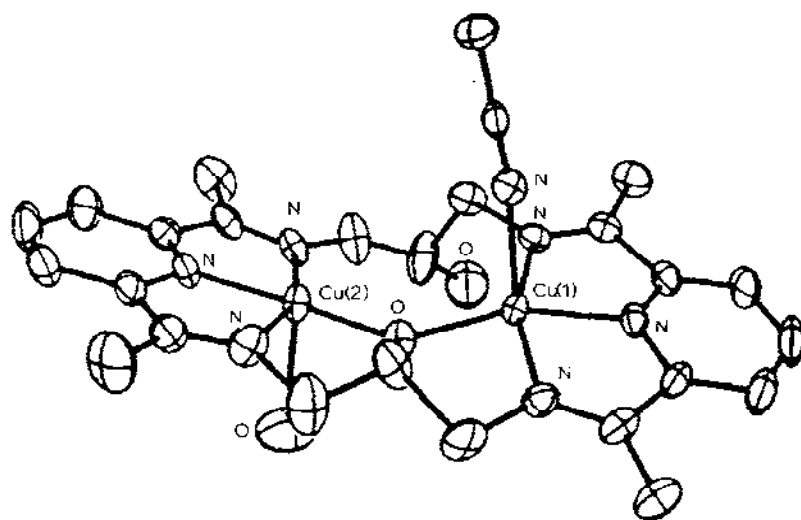


Fig. 15. Structure of the complex  $[Cu_2(HL_n)(CH_3CN)(H_2O)](ClO_4)_3$ . Reprinted with permission from ref. 44.

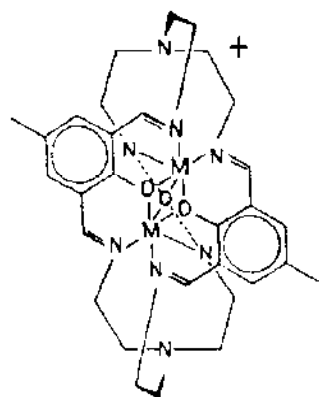


Fig. 16. A schematic representation of the trinuclear complexes with the ligand derived by condensation of 2,6-diformyl-4-methylphenol and diethylenetriamine. Reprinted with permission from ref. 46. Copyright 1986 American Chemical Society.

nature of the ligand was established by the single X-ray structure of the heterodinuclear cobalt(II)–iron(II) tetrafluoroborate complex [46].

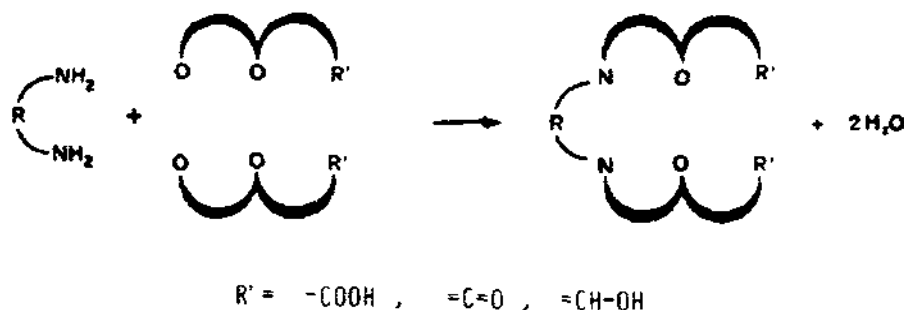
Room temperature X-ray powder patterns for the homo- and heterodinuclear complexes with this chelate ligand indicated that all the samples were probably isostructural, except for the homodinuclear copper(II) tetrafluoroborate monohydrate complex.

The magnetic exchange interaction in these complexes is intramolecularly propagated by the bridging oxygen atoms: X-ray results have not indicated intermolecular interactions. The net exchange interaction in each dimer is antiferromagnetic and is quite weak ( $J = -33 \text{ cm}^{-1}$  for  $\text{Cu}_2$ ,  $J = -0.93 \text{ cm}^{-1}$  for  $\text{Co}_2$ ,  $J = -0.82 \text{ cm}^{-1}$  for  $\text{Fe}_2$ ,  $J = -2.8 \text{ cm}^{-1}$  for  $\text{Mn}_2$  with  $\text{BF}_4^-$  as counteranion,  $J = -2.3 \text{ cm}^{-1}$  for  $\text{Mn}_2$  with  $\text{PPh}_4$  as counteranion). It appears that the metal coordination and bridging geometries found in these complexes either give rise to a relatively poor overlap of the magnetic orbitals on the adjacent metal centers, or enhance a ferromagnetic interaction that lowers the net antiferromagnetism [46].

### (iii) Complexes with acyclic side-off ligands

The reaction of an  $\alpha,\omega$ -diamine with one terminal keto-function of a triketone, keto-phenol or keto-carboxylic acid, (Scheme 6) would lead to the formation of a Schiff base, having available adjacent, dissimilar coordination compartments.

One of the compartments would resemble a Schiff base and can be designated  $\text{N}_2\text{O}_2$  or  $\text{N}_2\text{XO}_2$  (according to the donor atoms contained in the Schiff base); the other compartment may be compared with a  $\beta$ -diketone, keto-phenol or keto-carboxylic acid and is designated  $\text{O}_2\text{O}_2$ . The subsequent

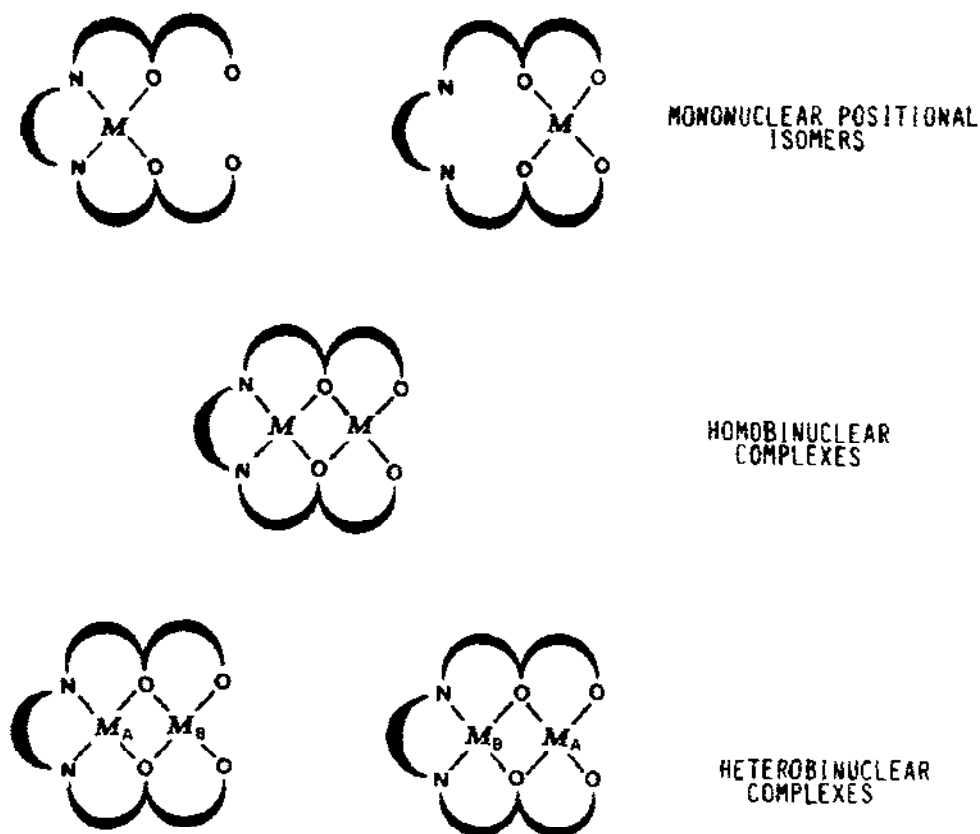


Scheme 6.

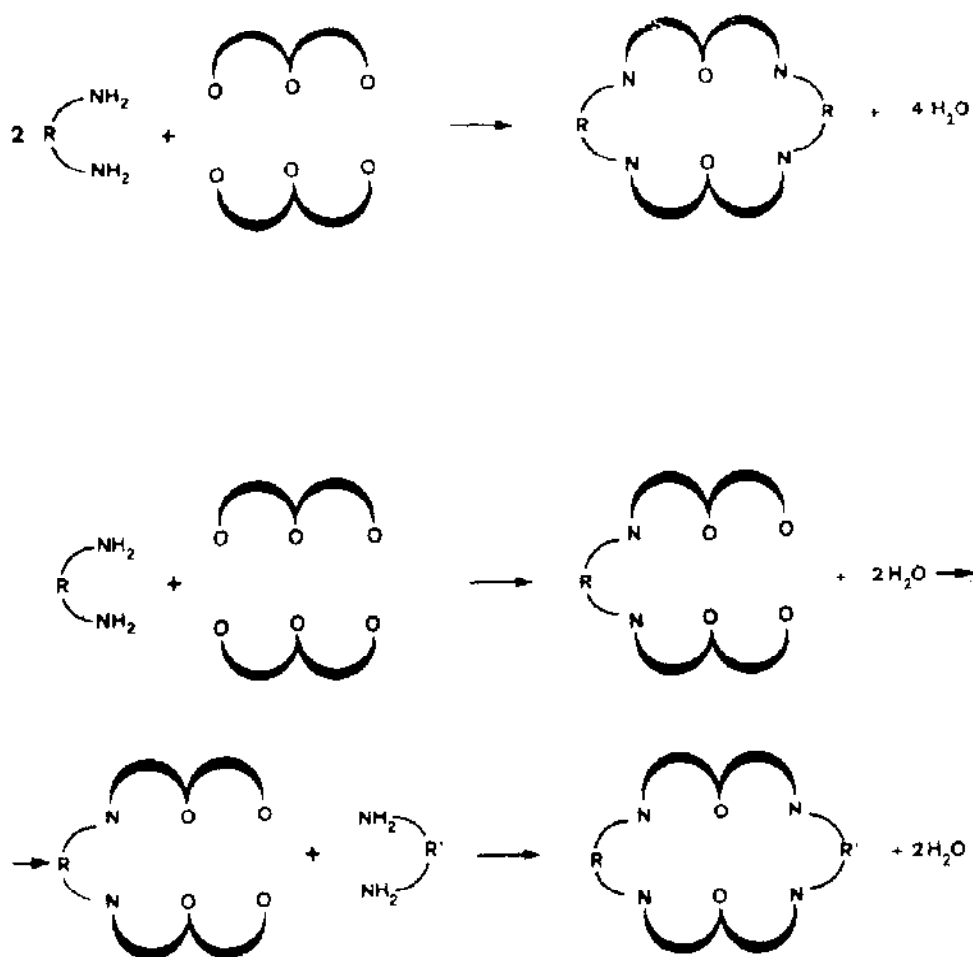
metal incorporation presents the opportunities shown in Scheme 7.

When the terminal keto-functions are two, their condensation with polyamine leads to the formation of asymmetric or symmetric compartmental ligands, according to the reactions reported in Scheme 8.

It has already been reported [1-5] that polyamines condense very readily at the carbonyl carbon of an acetyl group whether it be a diketone or a



Scheme 7.



Scheme 8.

triketone. Therefore in an unsymmetrically substituted 1,3,5-triketone in which the 1-substituent is  $-\text{CH}_3$  and the 5-substituent is  $-\text{C}_6\text{H}_5$  or  $\text{ter-C}_4\text{H}_9$ , a diamine condenses exclusively at the methyl end. Condensation was not observed at the central carbonyl carbon.

As a consequence mono-, homo- or heterodinuclear complexes of the type shown in Fig. 17 have been prepared and their properties studied in detail [47–49].

Several X-ray structural investigations [50–52] have shown the existence of heterodinuclear complexes and the site occupancy for the different metal ions used.

In the copper–vanadyl complex [50] ( $\text{R} = \text{CH}_3$ ,  $\text{M}_\text{A} = \text{Cu}$ ,  $\text{M}_\text{B} = \text{VO}$ ) the inner  $\text{N}_2\text{O}_2$  site is occupied by the copper(II) ion in an approximately square planar environment while the vanadyl(IV) group is coordinated in the outer  $\text{O}_2\text{O}_2$  compartment with square-base pyramidal geometry (Fig. 18). In this

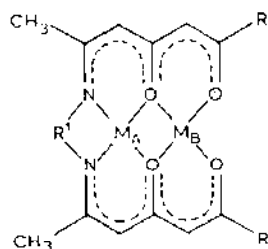


Fig. 17. Schematic representation of homo- and heterodinuclear complexes derived from acyclic hexadentate Schiff bases.

complex the planes of the diketone and of the keto-imine chelates are approximately coincident and the bond lengths indicate extensive electron delocalisation across each diketo-imine skeleton.

The nickel-copper complex ( $R = C_6H_5$ ;  $M_A = Ni$ ,  $M_B = Cu$ ) [51] consists of discrete dinuclear molecules in which the nickel atom is coordinated in the inner  $N_2O_2$  chamber and the copper in the outer  $O_2O_2$  chamber. All the atoms except for those in the phenyl group and the methylene and methyl hydrogens are within about  $0.1 \text{ \AA}$  of the mean molecular plane. There is a fairly good molecular plane of symmetry normal to the molecular plane and passing through the copper and nickel atoms. The planar molecules are arranged approximately in stacks long the  $b$  axis to which they are inclined by  $39^\circ$ . Neighbouring molecules in the stack are related by inversion centers with the distances between mean molecular planes of  $3.21$  and  $3.50 \text{ \AA}$  for neighbours related by inversion center at  $(0, 0, 0)$  and  $(0, 1/2, 0)$  respectively. One of the methylene carbons of the ligand backbone of one molecule lies  $3.06 \text{ \AA}$  above the copper atom of the second molecule. The coordination

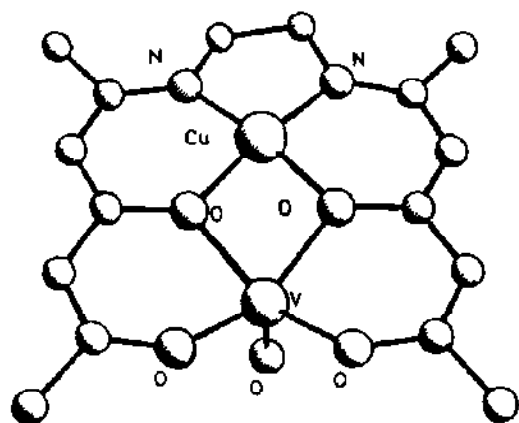


Fig. 18. Structure of [6,11-dimethyl-7,10-diazaheptadeca-5,11-diene-2,4,13,15-tetraonato(4-)]copper(II) oxovanadium(VI). Reprinted with permission from ref. 50.

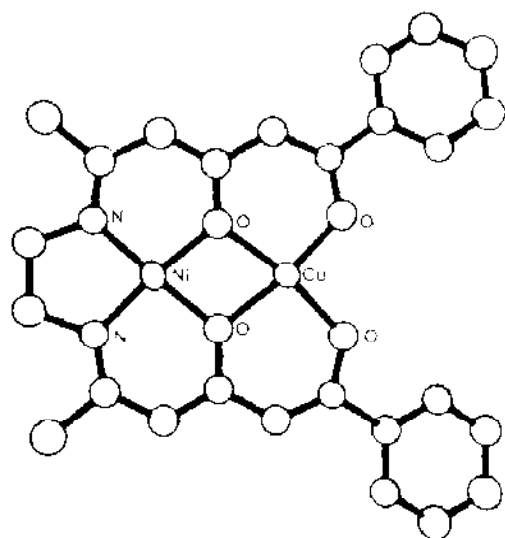


Fig. 19. Structure of  $[5,5'-(1,2\text{-ethanediyldinitrilo})\text{bis}(1\text{-phenyl-1,3-hexanedionato})](4-)\text{-nickel(II) copper(II)}$ . Reprinted with permission from ref. 51. Copyright American Chemical Society.

about the nickel atom is strictly planar while the copper atom is displaced  $0.11 \text{ \AA}$  from the plane toward this carbon in a square-pyramidal fashion as shown in Fig. 19.

The pronounced planar structure of these systems has also been used for the preparation of new  $\pi$ -materials. The dinuclear copper(II) complexes derived from 1,3,5-triketones in which one terminal carbonyl oxygen has been replaced by an aniline or 4-nitroaniline, have been prepared and the X-ray structure reported [53]. Although these two complexes do not have a side-off ligand, they are strictly correlated to the above compounds and can offer a useful basis for the development of  $\pi$ -systems. The complex bis-2,2-dimethyl-7-phenylimino-3,5,7-octanetrionato dicopper(II) crystallizes from benzene with one molecule of benzene, whilst bis-2,2-dimethyl-7-(4-nitrophenyl)imino-3,5,7-octanetrionato dicopper(II) crystallizes from benzene with two molecules of benzene. Both complexes are unusually stable with respect to loss of benzene [53]. The two compounds have a very different solid state structure. The aniline complex shown in Fig. 20 is composed of staggered stacks of alternating dinuclear copper(II) chelate molecules and benzene molecules which are equidistant between two chelate molecules. The benzene molecules are centered above and below the inversion center of the complex with a distance of  $3.258 \text{ \AA}$  between the mean position of the benzene carbons and the center of the chelate [53] thereby forming an ADADAD arrangement where the complex is the acceptor (A), and benzene the donor (D). The nitroaniline complex depicted in Fig. 21 has



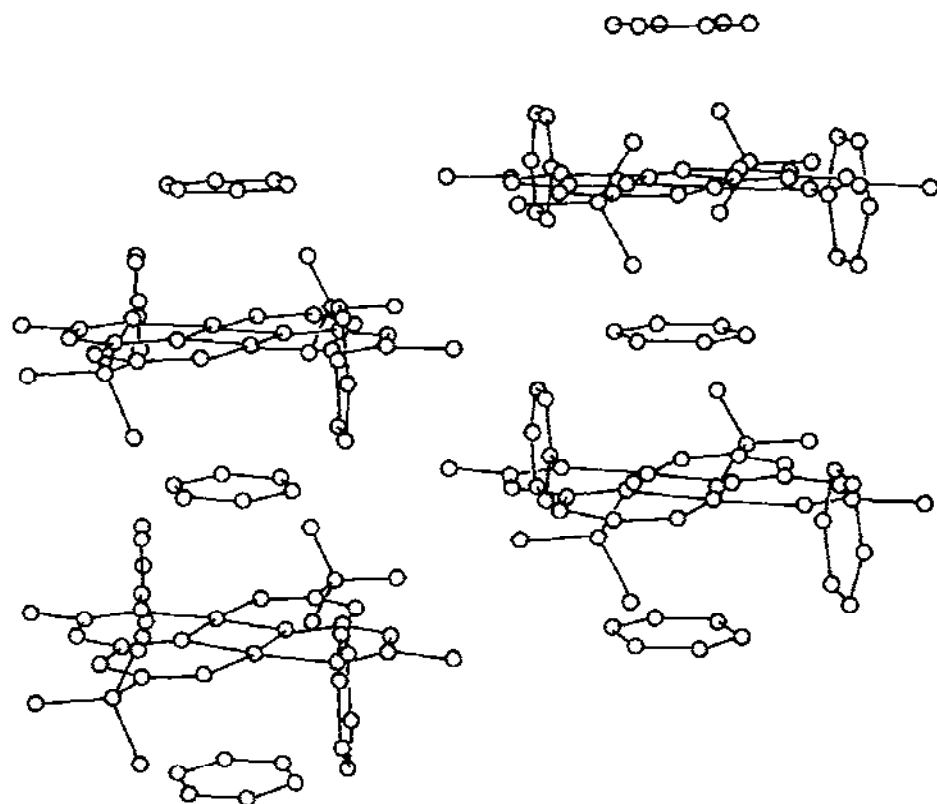


Fig. 20. The crystal packing of bis-2,2-dimethyl-7-phenylimino-3,5,7-octanetrionato dicopper dibenzene. Reprinted with permission from ref. 53. Copyright 1986 American Chemical Society.

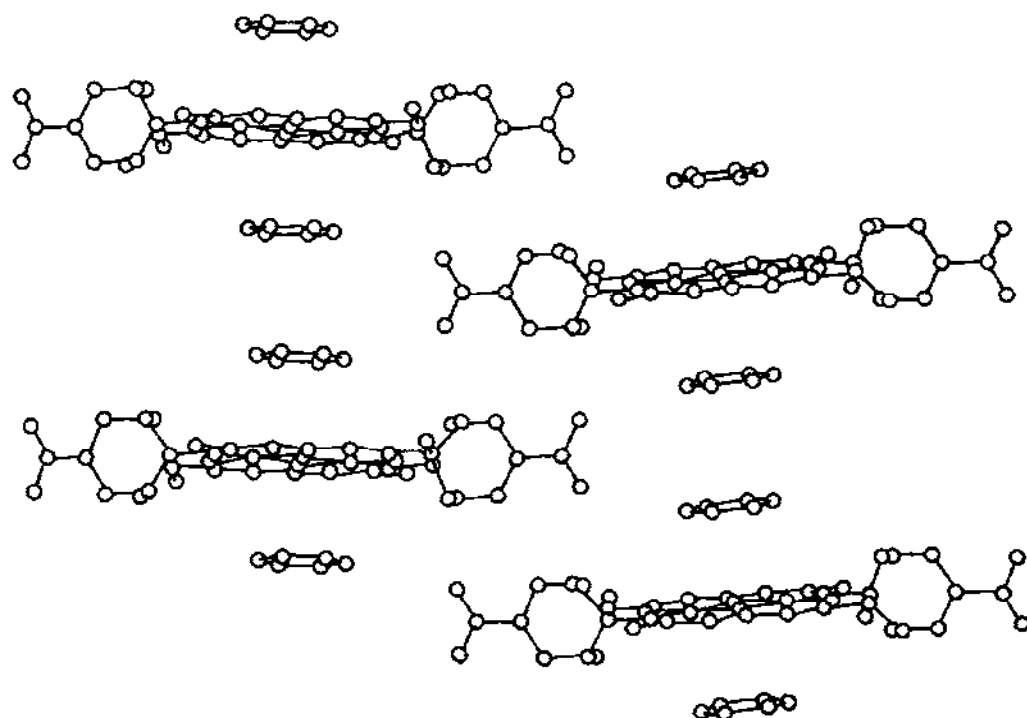


Fig. 21. The crystal packing of bis-2,2-dimethyl-7-(4-nitrophenyl)imino-3,5,7-octanetrionato dicopper dibenzene. Reprinted with permission from ref. 53. Copyright American Chemical Society.

two benzene molecules associated with each chelate molecule; it is also composed of staggered stacks in a sequence DADDAD. The unit cell contains four molecules of the dinuclear chelate and eight molecules of benzene. The benzene molecules are centered above and below the chelate inversion center with a distance of 3.262 Å between the mean position of the benzene carbon atoms and the center of the chelate. The interplanar spacing between neighboring benzene molecules located in the same stack but associated with different chelate molecules is 3.86 Å. The benzene and the chelate planes are very nearly parallel with a dihedral angle of 1.4° [53].

Magnetic susceptibility measurements proved that both compounds are diamagnetic at room temperature, with an estimated singlet-ground-state-triplet-excited-state separation greater than 850 cm<sup>-1</sup> [53], attributed to the coplanarity of the system. The other structural feature considered to be of primary importance in determining the strength of the exchange is the Cu-O-Cu bridging angle and the O-Cu-O angle. Both are comparable with other binuclear 1,3,5-triketonato complexes of copper(II).

The solid state structures are consistent with the accepted definition of  $\pi$ -molecular complexes [54]; the commonly accepted range for interplanar distances between donor and acceptor molecule in  $\pi$ -molecular complexes being 3.20–3.30 Å [53,54]. For organic  $\pi$ -molecular complexes of the type ADAD and DADDAD the periodicity along the stacks is about 7 and 10.5 Å respectively [53]; for the aniline and nitroaniline complex values of 6.52 and 10.38 Å were found [53].

The stoichiometry change accompanying the addition of the *p*-nitro group was assumed as additional proof of the  $\pi$ -molecular interaction; the electron withdrawing of the nitro group increases the Lewis acidity of the copper ions and hence their acceptor properties. As a consequence two benzene donors per acceptor were found.

The location of the benzene molecules directly over the four-membered Cu<sub>2</sub>O<sub>2</sub> ring in the center of the molecule is another indication of the active role played by copper ions in the  $\pi$ -interaction.

Both homodinuclear and heterodinuclear complexes have been prepared from the Schiff base 3,8-dimethyl-1,10-di(*o*-dihydroxyphenyl)-4,7-diazadeca-2,8-diene-1,10-dione (H<sub>4</sub>aapen) obtained by condensation in alcoholic medium of *o*-acetoacetylphenol [55] and ethylenediamine [56].

For the heterodinuclear complexes there is also the opportunity for positional isomers to occur.

For the copper(II)–uranyl(VI) (Cu-UO<sub>2</sub>(aapen)(DMSO)<sub>2</sub>) complex with H<sub>4</sub>aapen the X-ray crystal structure has been solved [57] and is shown in Fig. 22. The polyhedron around the uranium atom is a slightly distorted pentagonal bipyramid. The five oxygen atoms, equatorially bonded to uranium, are not coplanar, but their regularly alternating disposition indi-

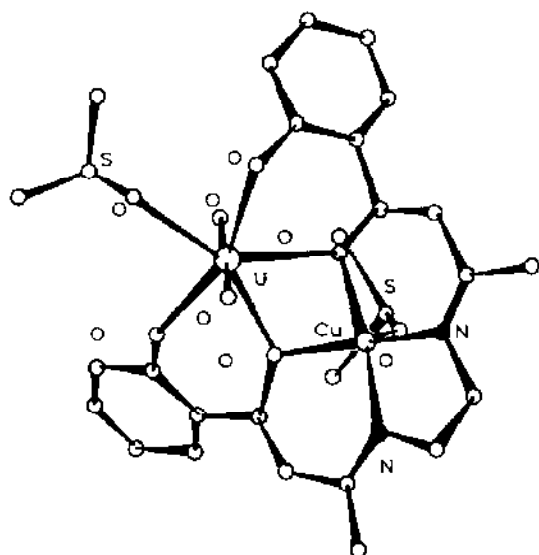


Fig. 22. Structure of  $\text{CuUO}_2(\text{aapen})(\text{DMSO})_2$ . Reprinted with permission from ref. 57.

cates the presence of a puckered arrangement. The copper(II) ion, retained in the inner  $\text{N}_2\text{O}_2$  chamber, is five coordinate, also being bonded to a DMSO molecule.

In the homodinuclear  $\text{Cu}_2(\text{aapen})(\text{H}_2\text{O})$  [58] shown in Fig. 23, one copper is four-coordinate and square planar, being retained in the inner  $\text{N}_2\text{O}_2$  chamber, while the other, which is incorporated in the outer  $\text{O}_2\text{O}_2$  chamber, is five-coordinated.

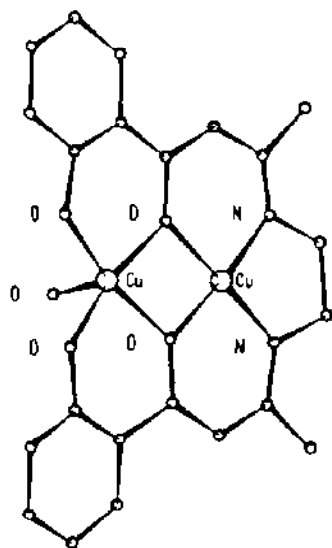


Fig. 23. Perspective view of the complex  $\text{Cu}_2(\text{aapen})\text{H}_2\text{O}$ . Reprinted with permission from ref. 58.

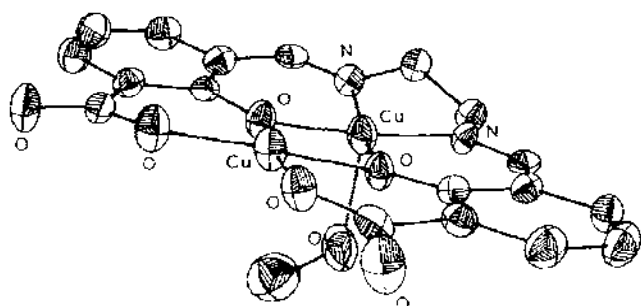


Fig. 24. Structure of  $\text{Cu}_2(\text{fsalacen})(\text{MeOH})$ . Reprinted with permission from ref. 60.

The structure of the nickel(II)–copper(II)–aapen complex is very similar to that of the related homodinuclear copper(II) complex. The nickel atom is four coordinate, square planar in the inner  $\text{N}_2\text{O}_2$  chamber, while the copper is five coordinate and square pyramidal in the outer  $\text{O}_2\text{O}_2$  chamber; a water molecule occupies the apical position [59].

The reaction of 3-formylsalicylic acid with ethylenediamine yields the binucleating Schiff base *N,N'*-(2-hydroxy-3-carboxybenzylidene)-1,2-diaminoethane ( $\text{H}_4\text{fsalacen}$ ) which forms homo- or heterodinuclear complexes, for some of which the X-ray structure has been solved and the magnetic behaviour studied in detail [60–66].

The homodinuclear copper(II) complex displayed in Fig. 24 consists of discrete units where the inner copper(II) ion is five-fold coordinate in a square pyramid; the fifth apical position is occupied by the oxygen of a methanol. The outer copper(II) is located in an essentially planar environment [60].

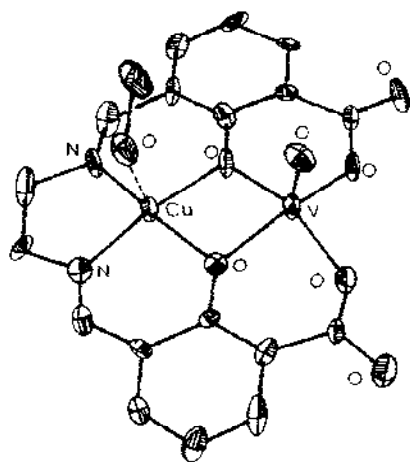


Fig. 25. Structure of  $\text{CuVO}(\text{fsalacen})(\text{MeOH})$ . Reprinted with permission from ref. 61. Copyright 1986 American Chemical Society.

A very similar structure was found for the copper(II)–vanadyl(IV) complex in which a vanadyl group is substituted to the outer copper(II) ion [61]. The metal ions and the oxygen of the methanol molecule and of the vanadyl groups are in the mirror plane for the two square pyramids (Fig. 25) which point in the same direction.

During the copper–vanadyl crystal growing attempts, in addition to the above heterodinuclear complex, two other species were detected [61]. The first is built up from molecules with  $\text{CuN}_2\text{O}_3$  and  $\text{VO}_5$  pyramids oriented up–up and up–down in the respective proportions of 80% and 20% and randomly distributed within the crystal. The second species consists of random distributions of molecules with conformation close to the above hetero-copper–vanadyl complex having the proportions of 85% and 15% respectively (Fig. 26) [61].

In the structural determination of copper(II)–magnesium(II), copper(II)–nickel(II), and copper(II)–cobalt(II) complexes with  $\text{H}_4\text{fsalacen}$  [62,65], the copper(II) ion is always in the inner  $\text{N}_2\text{O}_2$  chamber in an almost square planar geometry. The hetero-metal ion is bound to the outer  $\text{O}_2\text{O}_2$  compartment in an octahedral coordination; the two apical positions are filled by the oxygen atoms of water molecules. A similar geometry was also reported for the copper(II)–chromium(III), and the homodinuclear nickel(II) complexes [64,66]. For the copper(II)–cobalt(II) complex, in addition to this structure, a structure was found in which the cobalt is five coordinate in a square pyramidal geometry [62,63]. In this complex (Fig. 27) two binuclear molecules related by a symmetry center are packed together forming a tetramer in which the two metal ions occupy the center of octahedra sharing edges and corners. Such units are encapsulated in a three-dimensional network of water molecules [63].

The homodinuclear copper(II) complex with  $\text{H}_4\text{fsalacen}$  shows strong antiferromagnetic coupling with a singlet–triplet separation of  $-650\text{ cm}^{-1}$ . The copper(II)–vanadyl(IV) complex reveals intramolecular ferromagnetic

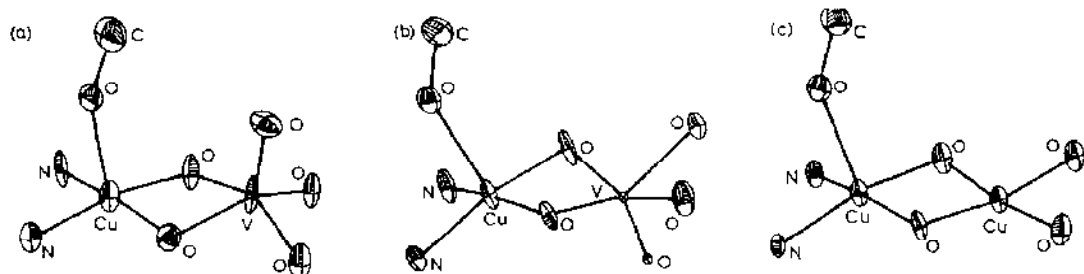


Fig. 26. The different core of the three binuclear complexes present in the copper–vanadyl crystals. Reprinted with permission from ref. 61. Copyright 1986 American Chemical Society.

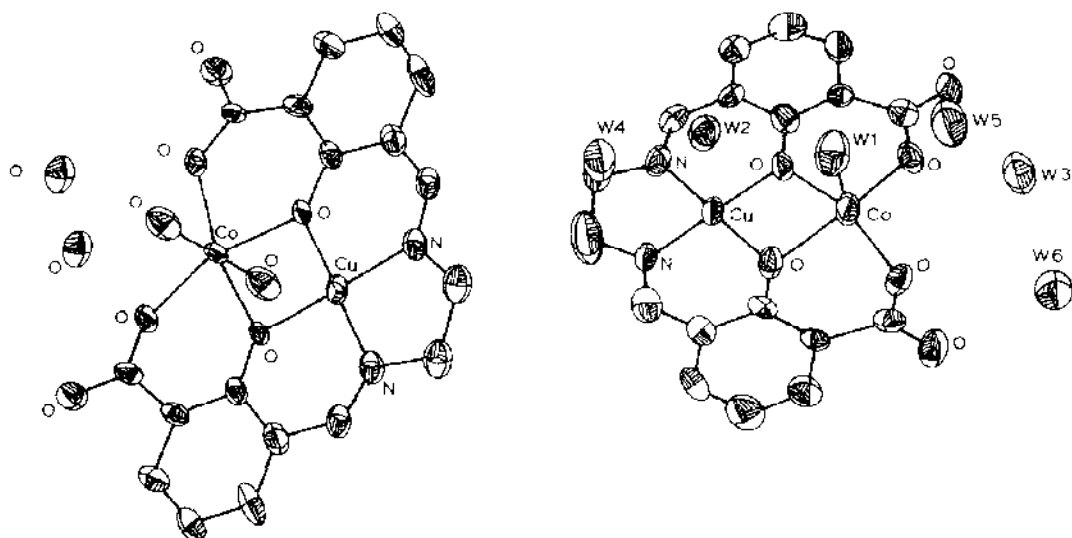


Fig. 27. Structure of (a)  $\text{CuCo}(\text{fsalacen})(\text{H}_2\text{O})_2$  and (b)  $\text{CuCo}(\text{fsalacen})(\text{H}_2\text{O})$ . Reprinted with permission refs. 62(a), 63(b). Copyright 1986 American Chemical Society.

coupling, characterized by a ground triplet state separated by about  $118\text{ cm}^{-1}$  from the excited singlet state [60,61]. The magnetic results for copper-magnesium and nickel-nickel complexes (in the homodinuclear complex the inner nickel(II) is diamagnetic so that the magnetic properties are those of the outside nickel(II) in a pseudooctahedral environment) show that, above 20 K, there is no intermolecular exchange; at lower temperatures, weak intermolecular antiferromagnetic interactions occur [64]. For the copper(II)-nickel(II) analogue, magnetic and EPR data suggest that the energy separation between the ground doublet and the excited quartet level is about  $-213\text{ cm}^{-1}$  [64]. A strong ferromagnetic interaction was observed for the copper(II)-chromium(III) complex [66].

The internal  $\text{N}_2\text{O}_2$  chamber of the binucleating side-off hexadentate ligands cannot coordinate a uranyl(VI) ion. Thus the enlargement of this site by means of a hydrocarbon chain containing a fifth donor atom offers a very appropriate coordination geometry for  $\text{UO}_2^{2+}$  with the consequent formation of binuclear species [67].

Mononuclear and dinuclear complexes with the potentially dinucleating ligands obtained by condensation of 3-formylsalicylic acid and polyamines of the type  $\text{NH}_2-(\text{CH}_2)_n-\text{X}-(\text{CH}_2)_n-\text{NH}_2$  ( $n = 2$ ,  $\text{X} = \text{NH}$  or  $\text{S}$ ;  $n = 3$ ,  $\text{X} = \text{PPh}$ ) have been reported [68,69]. A typical reaction pathway of these heptadentate ligands with copper(II), nickel(II) and uranyl(VI) ions is shown in Scheme 9.

In the mononuclear and heterodinuclear complexes, uranyl(VI) occupies the outer  $\text{O}_2\text{O}_2$  chamber. It is easy also to obtain homodinuclear uranyl(VI) complexes.



Scheme 9.

#### (iv) Complexes with acyclic end-off ligands

In 1970 complexes of various metals including copper(II) with pentadentate compartmental ligands, derived from the reaction of 2-aminophenol and 2,6-diformyl-4-methylphenol, were synthesized [17,18] (Fig. 28).

These compartmental ligands provide only one endogenous bridging donor and so have a labile bridging site available between the metals into which a variety of anions ( $X^-$ ) can be introduced as exogenous bridges. This bridging ligand  $X$  may donate one (OH, OR, Cl, etc.) or two atoms (pyrazolate, 3,5-dimethylpyrazolate, acetate, azide, etc.). The original ligand has been modified extensively and a wide range of new binucleating compounds has been prepared with the same basic structural framework. The complexes, almost exclusively homodinuclear copper(II), have been synthe-

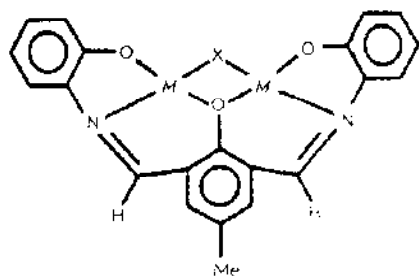


Fig. 28. Schematic representation of the binuclear end-off complexes derived from 2,6-diformyl-4-methylphenol.

sized by template procedure, sometimes by prior formation of the ligand followed by metal complexation.

2,6-Diformyl-4-methylphenol was condensed in alcoholic media, with aminophenols [17,18,70], aminothiophenols [71], aminoacids [72,73], dialkylalkanediamines [74–76], 2-aminoalkylpyridines [77,78], histamine [77,78], thiosemicarbazide [79] and diamines [76,87,88].

Potentially dinucleating ligands containing a bridging sulphur donor derived from 2-mercapto-5-methylisophthalaldehyde, especially designed for containing two soft metal centres (i.e., palladium) have been prepared [77–82]. They have been obtained in the form reported in Fig. 29a and give rise, under appropriate experimental conditions, to complexes of the type in Fig. 29b.

As an extension of the ligands designed to obtain soluble dinuclear complexes, 4-*tert*-butyl-2,6-bis(*N*-[(heptylthio)thiocarbonyl amino] formidoyl}phenol and the related binuclear copper(II) and nickel(II) complexes of the type reported in Fig. 30 were synthesized [83]. In these complexes the

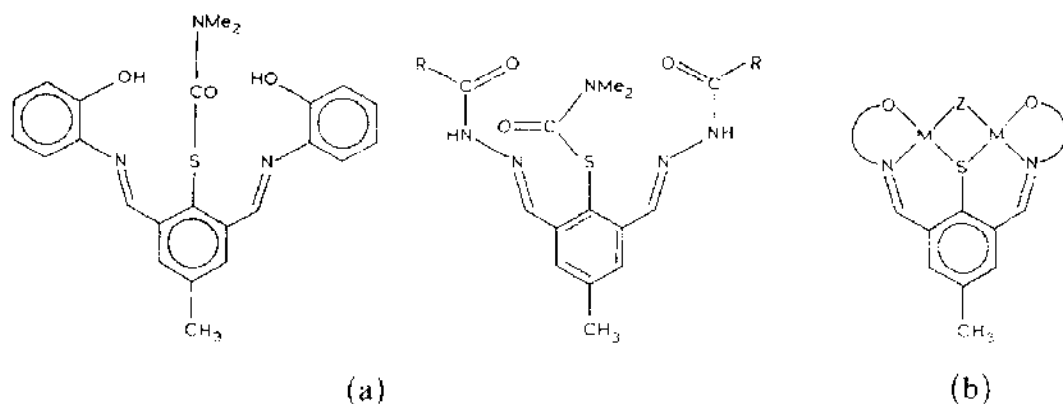


Fig. 29. End-off ligands related to (a) 2,6-diformyl-4-methylthiophenol and (b) the corresponding binuclear complexes.



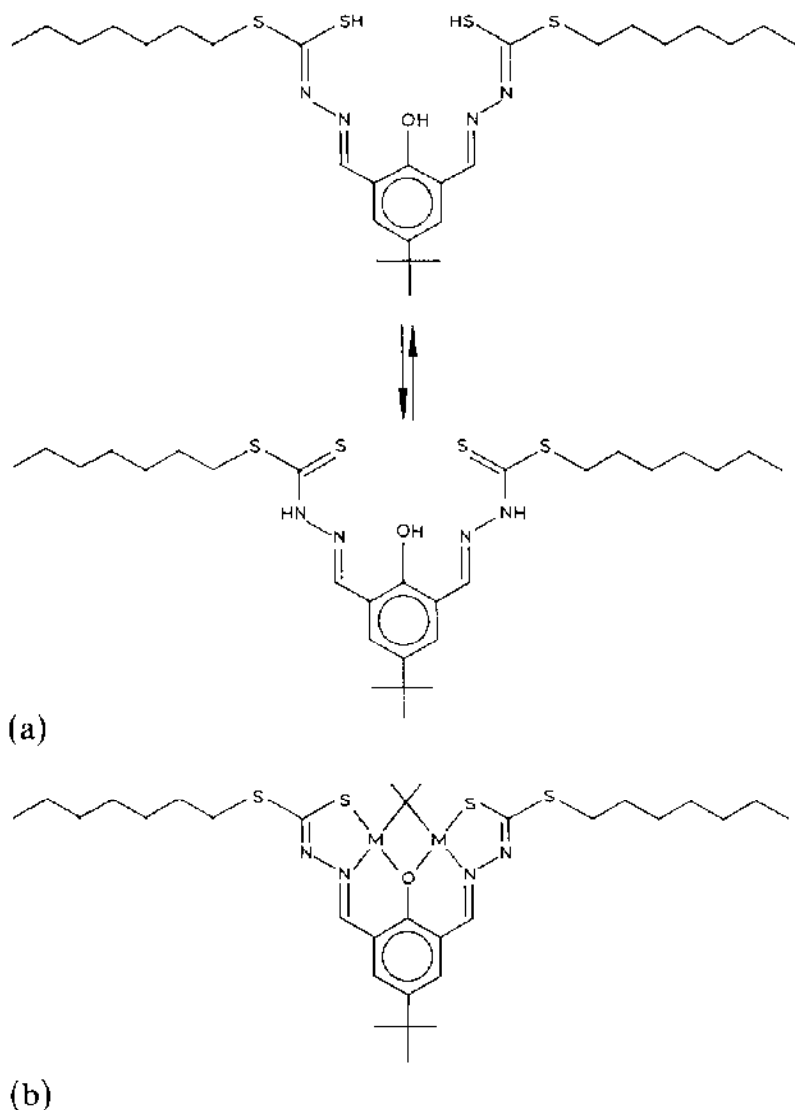


Fig. 30. Tautomerism of (a) the ligand 4-t-butyl-2,6-bis[N[(heptylthio)thiocarbonyl]aminoformidoyl] phenol and (b) the binuclear complexes derived from it.

bridging group X has been varied ( $\text{OH}^-$ ,  $\text{OEt}^-$ ,  $\text{Br}^-$ ,  $\text{CN}^-$ ,  $\text{N}_3^-$ , pyrazolate) in order to study their role in the metal-metal interaction and in redox reactions in coordinating and non-coordinating solvents. The complexes are very soluble in toluene, chlorinated hydrocarbons, acetone, *N,N*-dimethylformamide and tetrahydrofuran. IR and  $^1\text{H}$  NMR data suggest that azide and pyrazolate groups act as bidentate groups, in a 1,3- and 1,2-nitrogen system.

The nickel(II) complexes are diamagnetic while in the copper(II) complexes, antiferromagnetic coupling is occurring; the extent of metal-metal

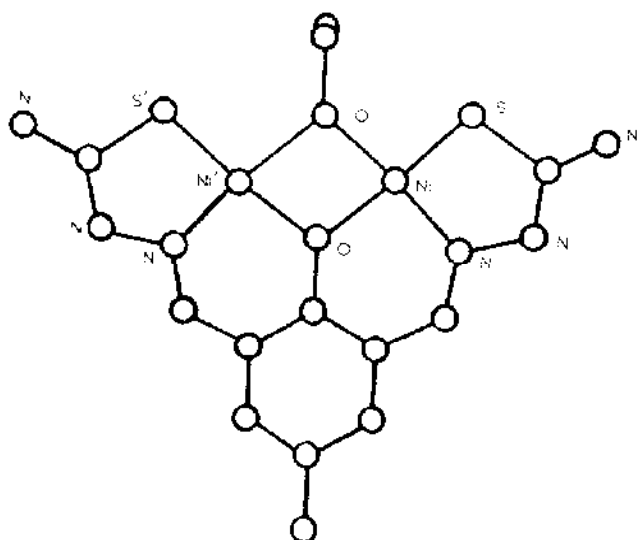


Fig. 31. Nickel(II) ethoxide complex with 3-formyl-5-methylsalicylaldehydedithiosemicarbazone.

interaction in the solid state and in solution is approximately the same and depends upon X. Moderate interactions exist with  $\text{OH}^-$  or  $\text{OEt}^-$ , weaker ones for  $\text{N}_3^-$ ,  $\text{Br}^-$  and  $\text{CN}^-$ , the weakest for pyrazolate. Room-temperature EPR spectra generally indicate a four-line pattern, although the spectra are not completely isotropic. When the solutions are heated at 333 K, isotropic spectra have been observed except in the case of the ethoxy and hydroxy bridged species. The anisotropy observed in solution is attributed to intermolecular interactions resulting from aggregation of the complex. Thus EPR spectra show that such an aggregation depends largely on the bridging group. The solution spectrum of the pyrazine-bridging system is nearly isotropic at room temperature while the spectra of the  $\text{N}_3^-$ ,  $\text{OEt}^-$  and  $\text{OH}^-$  systems are increasingly anisotropic, in the order shown, even at 333 K [83].

The dinuclear nature of the complexes with the acyclic end-off ligand has been proven by X-ray structural determinations.

The ligand 3-formyl-5-methyl-salicylaldehydedithiosemicarbazone, obtained by condensation of the two precursors in aqueous ethanol, reacts with copper(II) or nickel(II) carboxylate in the presence of a source of  $\text{X}^-$ , or by subsequent exchange of  $\text{X}^-$ , giving solvate (DMSO or DMF) dinuclear complexes. The structure of the nickel(II) ethoxylate complex [79] (Fig. 31) is composed of discrete molecules of the neutral complex. Two molecules of dimethylformamide per complex formula, neither coordinated nor hydrogen bonded to the ligand, occupy lattice sites in the crystal. The  $\text{Ni} \cdots \text{Ni}$  distance is 2.879 Å and the  $\text{Ni}-\text{O}(1)-\text{Ni}$  angles are  $100.4^\circ$  and  $101.1^\circ$ .

In the complex  $\mu$ -[2,6-bis[(2-pyridyl)methyl]iminomethyl]-*p*-cresolato-*N,N',N'',N'''*- $\mu$ -O]- $\mu$ -chloro-dichlorodicopper(II) dihydrate [84] (Fig. 32) the

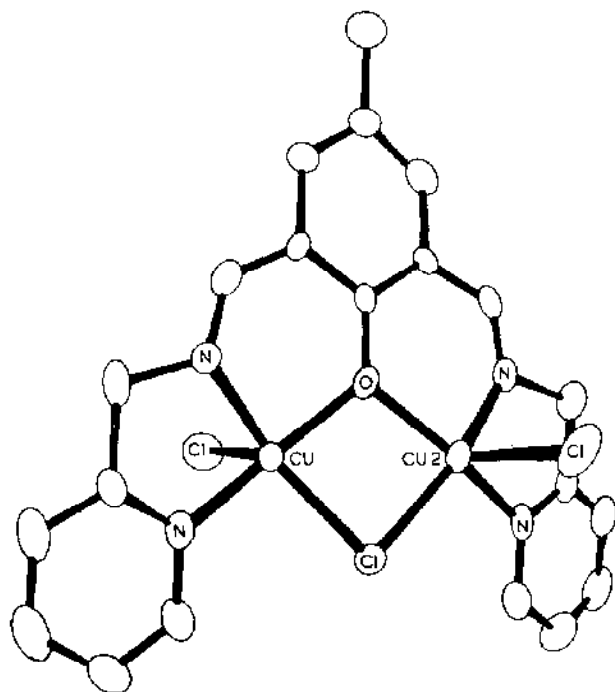
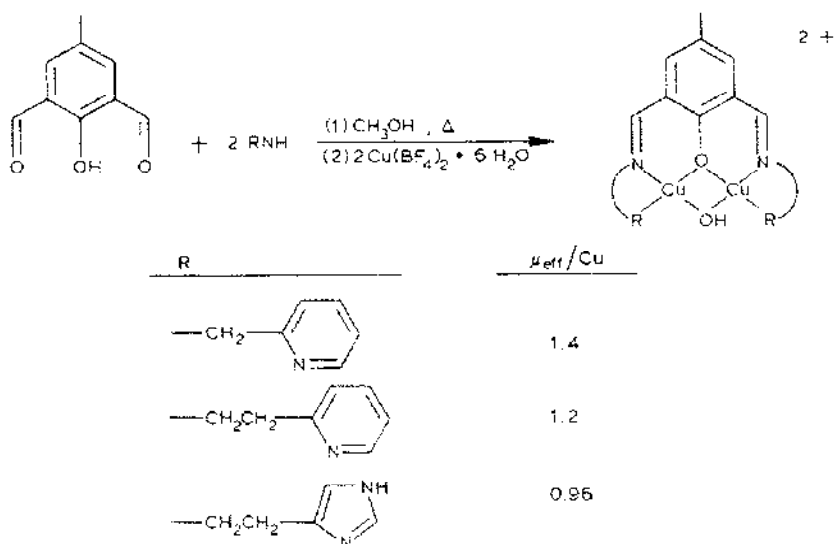


Fig. 32. Structure of  $\mu$ -[2,6-bis((2-pyridyl)methyliminoethyl)-*p*-cresolato- $N,N',N'',N'''$ , $\mu$ -*O*]chlorodichloro dicopper(II) dihydrate. Reprinted with permission from ref. 84.

ligand is near planar and acts as pentadentate while both copper(II) ions are double bridged by a phenolic oxygen and a chlorine atom. Two non-bridging chlorine atoms at the apex of distorted square pyramidal geometries coordinate to the central coppers on opposite sites of the molecule. The hydrogen bonds of the two water molecule of hydration link together two adjacent dinuclear complexes forming an infinite linear chain of dinuclear molecules.

The magnetic properties of this complex together with the analogous hydroxo-bridged complex (in this case two  $\text{ClO}_4^-$  counter anions are also present) have been studied in the 6–300 K region. A  $J$  value of  $-160 \pm 5 \text{ cm}^{-1}$  was found for the hydroxo-complex and a  $J$  value of  $-42 \pm 2 \text{ cm}^{-1}$  for the chlorocomplex [52]; in both complexes an antiferromagnetic intradimer interaction is operating. The chloride-bridged complex shows additional weak interdimer magnetic interaction ( $J' = -1.1 \text{ cm}^{-1}$ ), resulting from hydrogen bonding in the crystal lattice.

By condensation of 2,6-diformyl-4-methylphenol with primary amines, followed by addition of  $\text{Cu}(\text{BF}_4)_2 \cdot 6\text{H}_2\text{O}$  the complexes of Scheme 10 have been prepared [77,78]. In these complexes both copper atoms are presumably bound to an aromatic nitrogen as shown for the complex with histidine where each copper is five coordinate with one of the copper atoms bound to



Scheme 10.

the oxygen of a water molecule and the other copper bound to the oxygen of the hydroxy bridge of an adjacent molecule [85] (Fig. 33).

With the same precursors copper(II) air sensitive complexes have also been prepared in helium atmosphere according to Scheme 11 [77]. The crystal

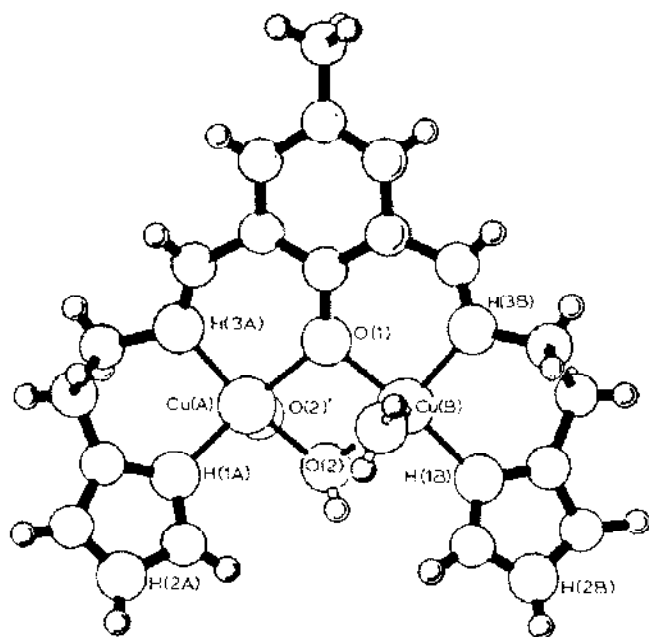
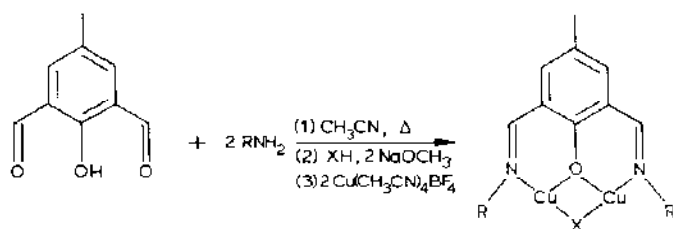


Fig. 33. Structure of the binuclear copper(II) cation with the ligand 2,6-bis{N-[2-(4-imidazolyl)ethyl]iminomethyl-4-methylphenol}. Reprinted with permission from ref. 85.



Scheme 11.

structure of one of these compounds ( $R = \text{CH}_2\text{--CH}_2\text{--C}_5\text{H}_4\text{N}$ ) confirms the geometry proposed in Scheme 11 [77] (Fig. 34). Each copper is bound to three atoms: a phenoxide oxygen, an imine nitrogen and a pyrazolate nitrogen. The pyridine was found not to be coordinated to copper. The intermolecular copper  $\cdots$  copper distance is 3.304 Å. The molecules form an infinite stack in the direction of the  $b$  axis.

2,6-Diformyl-4-methylphenol and dimethylamino-1-propylamine, in the presence of  $\text{Cu}(\text{ClO}_4)_2 \cdot 6\text{H}_2\text{O}$  followed by addition of  $\text{NaN}_3$ , gave the tetramer in Fig. 35 [86]. This tetramer is formed by two dinuclear subunits which are inverted by a center of symmetry in  $(1/2, 1, 1/2)$  resulting in  $C_i$  symmetry. In each subunit the compartmental ligand acts as tridentate; the phenolate oxygen bridges the two copper atoms while the two imino nitrogens each coordinate to the copper atoms. An additional bridge in the dinuclear subunit is formed by an azido-group; the other two azido groups are terminal, each bonded to one copper atom. Interdimeric azide bridges form the tetranuclear unit [86].

An interesting series of dinuclear copper(II) complexes has been prepared by reaction of sodium salts of 2,6-diformyl-4-methylphenol or 2,6-diacetyl- and 2,6-dibenzoyl-derivatives with  $\alpha,\omega$ -diaminoalkanes in the presence of

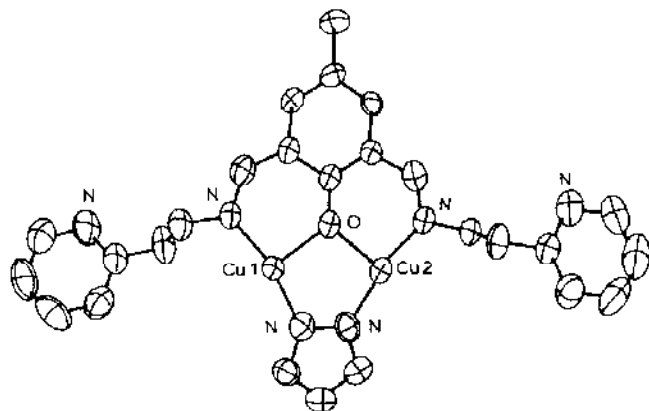


Fig. 34. Structure of binuclear copper(II) pyrazolate complex with the ligand obtained by condensation of 2,6-diformyl-4-methylphenol and 2-(2'-aminoethyl)-pyridine. Reprinted with permission from ref. 77. Copyright 1986 American Chemical Society.

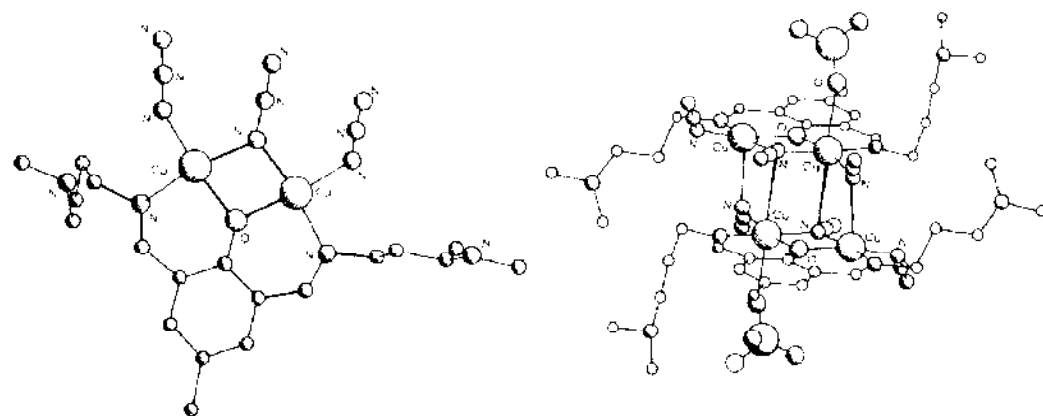
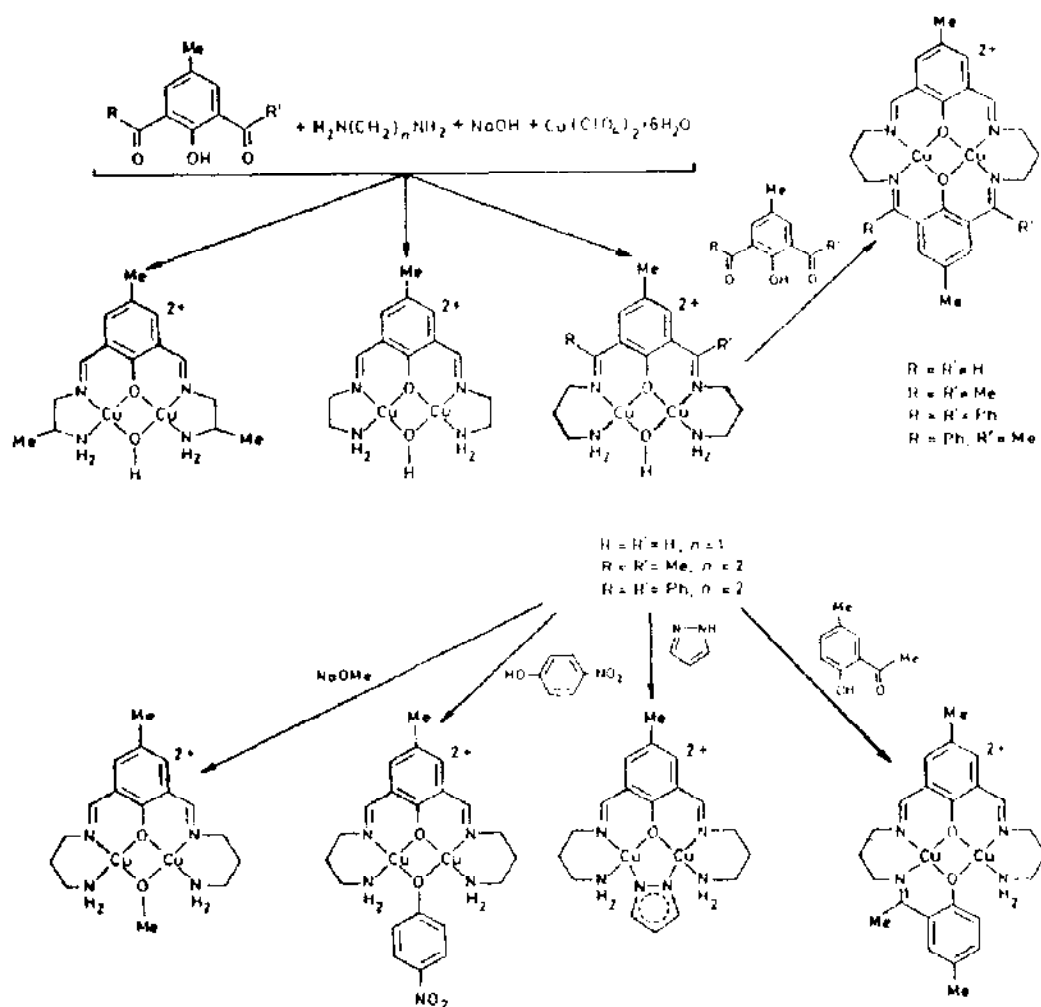


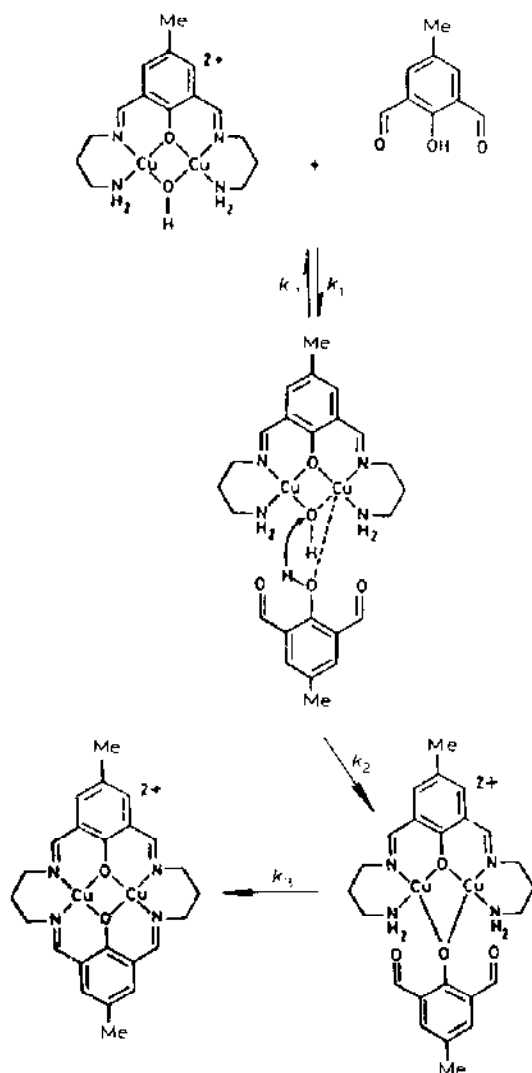
Fig. 35. The tetramer copper(II) complex with the ligand derived from 2,6-diformyl-4-methylphenol and 3-dimethylamino-1-propylamine: (a) the dimeric subunit; (b) tetrameric structure. Reprinted with permission from ref. 86.



Scheme 12.

copper perchlorate in very dilute aqueous methanol solution [87,88]. Only one end of the diamine condenses with each part of the carbonyl moiety with formation of hydroxo-bridged copper(II) complexes according to Scheme 12. The hydroxy group can be replaced by a methoxy bridge and generally by weak organic acids.

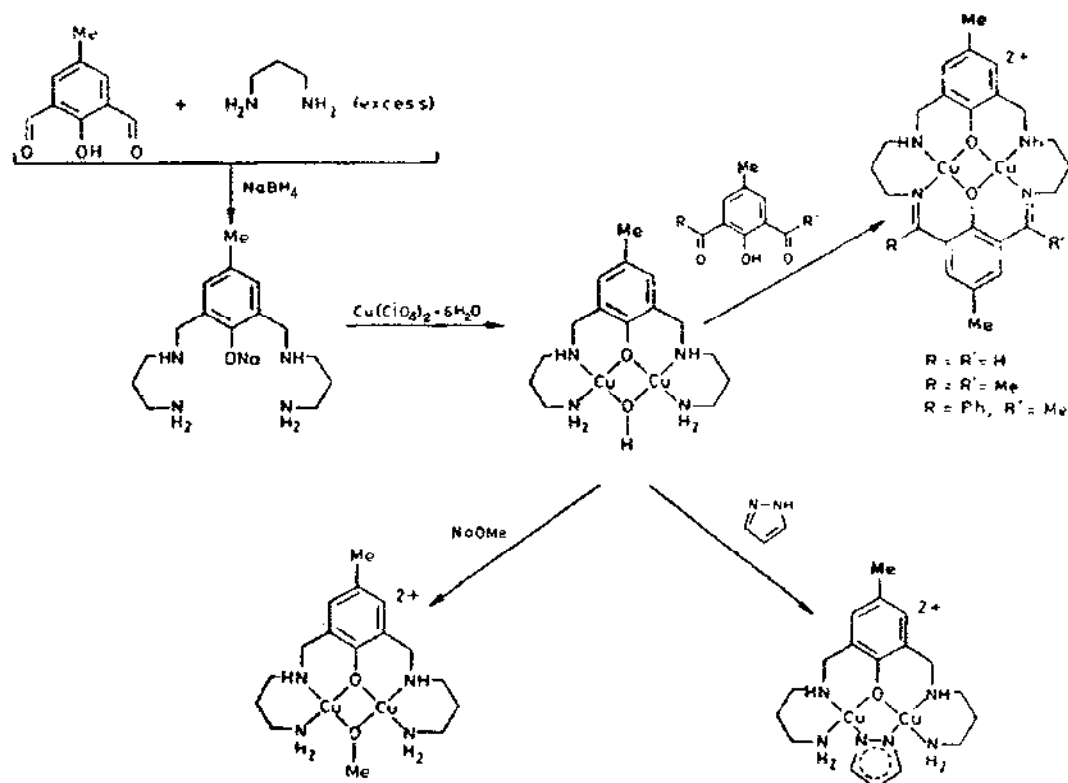
The formation of the macrocyclic complexes from the hydroxo-bridged compound is remarkable because, by using this reaction it is possible to generate variously substituted macrocyclic complexes which otherwise are not accessible. The mechanism for the formation of these macrocyclic complexes is proposed to involve the pathway in Scheme 13. The equilibrium constant  $K(k_1/k_{-1})$  for the formation of the hydroxo complex is



Scheme 13.

$4.8 \text{ dm}^3 \text{ mol}^{-1}$  and  $k_2 = 1.78 \times 10^{-2} \text{ s}^{-1}$ . The rate constant  $k_3$  for the cyclization reaction is  $7.4 \times 10^{-5} \text{ s}^{-1}$ . It was suggested, on the basis of these results [87,88], that the condensation of the two amino and aldehyde functions takes place in a concerted fashion.

Another series of more flexible ligands, with fully saturated side arms, have been synthesized by reaction of 2,6-diformyl-4-methylphenol with an excess of ethylenediamine [87,88] or 1,3-diaminopropane [76] in boiling methanol, followed by reduction of the condensation product with sodium borohydride. By using these ligands, copper(II) complexes have been obtained according to Scheme 14. Again the hydroxy group can be substituted



Scheme 14.

by weak potentially monodentate or bidentate acids. The macrocyclic compounds, obtained by condensation of hydroxo complexes with 2,6-diformyl-4-methylphenol, are particularly interesting because in these compounds the two halves of the ring contain diamino and diaza moieties.

For the copper(II) complex with the ligand in Fig. 36a the X-ray structure was determined [75] to be as shown in Fig. 36b.



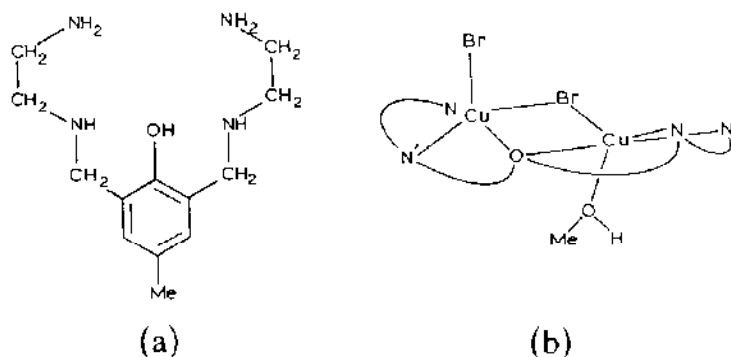


Fig. 36. (a) The ligand 2,6-bis(*N*-2'-aminoethylaminomethyl)-*p*-cresol and (b) the related copper(II) dibromo complex.

The complex is composed of discrete cations and  $\text{ClO}_4^-$  anions. The cations have two five coordinate copper(II) atoms in different environments; one copper has a  $\text{N}_2\text{OBr}_2$  donor set in an almost square-pyramidal environment with a bromine atom at the apex; the other copper has a  $\text{N}_2\text{O}_2\text{Br}$  donor set in a configuration between trigonal-bipyramidal and square-pyramidal with a methanol molecule at the apex. A second bromine atom bridges two copper ions [76].

The dicopper(II) complexes of Fig. 37 [78] have been prepared by reaction of the corresponding Schiff base ligand with sodium borohydride prior to reaction with copper(II). For the complex with the ligand derived from histamine, the crystal structure has recently been reported [89]. It crystallizes as a binuclear copper(II) hydroxo cation with two related formula units of  $\text{ClO}_4^-$  anions and 1.5 water molecules in the asymmetric unit. The compartmental ligand is pentadentate; the two copper atoms are bridged by the oxygens of the hydroxyl and phenolate groups. Two amino and imidazole nitrogen atoms complete the coordination of the two copper atoms in the cation (Fig. 38). One perchlorate group is situated between two dinuclear cations, so the resulting structure has been interpreted as a one-dimensional infinite chain. One copper atom is square planar with two additional axial elongated ligands; the coordination polyhedron around the second copper is a distorted tetragonal pyramid with a water molecule at its apex. No bonding contacts between the remaining perchlorate group and the dimeric subunits have been observed [89].

A phenoxide group from a tyrosine residue is considered a likely candidate for the endogenous bridging group in oxyhemocyanine [16]; an alkoxo group has however, been proposed as an alternative [16]. A new series of potentially pentadentate compartmental ligands have accordingly been prepared by condensation of pyridine-2-carboxaldehyde, pyrrole-2-carbo-

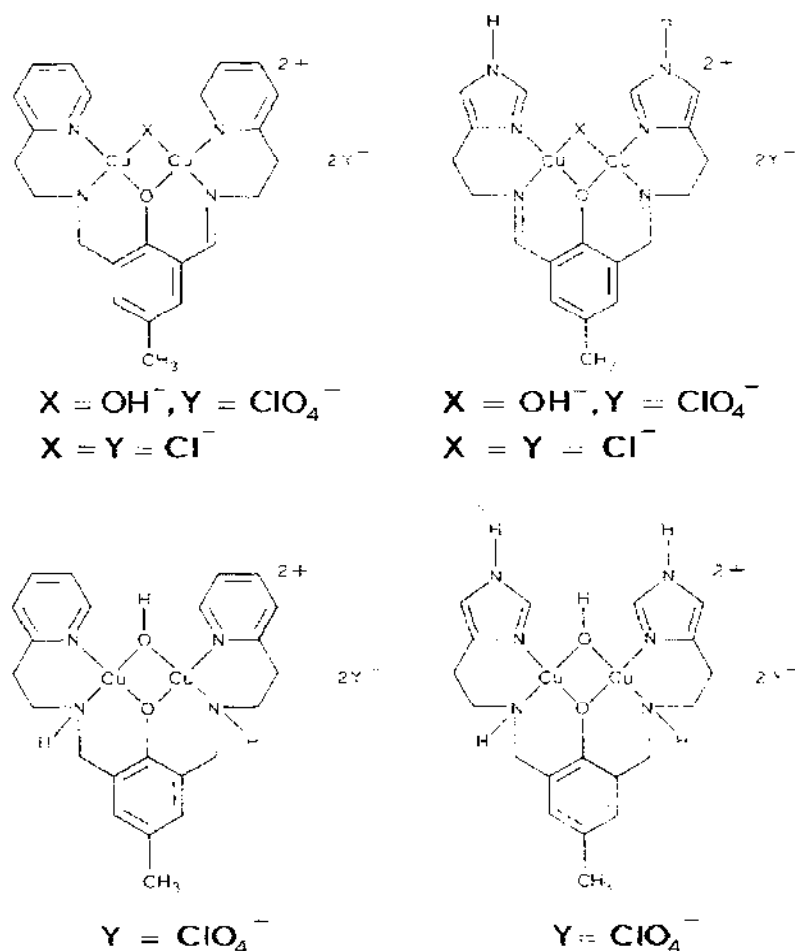


Fig. 37. Dicopper(II) complexes with a series of reduced ligands derived from 2,6-diformyl-4-methylphenol, 2-ethylaminopyridine or 2-ethylaminopyrazole.

aldehyde, salicylaldehyde, acetylacetone and  $\beta$ -diketones with 1,3-diaminopropan-2-ol or 1,5-diaminopentan-3-ol [90–94]. These ligands are more flexible than the corresponding ligands based on 2,6-diformyl-4-methylphenol and such flexibility can be increased by reducing them with sodium borohydride. The complexes prepared (Fig. 39) contain exogenous bridges having single (OH, Cl, OR) or two atoms (pyrazolate, acetate). The compartmental behaviour of these ligands has been confirmed by structural determination.

In the  $\mu$ -hydroxo dicopper(II) complex with 1,9-dipyridyl-5-hydroxy-2,8-diazanona-1,8-diene [90] shown in Fig. 40 there are alkoxo and hydroxo bridging groups. The  $N_2O_2$  donor sets around each copper are essentially planar. Both copper atoms are pentacoordinate in a square-pyramidal coordination, with very similar basal coordination but with different apical

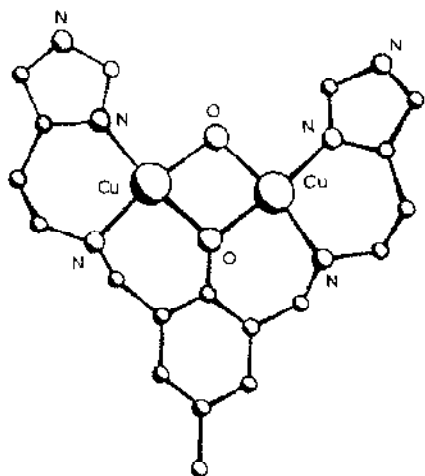


Fig. 38. Structure of the binuclear copper(II) cation with the ligand derived from 2,6-diformyl-4-methylphenol and histamine. Reprinted with permission from ref. 89.

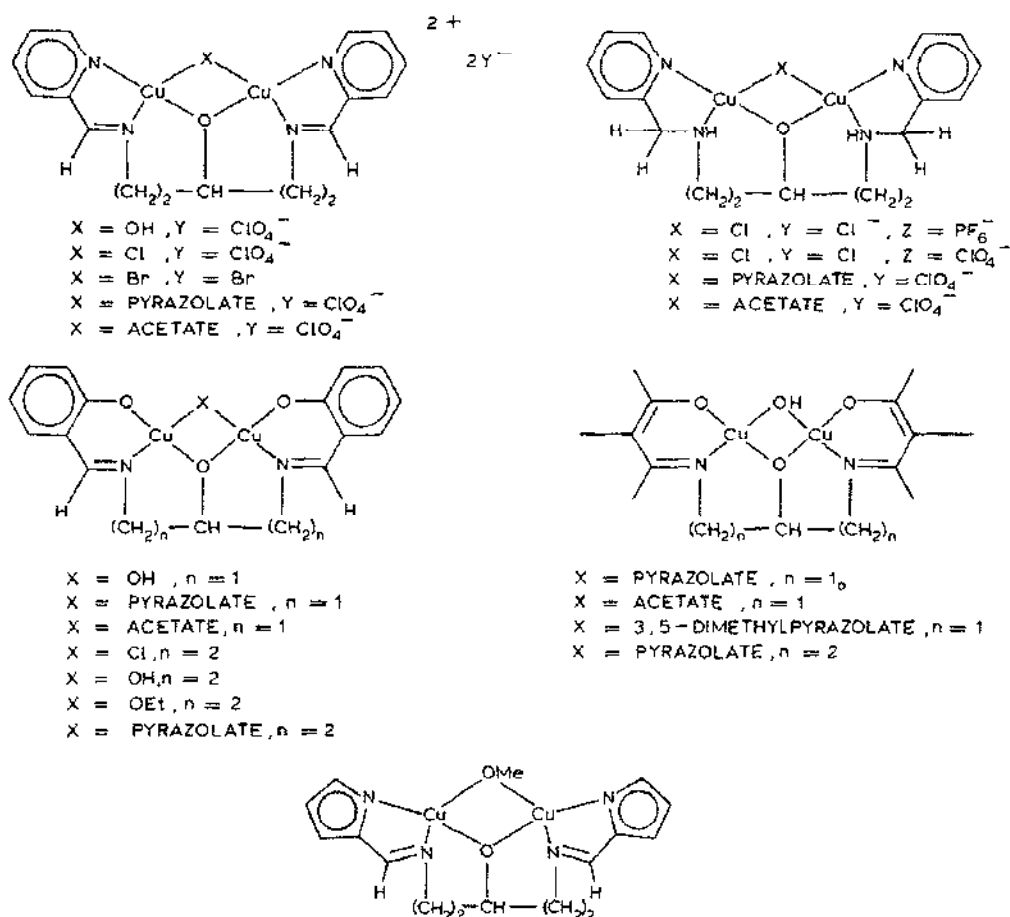


Fig. 39. A series of binuclear copper(II) complexes having an alkoxo bridge.

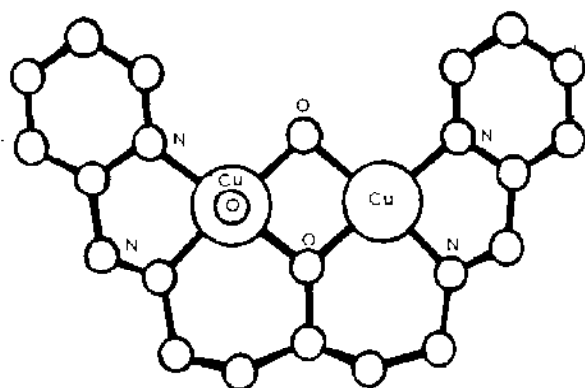


Fig. 40. Structure of  $\mu$ -hydroxo-dicopper(II) complex with 1,9-dipyridyl-5-hydroxy-2,8-diazanona-1,8-diene. Reprinted with permission from ref. 90. Copyright 1986 American Chemical Society.

ligands. One copper is bound to a water molecule while the second copper interacts with the oxygen of a neighboring dinuclear unit (a weaker interaction with the  $\text{ClO}_4^-$  ion is also present). The structure thus involves pairs of dinuclear complexes leading to tetranuclear units. In the  $\mu$ -pyrazolato dicopper(II) complex with 1,7-di(*o*-hydroxyphenyl)-4-hydroxy-2,6-diazahepta-1,6-diene (Fig. 41) [91] the copper atoms are bridged by the oxygen from the alkoxo group of the pentadentate ligand and by the two nitrogen atoms from the pyrazolate moiety. No evidence has been found for interdimer interaction: in addition the water molecule present in the compound is not coordinated. The intramolecular  $\text{Cu} \cdots \text{Cu}$  distance is 3.359 Å, while the copper-oxygen-copper angle of  $125.1^\circ$  represents a significant opening of this angle to accommodate the large bite of the pyrazolate bridge.

Recently two structural isomers of the  $\mu$ -acetato bridged copper(II) complex with 1,3-bis(salicylideneiminato)propan-2-ol [93,94] have been published, one anhydrous and one hydrated, which are shown, respectively, in Figs. 42 and 43. The most remarkable difference between the two isomers is the non-coplanarity of the two copper coordination spheres in the anhydrous

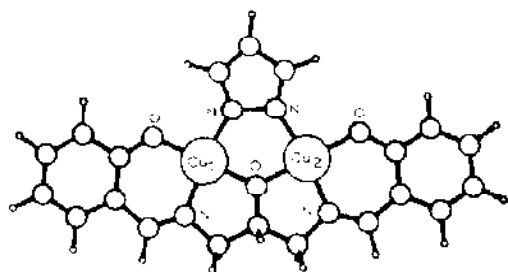


Fig. 41. Structure of  $\mu$ -pyrazolato dicopper(II) complex with 1,7-di(*o*-hydroxyphenyl)-4-hydroxy-2,6-diazahepta-1,6-diene. Reprinted with permission from ref. 91. Copyright 1986 American Chemical Society.

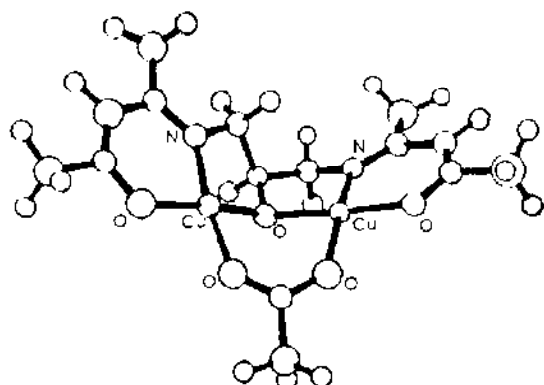


Fig. 42. Structure of  $\mu$ -acetato dicopper(II) with the ligand derived from acetylacetone and 1,3-diamino-2-propanol. Reprinted with permission from ref. 93.

complex, folded relative to each other, compared to the overall coplanarity of the dinuclear moiety in the hydrate complex.

The skeletal structures of the compounds of Fig. 44 are essentially the same as that of the hydrated complex. The copper atoms are bridged by the alkoxide and the carboxylate oxygens and the coordination planes are approximately coplanar [73]. Only an alkoxide bridge is present in the complex in Fig. 45 [94], where terminal  $\text{CH}_3\text{OH}$  and  $\text{CH}_3\text{O}^-$  complete the coordination geometry about copper(II) ions.

Recently, 2,6-bis[(salicylideneamino)methyl]-4-methylphenol has been synthesized [95] by reaction of 2,6-bis(aminomethyl)-4-methylphenol dihydrochloride and salicylaldehyde; the binuclear copper(II) complex (Fig. 46),

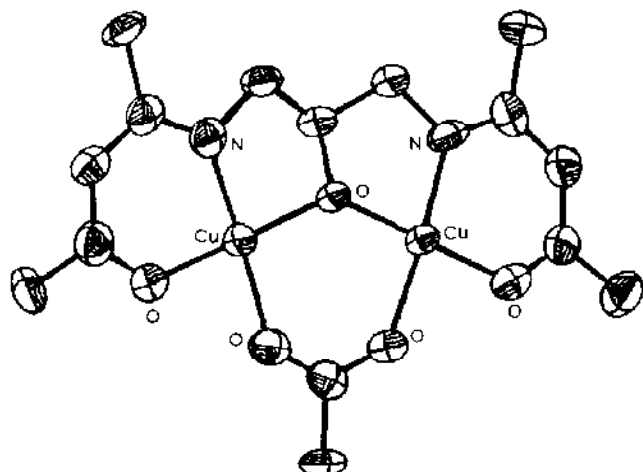


Fig. 43. Structure of the monoquo  $\mu$ -acetato dicopper(II) with the ligand derived from acetylacetone and 1,3-diamino-2-propanol. Reprinted with permission from ref. 92.

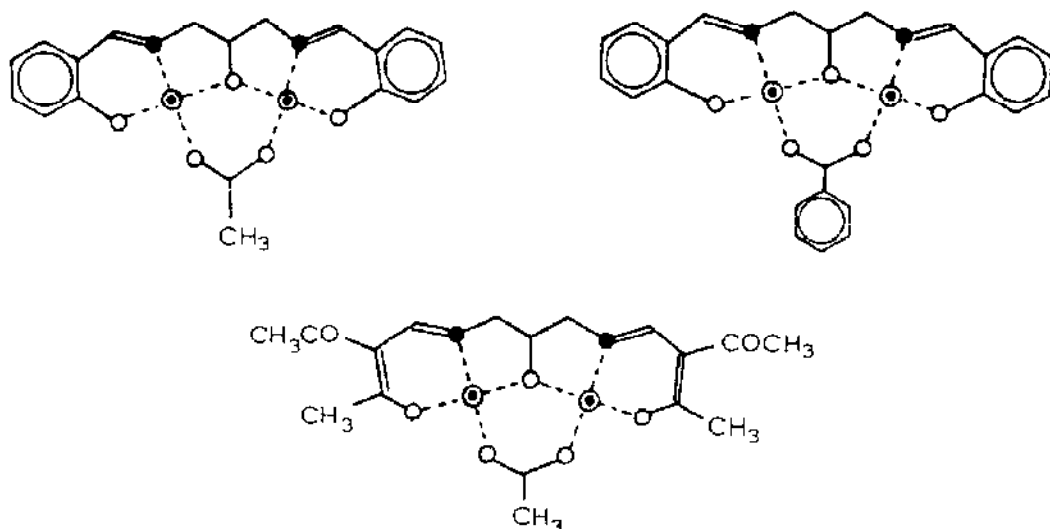


Fig. 44. Skeletal structure of  $\mu$ -alkoxo,  $\mu$ -carboxylato dicopper(II) complexes. Reprinted with permission from ref. 94.

where a pyrazolate anion has been introduced as an exogenous bridging unit, has been synthesized.

A comparison of the magnetic properties of the complexes, supplementary discussed above, can add useful information. Antiferromagnetic coupling has been observed in all the systems related to 2,6-diformylphenol, where a phenoxy bridging group occurs. Generally a high negative value of the exchange constant  $J$  was found, the differences being generally due to the second X bridge present.

For the complexes in Fig. 37,  $2J$  values range from  $-385$  to  $-545 \text{ cm}^{-1}$  for the hydroxo-bridged species and from  $-150$  to  $-230 \text{ cm}^{-1}$  for the chloro-bridged complexes. Strong antiferromagnetic coupling is also present

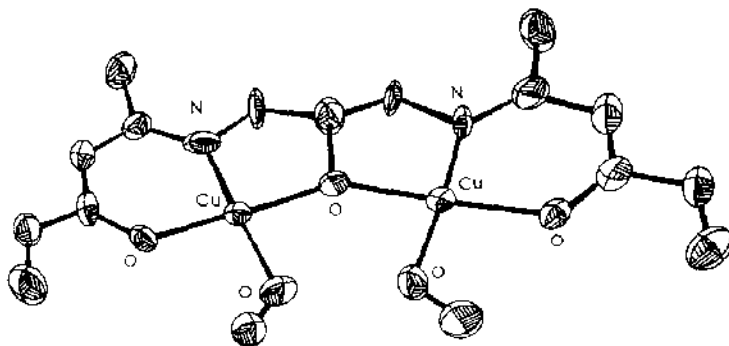


Fig. 45. Structure of dimethoxy dicopper(II) complex with the ligand derived from acetylacetone and 1,3-diamino-2-propanol. Reprinted with permission from ref. 94.

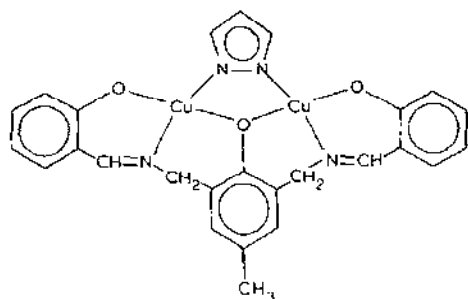


Fig. 46. Pyrazolate copper(II) complex with 2,6-bis[(salicylidene-amino)methyl]-4 methylphenol.

in the similar complexes with the more flexible ligands where the C=N groups have been reduced.

The complex in Fig. 46, derived from 2,6-bis(aminomethylphenol) has a magnetic susceptibility between 4.2 and 3.00 K compatible with a strong antiferromagnetically coupled  $\text{Cu}^{2+}\text{-Cu}^{2+}$  pair. The  $2J$  value for exchange between the two copper(II) ions may be compared with the values found for the similar complex reported in Fig. 28 ( $X = \text{pyrazolate}$ ) ( $2J = -460 \text{ cm}^{-1}$ ). The changes in the ligands have made a negligible difference in the overall magnetic interactions of the copper(II) ions.

Theoretical analysis using models for tetrameric and dimeric interactions have shown [86] that in these and similar systems the interdimeric interactions are small in those complexes for which a tetrameric structure was proven.

Finally antiferromagnetic interactions have also been observed in those complexes of the type reported in Fig. 30 where two oxygen donors have been substituted by sulphur donor atoms [83].

The occurrence of both antiferromagnetic and ferromagnetic coupling has been found for similar complexes based on 1,3-diaminopropan-2-ol and 1,5-diaminopentan-3-ol backbones, which furnish pentadentate ligands of greater stereochemical flexibility. For the complexes in Fig. 43, it was observed that  $-J$  decreases in the order  $\text{OR}^- = \text{pyrazolate} > \text{acetate} > \text{OH}^- > \text{Cl}^-$ . A comparison of the magnetic and structural data indicated that distortion from trigonal planar toward pyramidal geometry of the endogenous alkoxo-bridging group leads to a less negative value for  $J$ . In several compounds this effect leads to net ferromagnetism [90-94].

#### (v) Complexes with polypodal ligands

Recent EXAFS studies [7-11,16] have shown that each copper ion in oxyhemocyanin is four or five coordinate and the donor atoms are N and O.

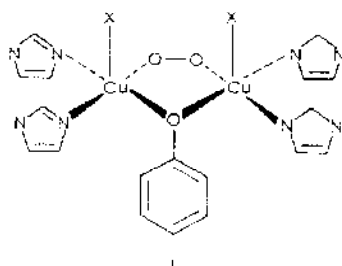


Fig. 47. Proposed binuclear copper(II) complex in oxyhemocyanine.

Two histidine imidazole N donors are bound to each copper and a symmetrically bridging peroxide ion occupies the exogenous site [7-11] (Fig. 47). A phenoxide group from a tyrosine is considered the most probable endogenous bridging group although an alkoxo group has been proposed as an alternative [7-11,16].

An extension of the availability of dinucleating ligands, containing an alkoxo bridge for the formation of copper(II) complexes, which can mimic the features of the hemocyanin-active site, is represented by the synthesis of *N,N,N',N'*-tetrakis (2-(1-ethylbenzimidazolyl))-2-hydroxy-1,3-diaminopropane prepared via condensation of *o*-phenylenediamine with 2-hydroxy-1,3-diaminopropanetetracetic acid followed by N-alkylation with bromoethane [96,97]. Treatment of this ligand with  $\text{Cu}(\text{BF}_4)_2$  or  $\text{Cu}(\text{ClO}_4)_2$ , followed by the addition of an anionic ligand X ( $\text{X} = \text{N}_3^-$ ,  $\text{OAc}^-$ , pyrazolate,  $\text{HCOO}^-$ ,  $\text{NO}_2^-$ , etc.) produces dinuclear complexes shown in Fig. 48 [96,97] ( $\text{Y} = \text{BF}_4^-$  or  $\text{ClO}_4^-$ ).

It was observed that simply by varying the bridge  $\text{X}^-$ , it is possible to obtain drastic changes in the copper-copper interactions: for this reason the structures of the weakly ferromagnetic acetate complex ( $\text{X} = \text{OAc}^-$ ) and the completely antiferromagnetically coupled azide complex ( $\text{X} = \text{N}_3^-$ ) have

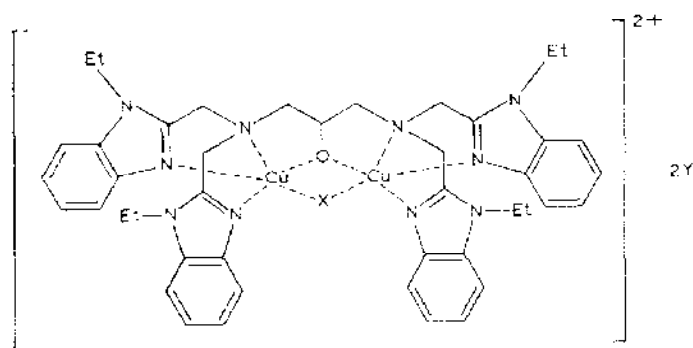
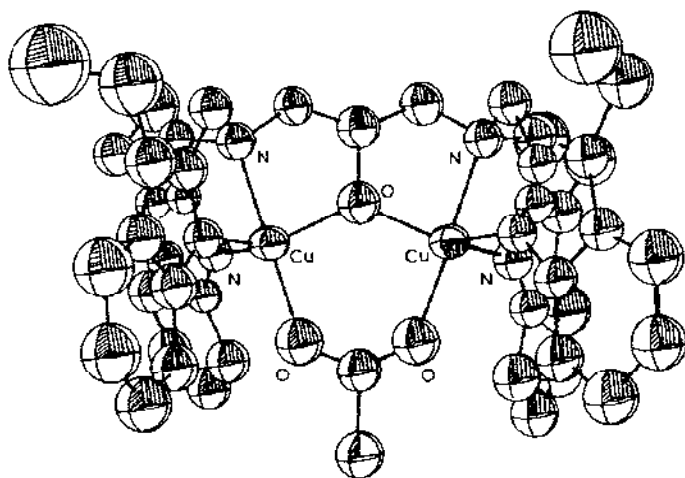


Fig. 48. Copper(II) complex with *N,N,N',N'*-tetrakis[2-(1-ethylbenzimidazolyl)]-2-hydroxy-1,3-diaminepropane ( $\text{Y} = \text{BF}_4^-$ ,  $\text{ClO}_4^-$ ).

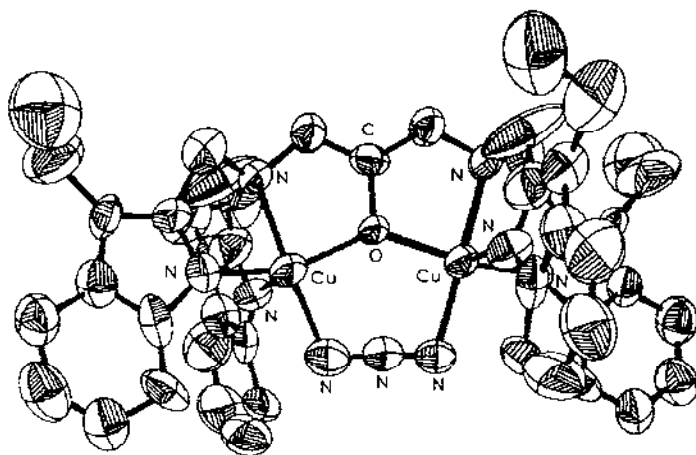


been determined [96,97]. The two structures are similar. Each copper atom is coordinated to a tertiary amine and to two *N*-ethylbenzimidazole ligands. The bridging alkoxide and the acetate or azide group complete the five coordination (Fig. 49).

There are, however, significant differences in the detailed coordination geometries. The stereochemistry about copper in the acetate complex closely approximates a trigonal bipyramid; by contrast the stereochemistry about copper in the azide complex more closely approximates a tetragonal pyramid than a trigonal bipyramid. The copper  $\cdots$  copper separation in the



(a)



(b)

Fig. 49. Structures of (a) dicopper(II)- $\mu$ -acetato and (b) dicopper(II)- $\mu$ -azide complexes with *N,N,N',N'*-tetrakis[2-(1-ethylbenzimidazolyl)]-2-hydroxy-1,3-diaminepropane. Reprinted with permission from refs. 96 and 97. Copyright 1986 American Chemical Society.

acetate complex is 3.459(2) Å; in the azide complex it is 3.615(3) Å. These different coordination geometries of the acetate and the azide complexes can explain their different magnetic behaviour. For the acetate complex the trigonal bipyramidal stereochemistry dictates a  $(d_{xy}^2)^1$  ground state and thus the major lobes of the magnetic orbital will be axially directed toward a single bridging ligand, the acetate. By contrast the stereochemistry of the azide complex dictates a  $(d_{xz}^2)^1$  ground state that orients the magnetic orbital lobes toward both bridging ligands, the alkoxide and the azide.

Polypodal ligands based on the separation, by a xylene bridge, of two tridentate donor groups containing nitrogen [98–100], sulphur [101], phosphorus [102] or arsenic [103] donor atoms have been prepared. The *p*-xylyl ligand, obtained by reaction of bis[2-(2-pyridyl)ethyl]amine with  $\alpha,\alpha'$ -dibromo-*p*-xylene in methanol in the presence of  $K_2CO_3$  gives with  $CuCl_2$  the complex shown in Fig. 50 [100]. The molecule is a dimer with a crystallographic center of symmetry located at the center of the benzene ring. The copper atoms exhibit distorted trigonal bipyramidal coordination geometry. The two pyridyl nitrogens occupy the axial positions while the equatorial plane is shared by the amine nitrogen and two chlorides. A large copper  $\cdots$  copper separation is present ( $Cu \cdots Cu = 11.71$  Å).

The *m*-xylyl ligand (Fig. 51a) has been used with the aim of stabilizing the reduced state of copper [101]. The copper(I) complex, obtained by reaction of this ligand with  $[Cu(CH_3CN)_4]PF_6$  is a polymer with the basic repeating sequence of Fig. 51b. The two copper(I) ions have a highly distorted

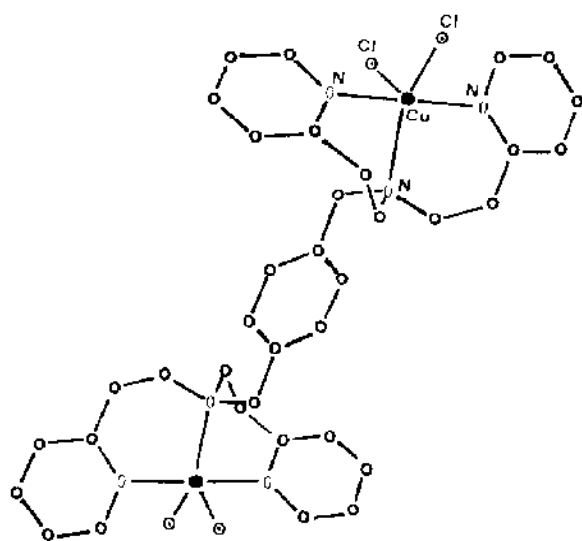


Fig. 50. Structure of the dicopper(II) dichloro complex with the ligand derived from bis[2-(2-pyridylethyl)amine and  $\alpha,\alpha'$ -dibromo-*p*-xylene.

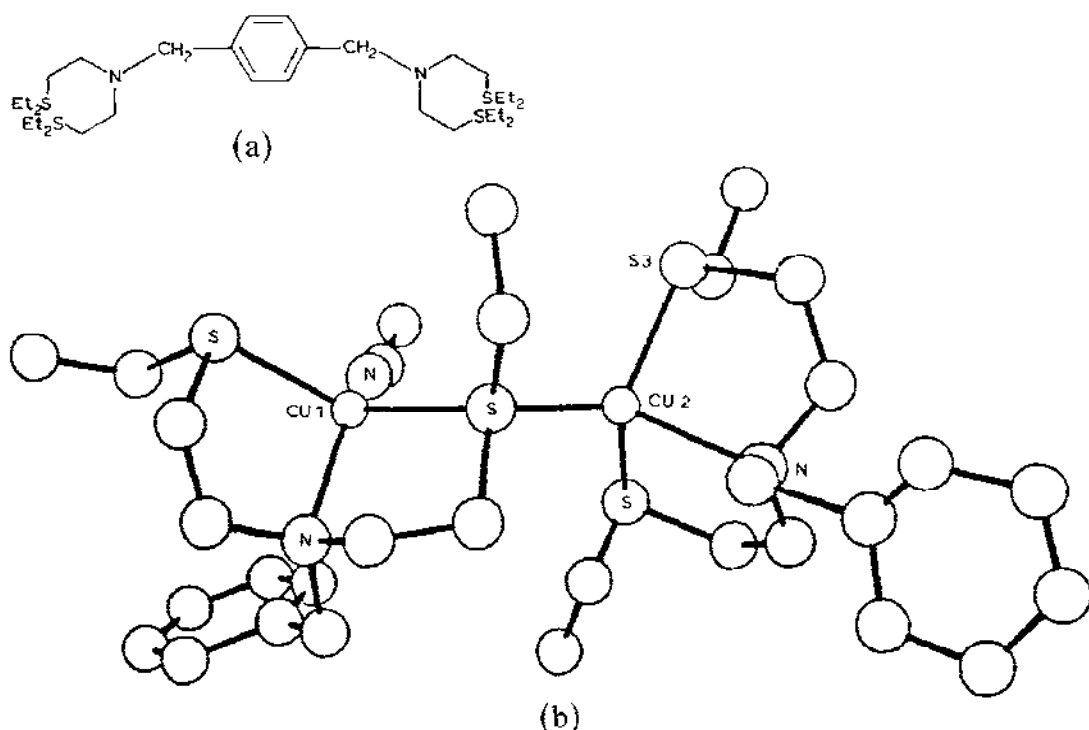


Fig. 51. (a) The *p*-xylyl ligand containing thioether groups and (b) the related dicopper complex. Reprinted with permission from ref. 101.

tetrahedral environment; one copper is coordinated by the tridentate  $\text{NS}_2$  group and an acetonitrile molecule, the other has a  $\text{NS}_3$  environment. One thioether sulphur atom acts as a bridging bidentate group.

The *m*-xylyl ligand, derived by reaction of bis-2-(2-pyridyl)ethylamine with  $\alpha, \alpha'$ -dibromo-*m*-xylene in ethylacetate in the presence of diisopropylethylamine, reacts with  $[\text{Cu}(\text{CH}_3\text{CN})_4]\text{PF}_6$  in  $\text{MeOH}/\text{CH}_2\text{Cl}_2$  to yield an extremely air sensitive dinuclear copper(II) complex, which reacts with  $\text{O}_2$  giving rise to the phenoxy and methoxy copper(II) bridged complex shown in Fig. 52, as confirmed by X-ray studies [104]. By this procedure a new compartmental ligand has been prepared in situ. The cation has a rigorously planar  $\text{Cu}_2\text{O}_2$  bridging unit with a crystallographic 2-fold axis which passes through the two oxygen atoms and the carbons bonded thereto. The ligand arranged around each copper atom is almost square pyramidal with an axial pyridyl nitrogen atom and a basal  $\text{N}_2\text{O}_2$  donor set which includes the tertiary amines and pyridyl atoms. Two  $\text{PF}_6^-$  groups form the counter anions.

Subsequent studies [105–107] have demonstrated that the reaction of the above *m*-xylyl ligand with copper(I) salts leads to the formation of complex **B** of Scheme 15, which reacts with oxygen to give complex **C**. Finally the

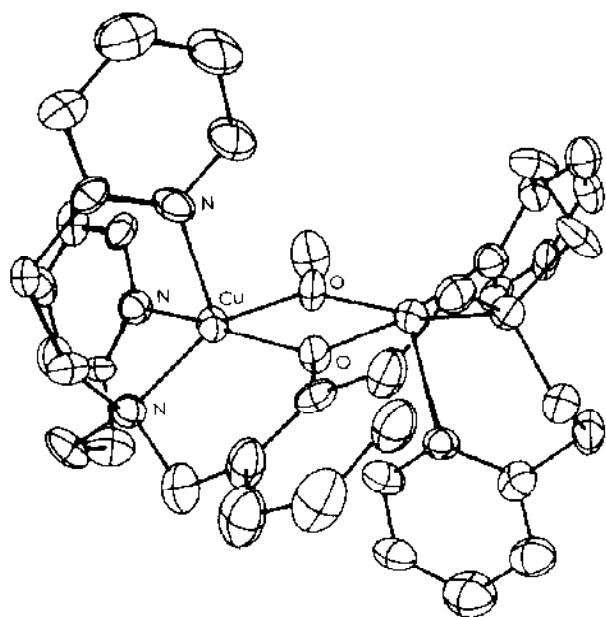
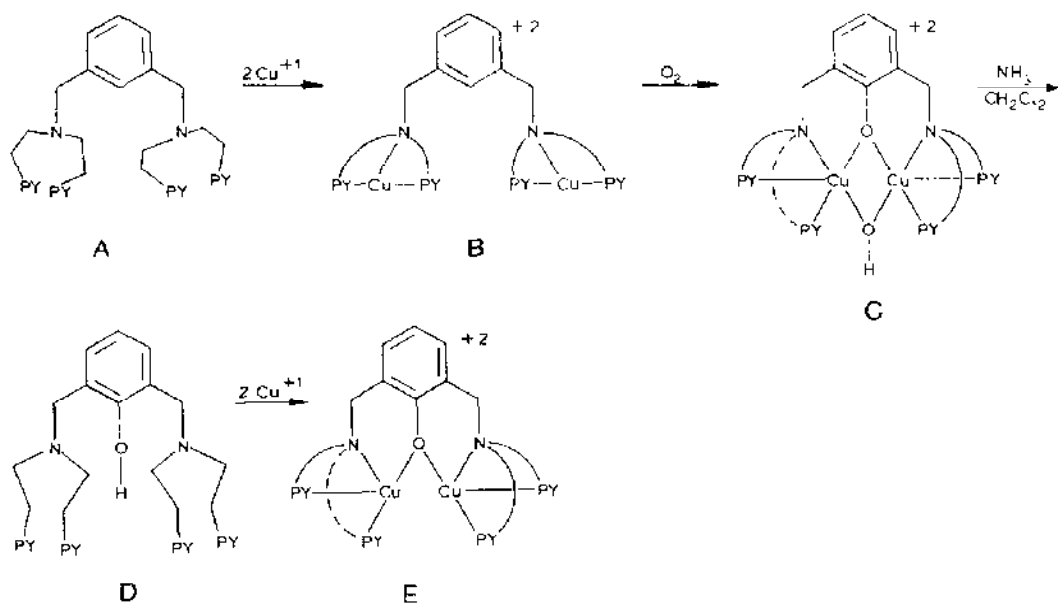


Fig. 52. Binuclear  $\mu$ -methoxy-dicopper(II) with  $N,N,N',N'$ -tetrakis[2-(2-pyridyl)ethyl] $\alpha,\alpha'$ -diamino-*m*-xylene. Reprinted with permission from ref. 104.

copper ions can be removed from **C** producing the phenolic compound **D** which by reaction with copper(I) gives **E**.

Manometric measurements of  $O_2$  uptake by **B** and mass spectrometric analyses of **C** prepared by using isotopically pure  $^{18}O_2$  proves that both atoms of dioxygen are incorporated into the oxygenation product [107].



Scheme 15.

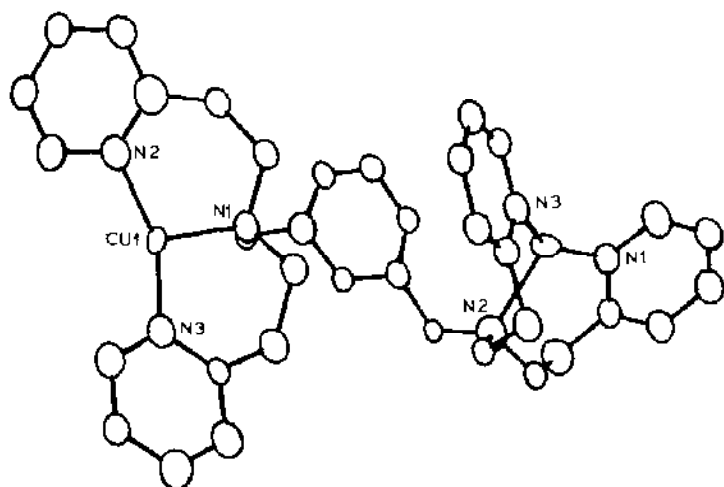


Fig. 53. Structure of dicopper(II) complex **B** of Scheme 15. Reprinted with permission from ref. 106. Copyright 1986 American Chemical Society.

The structural determination of **B**, **C** and **E** have unambiguously confirmed the pathway of Scheme 15.

The structure of **B** [105,106] consists of one discrete complex dication and two well-separated anions per asymmetric unit. The cation consists of two crystallographically independent cuprous ion coordination environments; each copper(I) is three coordinate with ligation from two pyridine and one tertiary amino donor group (Fig. 53). The chelating tridentate ligands cause considerable distortion from idealized trigonal planar coordination.

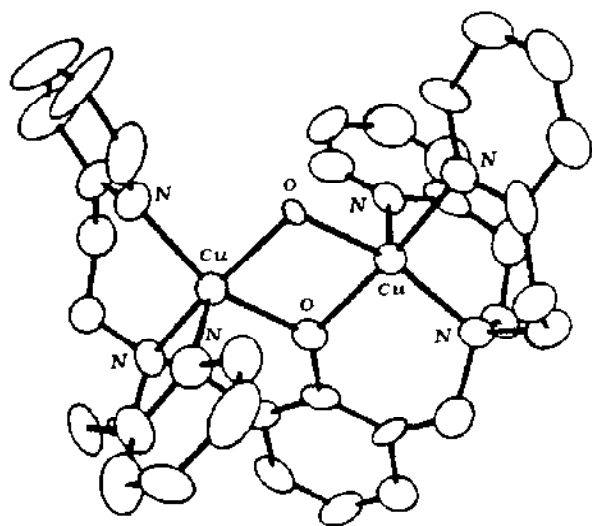


Fig. 54. Structure of  $\mu$ -hydroxo dicopper(II) complex **C** of Scheme 15. Reprinted with permission from ref. 106. Copyright 1986 American Chemical Society.

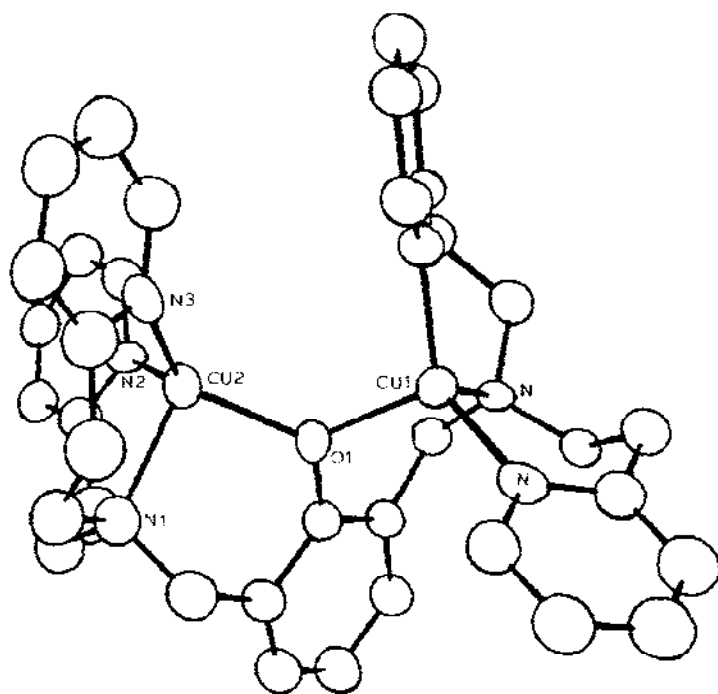


Fig. 55. Structure of dicopper(II) complex **E** of Scheme 15.

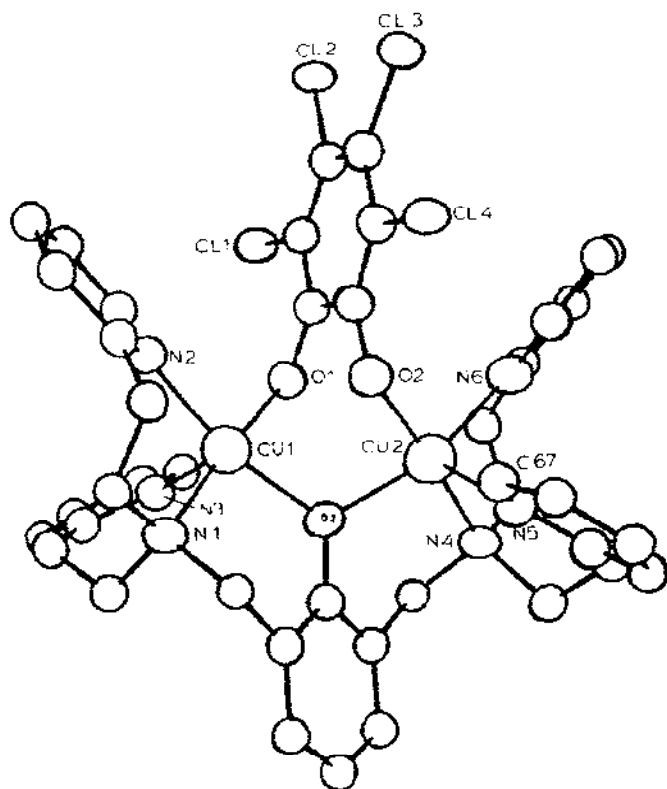
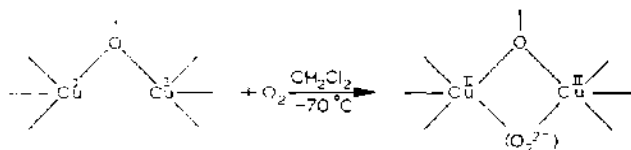


Fig. 56. Structure of tetrachloro-*o*-catecholate bridged dicopper(II) complex with *N,N,N',N'*-tetrakis[2-(2-pyridyl)ethyl] $\alpha,\alpha'$ -diamino-*m*-xylene. Reprinted with permission from ref. 109. Copyright 1986 American Chemical Society.

The structure of **C** [106] (Fig. 54) is composed of one discrete dication and two well-separated  $\text{PF}_6^-$  anions per asymmetric unit. The cation consists of two crystallographically independent but very similar copper(II) coordination environments in each dinuclear unit. Each copper ion is coordinated by the tertiary amine and two pyridine nitrogen atoms; the bridging-phenolate and hydroxide oxygen atoms complete the pentacoordination. The geometry around each copper is a tetragonal pyramid with two pyridine nitrogens occupying axial positions on opposite sides of the  $\text{Cu}_2\text{O}_2$  plane which is essentially planar.

The complex **E** [133] has been obtained by addition of **D**, containing  $\text{NaOH}$ , to  $[\text{Cu}(\text{CH}_3\text{CN})_4]\text{PF}_6$ . The structure of the cation is reported in Fig. 55. Each of the two crystallographically independent molecules in the asymmetric unit, consists of two four-coordinate copper(I) ions bonded to the amino nitrogen, to two pyridine nitrogens, and to a bridging phenoxo oxygen. The geometry about each copper(I) has been described as pyramidal, the basal plane being formed by the two pyridine donors and the oxygen atoms; the longer axial position is occupied by the tertiary amino nitrogen. The  $\text{Cu} \cdots \text{Cu}$  distances in the molecules are 3.619 and 3.715 Å, while the  $\text{Cu}-\text{O}-\text{Cu}$  angles are  $128^\circ$  and  $130^\circ$ . Reaction of this complex with oxygen is remarkable [106] (Scheme 16).

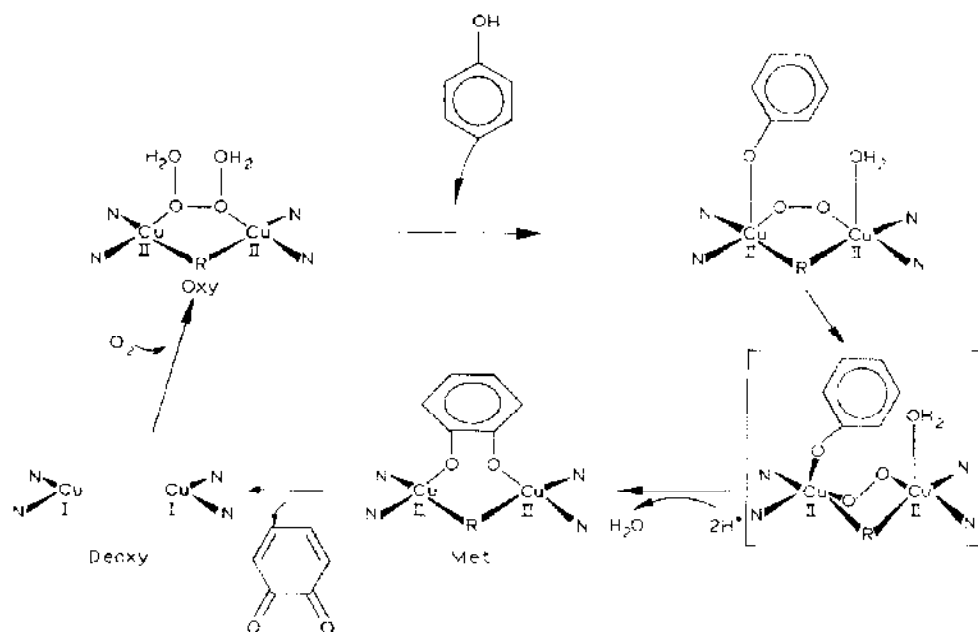


Scheme 16.

Manometric measurements at  $-78^\circ\text{C}$  indicated that 1 mol of dioxygen is taken up per mol of complex, and Raman and electronic spectra confirmed the formation of a copper peroxide complex. It was impossible to distinguish between  $\mu$ -1,1-,  $\mu$ -1,2- or terminally bound peroxide. The electronic spectrum of this copper(II)-peroxide complex, significantly different from that of oxyhemocyanin, suggests a different coordination mode for the peroxo-groups in the two cases.

The proposed mechanism of phenol oxygenation and oxidation by the tyrosinase coupled dinuclear copper site [108] is reported in Scheme 17. An intramolecular two-electron-transfer reaction produces the *o*-quinone product and regenerates the copper(I) center.

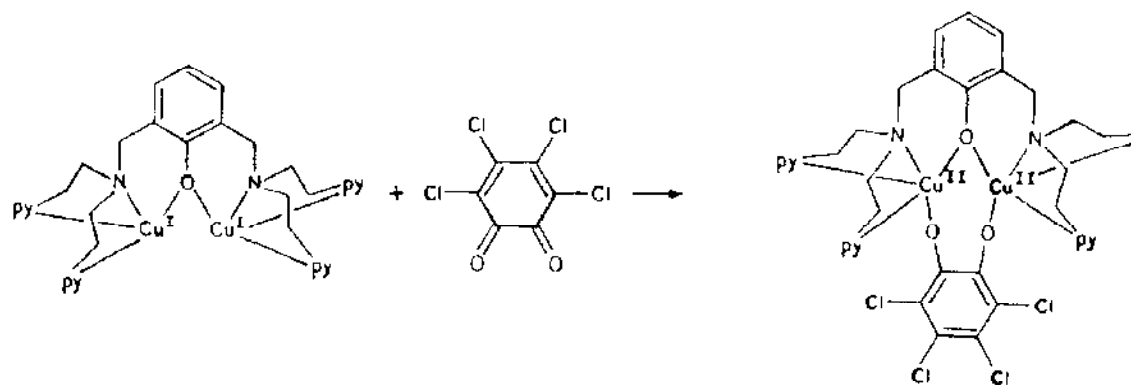
A dinuclear phenoxo-bridged copper(II) complex containing a catecholate bridging group has been obtained through the oxidation and coordination of tetrachloro-*o*-benzoquinone, according to Scheme 18 [109]. The copper(II)-tetrachloro-*o*-benzoquinone complex is stable in the presence of



Scheme 17.

$\text{O}_2$  and has a magnetic moment of  $\sim 1.5 \mu_{\text{B}}$ . In this complex the coordination geometry around each copper(II) has been described as square-based pyramidal with the amine nitrogen atoms, one pyridyl nitrogen atom, the bridging phenoxo oxygen and one of the catecholate oxygen donors forming the basal plane. The second pyridyl nitrogen atom occupies the apical position with a longer Cu–N distance. The Cu  $\cdots$  Cu distance is 3.248 Å. (Fig. 56).

This oxidation reaction is not a general route; 3,5-di-*t*-butyl-*o*-benzoquinone does not react with the copper(I) dinuclear complex in Scheme 18. The dinuclear phenoxo and hydroxo complex **C** of Scheme 15 catalytically



Scheme 18.



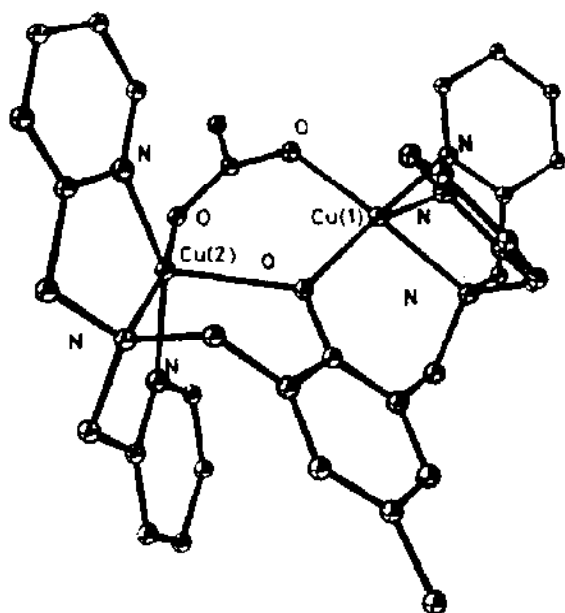


Fig. 57. Structure of  $\text{Cu}_2\text{L}_c(\text{CH}_3\text{COO})$ . Reprinted with permission from ref. 113.

oxidizes 3,5-di-*t*-butylcatechol to the corresponding 3,5-di-*t*-butylquinone. The catecholate complex, however, serves as a structural model for the probable intermediate in the catalytic oxidation of catechols by dicopper moieties [110–112].

More recently the ligands 2,6-bis(2-pyridylmethyl)-aminomethyl-4-methylphenol ( $\text{HL}_c$ ) and 2,6-bis(bis-2-(methylthio)ethylaminomethyl-4-methyl-

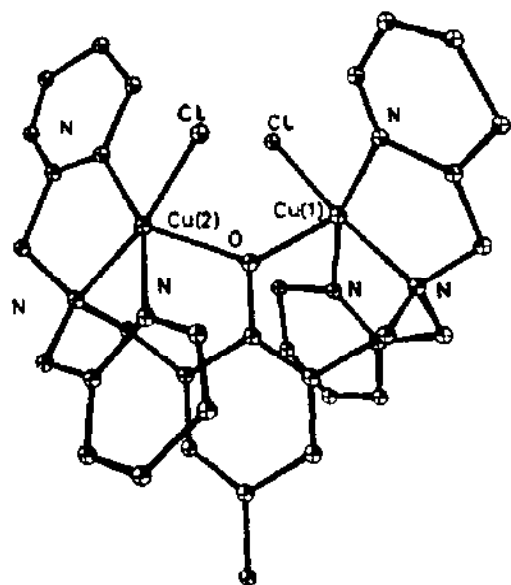


Fig. 58. Structure of  $\text{Cu}_2\text{L}_c(\text{Cl})_2$ . Reprinted with permission from ref. 113.

phenol ( $\text{HL}_d$ ) have been used for the preparation of a series of copper(II) complexes [113], and the structure of the copper(II) acetato and chloro complexes of  $\text{HL}_c$  and hydroxo complex of  $\text{HL}_d$  have been reported [113]. In the acetato complex the two copper(II) ions are bridged by the phenolate and the acetate groups as shown in Fig. 57. The two copper(II) ions have a different square pyramidal geometry; in one, the axial position is occupied by a pyridyl nitrogen, in the other by a bridging phenolate oxygen atom.

As a consequence the two copper-oxygen (phenolate) distances are different. Also for the chloro complex the coordination geometry around the copper atoms is square pyramidal. The two square pyramids share the phenolate oxygen at the axial position (Fig. 58). The two chlorine atoms are terminal. In this complex only a phenolate bridge is present.

In the hydroxo-complex shown in Fig. 59 the two copper(II) ions are bridged by phenolate and hydroxide oxygen atoms. The geometry around the copper atoms is trigonal bipyramidal.

As already reported in square-pyramidal copper(II) complexes, an unpaired electron is localized in the  $d_{x^2-y^2}$  orbital whose lobes are directed to the four ligand atoms in the basal plane. Therefore the exchange interaction between the copper(II) ions must be negligible when two square pyramids share an atom at their apices as with the chlorocomplex ( $-2J = 0 \text{ cm}^{-1}$ ). In the acetate complex, superexchange via the phenolate oxygen was considered negligible, the antiferromagnetism observed being due to a superexchange through the acetate bridge. This gives rise to a low antiferromagnetism ( $-2J = 80 \text{ cm}^{-1}$ ). For the hydroxo-complex  $-2J = 675 \text{ cm}^{-1}$  was observed. In this complex the unpaired electron is localized in the  $d_{z^2}$  orbital.

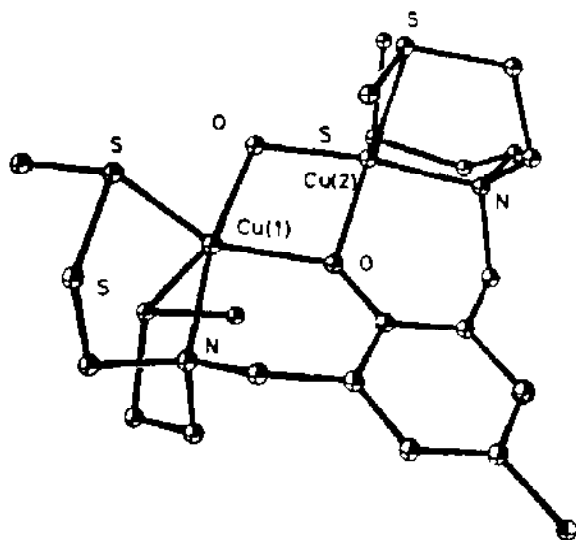


Fig. 59. Structure of  $\text{Cu}_2\text{L}_d(\text{OH})$ .

which is mainly spread along the trigonal axis of the trigonal bipyramid. Since the two trigonal axes interact at the hydroxide oxygen, substantial magnetic coupling is feasible through this pathway. The antiferromagnetic interaction through the phenolate is negligible; therefore the antiferromagnetism in the complex arises from the superexchange interaction through the bridging hydroxide ion. The Cu–O(hydroxide)–Cu angle of  $104.8^\circ$  is compatible with such an interaction. With  $HL_d$  double bridged ( $Cl^-$  and  $N_3^-$ ) complexes have also been obtained. These complexes have, at room temperature, a reduced magnetic moment, indicating the presence of an antiferromagnetic interaction between the copper(II) ions.

2,6-Bis{[bis(2-(1-pyrazolyl)ethyl)amino]methyl}-*p*-cresol gives, with  $Cu(BF_4)_2 \cdot 6H_2O$  in methanol, the dinuclear  $\mu$ -hydroxo complex [114] reported in Fig. 60. There is a significant difference in the two Cu–O(phenolate) bond lengths probably due to the different coordination geometry about each copper. For Cu(2) the geometry has been described as square pyramidal, for Cu(1) it is more distorted, bordering on trigonal bipyramidal. The copper–copper distance is 3.053 Å. Strong antiferromagnetic coupling was observed between the two copper(II) ions ( $-2J = 420 \text{ cm}^{-1}$ ) [114]. The unpaired electron on Cu(2), lies in the  $b_1(d_{x^2-y^2})$  orbital, while for Cu(1), which is considered trigonal bipyramidal, the unpaired electron resides in the  $a_1(d_{z^2})$  orbital. However whether the local symmetry of Cu(1) is te-

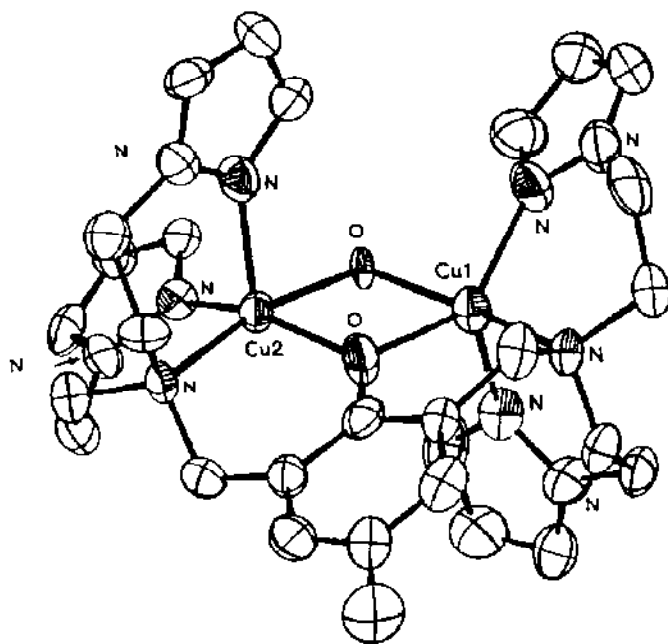
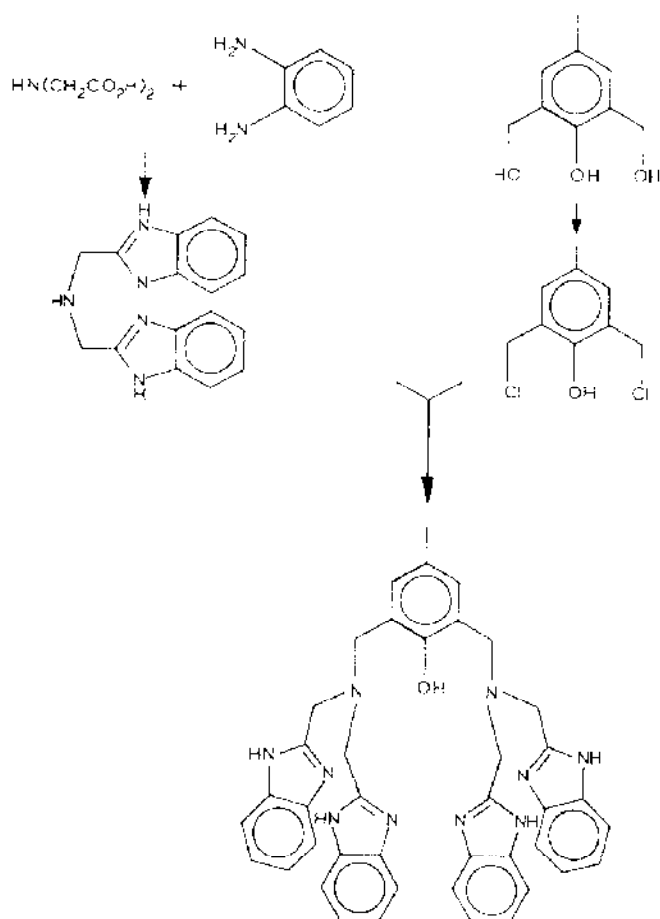


Fig. 60. The  $\mu$ -hydroxo-dicopper(II) complex with the ligand 2,6-bis{[bis-2-(1-pyrazolyl)ethyl]amino}methyl}-*p*-cresol. Reprinted with permission from ref. 114. Copyright 1986 American Chemical Society.

trigonal or trigonal bipyramid, the Cu(II) orbital containing the unpaired electron has a high electron density along the bond that forms the  $\mu$ -hydroxo bridge and provides a pathway for magnetic exchange. In addition, assuming that the pathway with the stronger magnetic coupling, i.e. the larger Cu–O–Cu angle, will predominate, a value of  $-450\text{ cm}^{-1}$  for the singlet–triplet separation can be obtained from the Hatfield–Hodgson tabulation [115,116].

A similar ligand has recently been prepared by the reaction pathway reported in Scheme 19 [117–119], copper(II) and cobalt(II) complexes being obtained, and the reaction with oxygen tested [117]. In the copper complex,  $\text{Cu}_2\text{L}_6(\text{H}_2\text{O})_5(\text{ClO}_4)_3$ , the copper atoms are in a non-equivalent distorted square pyramid; each of the copper atoms is coordinated to benzimidazole, a tertiary amine nitrogen and a water molecule; the bridging phenolate oxygen completes the coordination sphere [119]. The Cu  $\cdots$  Cu distance is 3.875 Å.



Scheme 19.

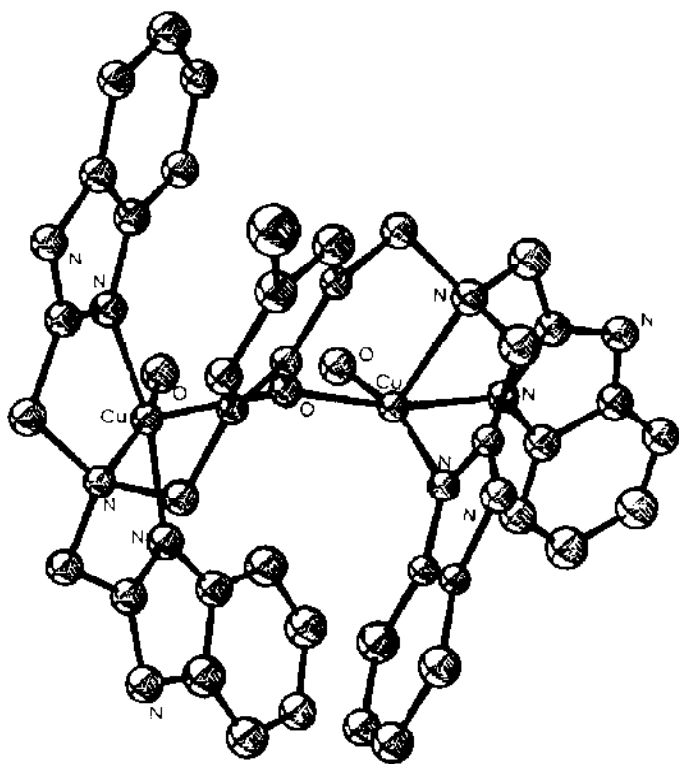


Fig. 61. Structure of the binuclear cation of the complex  $\text{Cu}_2\text{L}_c(\text{H}_2\text{O})_5(\text{ClO}_4)_3$ . Reprinted with permission from ref. 119.

This and related complexes [118] show a normal magnetic moment at room temperature. In the structure, disordering of solvent molecules and perchlorate anions precludes high accuracy in the structure determination (Fig. 61).

#### C. REDOX PROPERTIES IN NATURAL AND SYNTHETIC COMPOUNDS

Interest in the electrochemical behaviour of dinuclear copper complexes arises from metalloprotein chemistry. "Type 3" copper proteins contain a coupled dinuclear copper active site, involved in oxidoreductive biological functions, able to perform multicharge transfers at largely positive potentials. For example, in Table 1 the redox potentials of two "Type 3" copper

TABLE 1

Standard redox potentials (mV, vs. N.H.E.) of "Type 3" copper centers in Laccases <sup>a</sup>

<i>Polyporus versicolor</i>	+ 782
<i>Rhus vernicifera</i>	+ 434

<sup>a</sup> From ref. 120.

centres in the two-electron acceptor laccases are reported [120].

The electrochemistry of some classes of dicopper complexes has recently been reviewed [121], but a more systematic survey can help researchers in this area, and also in devising strategy in the synthesis of compounds with foreseeable redox properties.

Electrochemists use different reference electrodes, thus we have tried here to unify potential values by reporting them (unless otherwise specified) versus the normal hydrogen electrode (N.H.E.), according to known scales of reference electrode potentials [122].

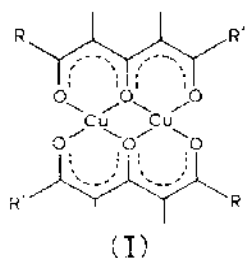
In addition we have considered, as is usual, the ferrocenium/ferrocene couple to be located at +0.40 V versus N.H.E., independently of the solvent [123] \*; although this assumption introduces some minor error due to unconsidered junction potentials, it is useful to have comparable potential values within the different compounds.

#### D. ELECTROCHEMISTRY OF DINUCLEAR COMPLEXES WITH SITES HAVING THE SAME DONOR SET

Dinuclear complexes having the same coordination donor set around each metal centre are here further subdivided between those having adjacent chambers and those having non-adjacent chambers; strictly speaking these latter compounds should not be covered in this topic devoted to "compartmental ligands".

##### (i) *Adjacent $O_2-O_2-O_2$ donor set*

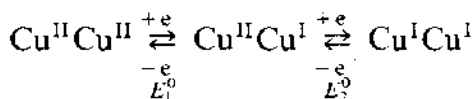
The first class of copper(II) compounds showing a  $M_2O_6$  unit, studied from the electrochemical viewpoint, belongs to the 1,3,5-triketonato chelates. I.



The electrochemistry of these complexes has been ascertained with some difficulty. In a first approach it was reported that these dicopper(II) com-

\* In fact, we disagree with this widely accepted extrathermodynamic assumption, since in our experience ferrocene is oxidized in various nonaqueous solvents at a mean value of +0.4 V versus saturated calomel electrode (SCE).

plexes in DMF solution undergo a two electron reduction in a single step, according to the sequence



with the two reversible one-electron charge transfers occurring at  $E_1^0 = E_2^0$  [19,20]. Figure 62 shows the relevant typical cyclic voltammetric response. This result was quite unexpected. In fact, even if the two-electron process does not proceed through two stepwise one electron changes at different potentials, it must likely be accompanied by a stereochemical change from square planar copper(II) geometry to distorted tetrahedral copper(I) geometry. In electrochemical terms this should involve an ECEC, or EEC mechanism (with C indicating the chemical (in this case stereochemical) complication following the charge transfer E), rather than a simple EE mechanism. At any rate, it is possible that the conformational change is too fast to be detected in the timescale of fast voltammetric techniques, i.e. the structural reorganization occurs concomitant with the charge transfer [124]. It seems likely that, according to the Marcus theory, the activation barrier to electron transfer is increased, slowing down the rate of heterogeneous charge transfer, i.e. causing a marked deviation from the pure reversible character of the charge transfer.

Later, it was shown that the previous results must be considered not as

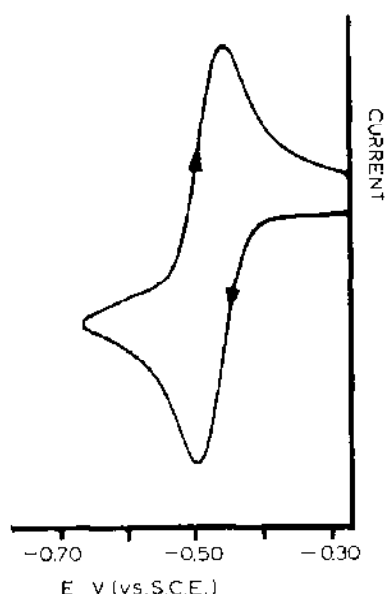


Fig. 62. Cyclic voltammogram of I ( $R = C_6H_5$ ,  $R' = CH_3$ ) in DMF solution containing tetraethylammonium perchlorate as supporting electrolyte. Hanging mercury drop indicator electrode [20].

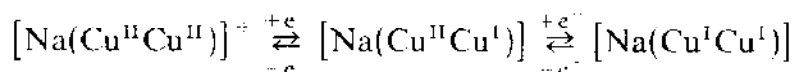
TABLE 2

Redox potentials (V) for the single two-electron reduction of I derivatives in DMF, in the presence and absence of Na<sup>+</sup> ions <sup>a</sup>

R	R'	R''	$E_{(Cu^{II}Cu^{II})/(Cu^ICu^I)}$	
			Na <sup>+</sup> absent	Na <sup>+</sup> present
CH <sub>3</sub>	C <sub>6</sub> H <sub>5</sub>	H	-0.58	-0.24
C <sub>6</sub> H <sub>5</sub>	C <sub>6</sub> H <sub>5</sub>	H	-	-0.22
CH <sub>3</sub>	<i>p</i> -CH <sub>3</sub> OC <sub>6</sub> H <sub>4</sub>	H	-	-0.41
<i>p</i> -CH <sub>3</sub> OC <sub>6</sub> H <sub>4</sub>	<i>p</i> -CH <sub>3</sub> OC <sub>6</sub> H <sub>4</sub>	H	-	-0.28
C <sub>6</sub> H <sub>5</sub>	C(CH <sub>3</sub> ) <sub>3</sub>	H	-	-0.25
CH <sub>3</sub>	C(CH <sub>3</sub> ) <sub>3</sub>	H	-0.63	0.33

<sup>a</sup> From refs. 19, 20, 47, 49 and 125.

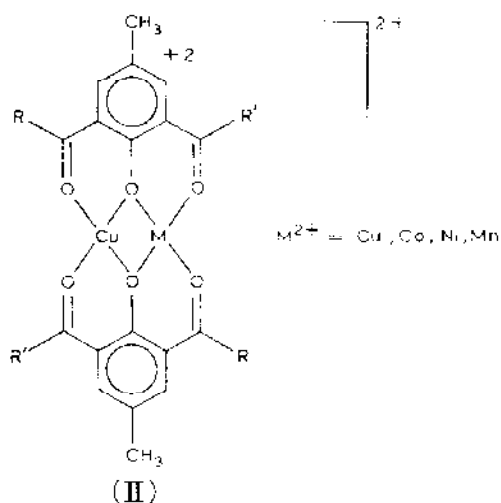
the reduction of the starting triketonato complexes, but as the reduction of the relevant sodium ion-paired complexes [47,49,125]



In addition it was confirmed that in the absence of Na<sup>+</sup> ions the single-stepped two-electron charge transfer is quasireversible in character. It seems surprising that conformational changes, affecting the rate of charge transfer, do not also occur in the reduction of the ion-paired complexes.

Table 2 reports the formal electrode potentials of the single two-electron redox change for the various triketonate complexes, both in the presence and absence of Na<sup>+</sup> ions.

Another series of compounds showing a M<sub>2</sub>O<sub>6</sub> unit comes from copper(II) complexes of 4-methyl-2,6-di(acylbenzoyl)phenol, II [21,126]. It is interesting to note that while the homodinuclear copper(II) species reduce in a single





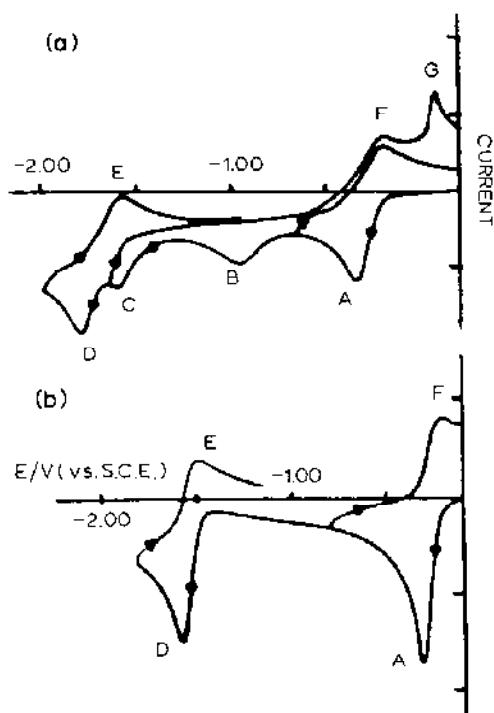
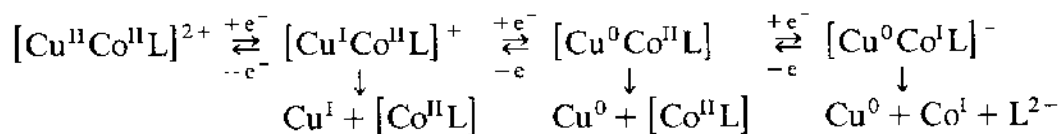


Fig. 63. Cyclic voltammograms recorded at mercury electrode for the heterodinuclear compound ( $\text{Cu}^{\text{II}}\text{-Co}^{\text{II}}$ ) in: (a)  $\text{MeCN-}[\text{NEt}_4]\text{ClO}_4$  ( $0.1 \text{ mol dm}^{-3}$ ); (b)  $\text{DMSO-}[\text{NEt}_4]\text{ClO}_4$  ( $0.1 \text{ mol dm}^{-3}$ ) [126].

two-electron step [21], the heterodinuclear complexes reduce in two sequential one-electron processes at different potentials [126]. Figure 63 schematizes the cyclic voltammetric responses recorded from the heterodinuclear  $\text{Cu}^{\text{II}}\text{Co}^{\text{II}}$  species in (a) both acetonitrile (MeCN) and (b) dimethylsulphoxide (DMSO) solutions and shows the often neglected influence of the solvent on the redox behaviour of dinuclear compounds.

In both solvents the two redox couples A/F and D/E may be assigned to the  $\text{Cu}^{\text{II}}/\text{Cu}^{\text{I}}$  and  $\text{Co}^{\text{II}}/\text{Co}^{\text{I}}$  redox couples, respectively. These redox changes are quasi-reversible in character, and kinetically coupled to decomplexation of the electrogenerated metal(I) centres. In MeCN the voltammetric picture is complicated by the presence of the adsorption peak B and by the cathodic step C, which in the reverse scan causes the appearance of the characteristic stripping peak G, due to redissolution of electrodeposited copper metal. A reliable explanation assumes that in the less coordinating MeCN solvent the following mechanism takes place:



In the more coordinating DMSO solvent the electrode process is simplified

TABLE 3

Formal electrode potentials (V) of the charge transfers observed in the cathodic reduction of homo- and heterodinuclear derivatives **II**

M	R	R'	$E_{(Cu^{II}M^{II}) \rightarrow Cu^I M^{II}}$	$E_{(Cu^I M^{II}) \rightarrow Cu^I M^I}$	Solvent	Ref.
Cu	H	H	+ 0.20	+ 0.20	DMF	21
Cu	CH <sub>3</sub>	CH <sub>3</sub>	+ 0.19	+ 0.19	DMF	21
Cu	n-C <sub>3</sub> H <sub>7</sub>	n-C <sub>3</sub> H <sub>7</sub>	+ 0.19	+ 0.19	DMF	21
Cu	C <sub>6</sub> H <sub>5</sub>	C <sub>6</sub> H <sub>5</sub>	+ 0.20	+ 0.20	DMF	21
Cu	C <sub>6</sub> H <sub>5</sub>	CH <sub>3</sub>	+ 0.20	+ 0.20	DMF	21
Ni	CH <sub>3</sub>	CH <sub>3</sub>	- 0.03	- 1.60	MeCN	126
Ni	CH <sub>3</sub>	CH <sub>3</sub>	- 0.03	- 1.31	DMSO	126
Co	CH <sub>3</sub>	CH <sub>3</sub>	- 0.04	- 1.54	MeCN	126
Co	CH <sub>3</sub>	CH <sub>3</sub>	- 0.03	- 1.31	DMSO	126
Mn	CH <sub>3</sub>	CH <sub>3</sub>	- 0.03	- 1.65	MeCN	126
Mn	CH <sub>3</sub>	CH <sub>3</sub>	0.02	- 1.49	DMSO	126

by the stabilizing effect of the solvent on the electrogenerated copper(I) centre

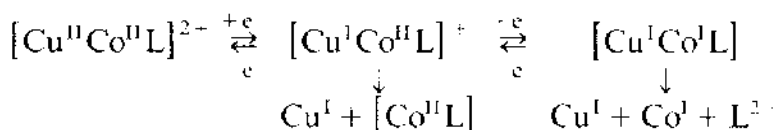


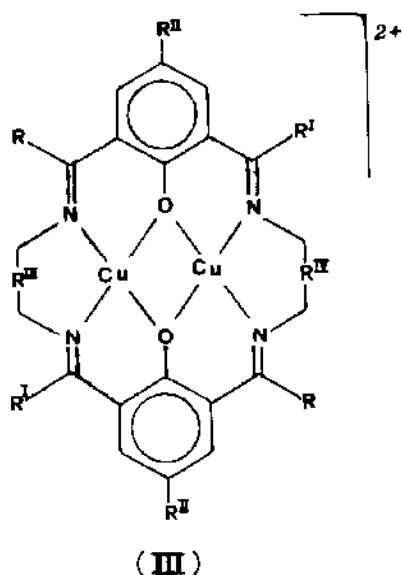
Table 3 summarizes the redox potentials of the charge-transfer involved in the cathodic reduction of type **II** derivatives.

A comparison between the homodinuclear copper(II) complexes **II** and **I** shows that the former reduce at potentials significantly less negative than the latter. This has been attributed not only to the fact that compounds **II** are cationic and hence favour electrostatically the addition of electrons, but also to their tetrahedrally distorted geometry (with respect to the planar geometry of triketonato complexes) which thermodynamically favours access to copper(I) species. For these bimetallomers, homodinuclear Cu–Cu species are more easily reducible than heterodimetal Cu–M species.

Indeed, this behaviour is quite common to other dinuclear complexes, reported below, and can be explained both on the basis of resonance-stabilized, delocalized mixed-valent Cu<sup>II</sup>Cu<sup>I</sup> species [127,128], and on the basis of electronic synergistic interactions accompanying the redox chemistry of the dinuclear compounds [83].

#### (ii) Adjacent N<sub>2</sub>–O<sub>2</sub>–N<sub>2</sub> donor set

A great deal of work was devoted to dinuclear complexes in which each metal site is coordinated to a N<sub>2</sub>O<sub>2</sub> atom set. The redox behaviour of



compounds **III**, [36,37,39,40,88], has been investigated thoroughly. In all cases, these dinuclear copper(II) derivatives undergo two one-electron successive reversible, or quasireversible, cathodic charge transfers at different potentials, indicating that the mixed-valent  $\text{Cu}^{\text{II}}\text{Cu}^{\text{I}}$  species is stable, its stability increasing with the increasing separation between the potential of the two reduction steps. In fact the difference  $\Delta E$  between the standard electrode potentials of the  $\text{Cu}^{\text{II}}\text{Cu}^{\text{II}}/\text{Cu}^{\text{II}}\text{Cu}^{\text{I}}$  and  $\text{Cu}^{\text{II}}\text{Cu}^{\text{I}}/\text{Cu}^{\text{I}}\text{Cu}^{\text{I}}$  redox couples is a measure of the comproportionation constant,  $K_{\text{com}}$

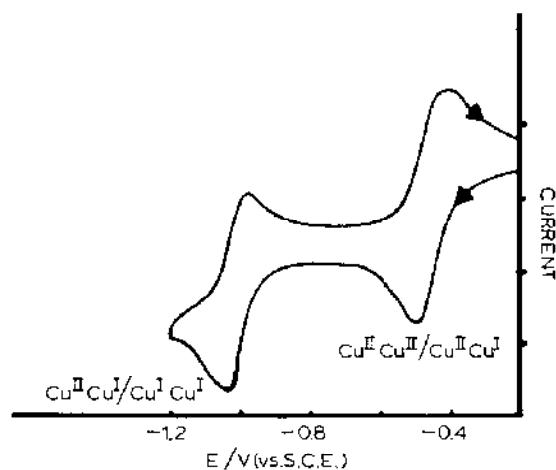
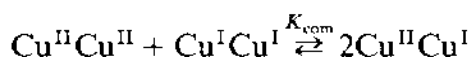
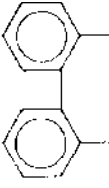
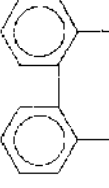
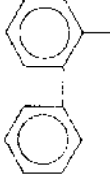


Fig. 64. Cyclic voltammetric response typical for the reduction of compounds **III**. Present compound  $\text{R} = \text{R}' = \text{C}_6\text{H}_5$ ,  $\text{R}'' = \text{CH}_3$ ,  $\text{R}''' = \text{R}^{\text{IV}} = (\text{CH}_2)_5$ ;  $\text{MeCN} - [\text{NEt}_4]\text{ClO}_4$  (0.1 mol  $\text{dm}^{-3}$ ) solution. Hanging mercury drop working electrode. Scan rate:  $0.05 \text{ V s}^{-1}$  [88].

TABLE 4

Redox potentials (V) for the two successive  $\text{Cu}^{\text{II}}\text{Cu}^{\text{II}}/\text{Cu}^{\text{II}}\text{Cu}^{\text{I}}$  and  $\text{Cu}^{\text{II}}\text{Cu}^{\text{I}}/\text{Cu}^{\text{I}}\text{Cu}^{\text{I}}$  one-electron reduction steps displayed by dicopper(II) complexes of type III

R	R'	R <sup>II</sup>	R <sup>III</sup>	R <sup>IV</sup>	( $E^{\text{III}}$ ) <sup>1</sup>	( $E^{\text{IV}}$ ) <sup>2</sup>	Solvent	Ref.
H	H	CH <sub>3</sub>	CH <sub>3</sub> CH <sub>2</sub> CH <sub>2</sub>	CH <sub>3</sub> CH <sub>2</sub> CH <sub>2</sub>	-0.52	-0.91	DMF	36, 37
H	H	CH <sub>3</sub>	CH <sub>3</sub> CH <sub>2</sub> CH <sub>2</sub>	CH <sub>3</sub> CH <sub>2</sub> CH <sub>2</sub>	0.27	-0.61	DMF	88
H	H	CH <sub>3</sub>	CH <sub>3</sub> CH <sub>2</sub> CH <sub>2</sub>	CH <sub>3</sub> CH <sub>2</sub> CH <sub>2</sub>	0.22	-	MeCN	88
CH <sub>3</sub>	CH <sub>3</sub>	CH <sub>3</sub>	CH <sub>3</sub> CH <sub>2</sub> CH <sub>2</sub>	CH <sub>3</sub> CH <sub>2</sub> CH <sub>2</sub>	-0.22	-0.99	MeCN	88
CH <sub>3</sub>	CH <sub>3</sub>	CH <sub>3</sub>	CH <sub>3</sub> CH <sub>2</sub> CH <sub>2</sub>	CH <sub>3</sub> CH <sub>2</sub> CH <sub>2</sub>	-0.16	0.92	MeCN	39
CH <sub>3</sub>	CH <sub>3</sub>	CH <sub>3</sub>	CH <sub>3</sub> (CH <sub>2</sub> ) <sub>2</sub> CH <sub>2</sub>	CH <sub>3</sub> (CH <sub>2</sub> ) <sub>2</sub> CH <sub>2</sub>	-0.05	-	MeCN	39
n-C <sub>3</sub> H <sub>7</sub>	n-C <sub>3</sub> H <sub>7</sub>	CH <sub>3</sub>	CH <sub>3</sub> CH <sub>2</sub> CH <sub>2</sub>	CH <sub>3</sub> CH <sub>2</sub> CH <sub>2</sub>	-0.23	-1.01	MeCN	88
C <sub>6</sub> H <sub>5</sub>	C <sub>6</sub> H <sub>5</sub>	CH <sub>3</sub>	CH <sub>3</sub> CH <sub>2</sub> CH <sub>2</sub>	CH <sub>3</sub> CH <sub>2</sub> CH <sub>2</sub>	-0.23	-0.78	MeCN	88
C <sub>6</sub> H <sub>5</sub>	CH <sub>3</sub>	CH <sub>3</sub>	CH <sub>3</sub> CH <sub>2</sub> CH <sub>2</sub>	CH <sub>3</sub> CH <sub>2</sub> CH <sub>2</sub>	-0.24	-0.94	MeCN	88
H	H	C(CH <sub>3</sub> ) <sub>3</sub>	CH <sub>3</sub> CH <sub>2</sub> CH <sub>2</sub>	CH <sub>3</sub> CH <sub>2</sub> CH <sub>2</sub>	-0.53	-0.92	DMF	40
H	H	C(CH <sub>3</sub> ) <sub>3</sub>	CH <sub>3</sub> C(CH <sub>3</sub> ) <sub>2</sub> CH <sub>2</sub>	CH <sub>3</sub> C(CH <sub>3</sub> ) <sub>2</sub> CH <sub>2</sub>	-0.55	0.94	DMF	40
H	H	C(CH <sub>3</sub> ) <sub>3</sub>	CH <sub>3</sub> (CH <sub>2</sub> ) <sub>2</sub> CH <sub>2</sub>	CH <sub>3</sub> (CH <sub>2</sub> ) <sub>2</sub> CH <sub>2</sub>	-0.33	-0.81	DMF	40
H	H	C(CH <sub>3</sub> ) <sub>3</sub>			-0.23	-0.64	DMF	40
H	H	C(CH <sub>3</sub> ) <sub>3</sub>	CH <sub>3</sub> CH <sub>2</sub> CH <sub>2</sub>	CH <sub>3</sub> C(CH <sub>3</sub> ) <sub>2</sub> CH <sub>2</sub>	-0.54	0.94	DMF	40
H	H	C(CH <sub>3</sub> ) <sub>3</sub>	CH <sub>3</sub> CH <sub>2</sub> CH <sub>2</sub>		0.38	0.82	DMF	40
H	H	C(CH <sub>3</sub> ) <sub>3</sub>	CH <sub>3</sub> CH <sub>2</sub> CH <sub>2</sub>	CH <sub>3</sub> (CH <sub>2</sub> ) <sub>2</sub> CH <sub>2</sub>	0.40	0.92	DMF	40

through the relation

$$K_{\text{com}} = \exp\left(-\frac{F}{RT} \Delta E\right)$$

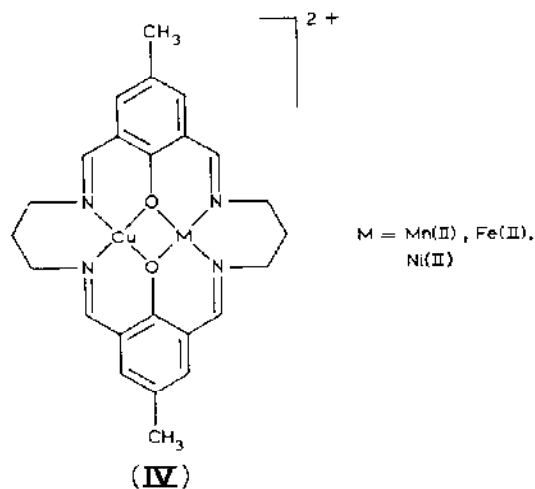
It has been suggested [36,37] that the value of  $K_{\text{com}}$  can be correlated to the extent of delocalization in the mixed valent species, according to the Robin–Day classification [129]. Valence-trapped “Class I” compounds should have  $K_{\text{com}} \leq 4$ ; slightly delocalized “Class II” compounds should have  $K_{\text{com}}$  ranging from 4 to  $10^2 - 10^3$ ; completely delocalized “Class III” compounds should have very high  $K_{\text{com}}$  values (from  $\sim 10^6$  to  $\sim 10^{38}$ ). These conclusions must however be viewed cautiously [83].

A cyclic voltammetric response typical for type **III** compounds is reported in Fig. 64, together with the relevant assignment for the sequential one-electron charge transfers. Table 4 summarizes the redox potentials for all dicopper(II) complexes of type **III**.

Discrepancies between potentials reported from different authors for same compounds are largely due to the previously cited assumption that ferrocene oxidizes at +0.4 V versus N.H.E. in every solvent.

Substituent electronic effects show that electron-donating substituents stabilize the 2+ copper oxidation state, while electron-withdrawing substituents favour access to the 1+ oxidation state. In addition the more flexible the cavity, through control of the diamine linkage, the more easily reducible are the complexes, because of a more favoured tetrahedral distortion around the electrogenerated copper(I) centre.

Heterodinuclear complexes of type **IV**, which are simply a form of the more general skeleton **III**, have been studied electrochemically [127,128]. All



complexes display a one-electron  $\text{Cu}^{\text{II}}\text{M}^{\text{II}}/\text{Cu}^{\text{I}}\text{M}^{\text{II}}$  step, well distinct from the oxidation or reduction of the second metal centre. Table 5 summarizes

TABLE 5

Redox potentials (V) for charge transfers observed for homodinuclear and heterodinuclear complexes of type IV<sup>a</sup>

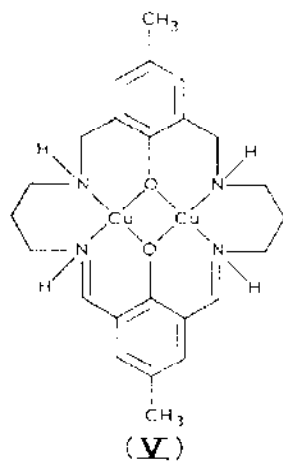
M	$E_{(Cu^{II}M^{II} \cdot Cu^{I}M^{II})}^{0/1}$	$E_{(Cu^{II}M^{II} \cdot Cu^{I}M^{I})}^{0/1}$	$E_{(Cu^{II}M^{II} \cdot Cu^{II}M^{III})}^{0/1}$	Solvent
Cu	-0.54	—	—	CH <sub>3</sub> OH
Cu	-0.52	0.91	—	DMF
Mn	-0.68	—	+0.55	DMF
Mn	-0.55	—	+0.70	CH <sub>3</sub> OH
Fe	0.66	—	+0.25	DMF
Ni	-0.69	-1.16	—	DMF

<sup>a</sup> From refs. 36, 37.

the redox potentials relevant to complexes IV, together with those of the corresponding homodinuclear complexes [36,37].

It has been pointed out that the potential for the copper(II)/copper(I) couple is not appreciably affected by the nature of the second metal centre, unless copper itself is the second metal; in this case reduction is easier, as discussed above.

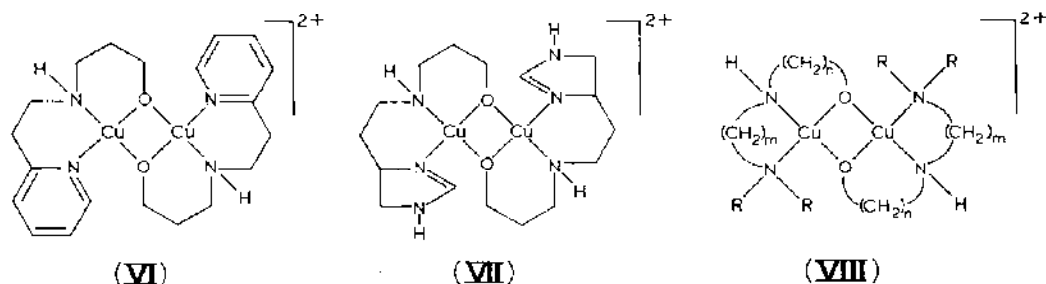
The diazadiamino copper(II) complex V, in MeCN, reduces in two separate one-electron quasireversible charge transfers at -0.28 V and -0.54 V, respectively [88].



Comparison with the corresponding unsaturated compounds (see Table 4) shows that the partial saturation of the ligands disfavors slightly the Cu<sup>II</sup>Cu<sup>II</sup>/Cu<sup>II</sup>Cu<sup>I</sup> step, while notably favouring access to the Cu<sup>I</sup>Cu<sup>I</sup> species, so destabilizing the mixed-valent Cu<sup>II</sup>Cu<sup>I</sup> species.

A further class of compounds showing the N<sub>2</sub>-O<sub>2</sub>-N<sub>2</sub> donor atom set, recently reviewed [130], is that constituted by alkoxo-bridged linear chain tridentate complexes VI–VIII.

Interestingly some of these dicopper(II) compounds are reduced in a



single  $\text{Cu}^{\text{II}}\text{Cu}^{\text{II}}/\text{Cu}^{\text{I}}\text{Cu}^{\text{I}}$  two-electron step or in two separate stepwise one-electron steps, depending upon the solvent. As an example, Fig. 65 shows the cyclic voltammetric response obtained from VI ( $R = \text{C}_2\text{H}_5$ ,  $m = 3$ ,  $n = 2$ ) in DMF and MeCN solvents.

Note the marked quasireversible character of the single two-electron step in DMF, as well as the chemical complications (likely decomplexation of electrogenerated copper(I)) following the second one-electron step in MeCN (as shown by the  $(i_p)^a/(i_p)^c$  ratio  $\ll 1$ ).

Whether adjacent binuclear complexes reduce in a single two-electron step or in two separated one-electron steps, it is clear that the solvent plays, in our opinion, a fundamental, but until now almost unrecognized, role.

Table 6 summarizes the redox potentials of compounds VI–VIII [130–132].

Potential data reported in Table 6 refer to electrochemistry in solutions containing  $[\text{NEt}_4]\text{ClO}_4$  as supporting electrolyte; in fact it was reported that the presence of different anions (like  $\text{BF}_4^-$  or  $\text{PF}_6^-$ ) in some cases splits the

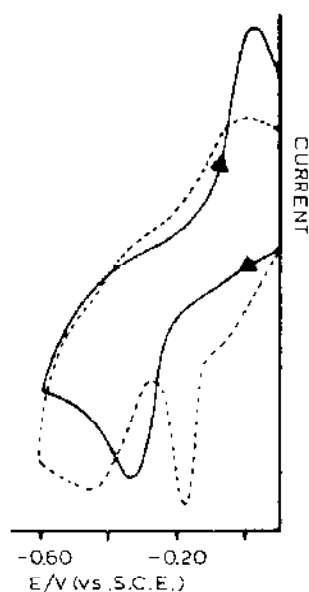


Fig. 65. Cyclic voltammograms recorded on one of the compounds VI ( $m = 3$ ,  $n = 2$ ,  $R = \text{C}_2\text{H}_5$ ) in: (—) DMF- $[\text{NEt}_4]\text{ClO}_4$  ( $0.1 \text{ mol dm}^{-3}$ ); (---) MeCN- $[\text{NEt}_4]\text{ClO}_4$  ( $0.1 \text{ mol dm}^{-3}$ ). Hanging mercury drop working electrode. Scan rate  $0.2 \text{ V s}^{-1}$  [131].

TABLE 6  
Redox potentials (V) for the alkoxo-bridged linear chain tridentate copper(II) complexes VI-VIII<sup>a</sup>

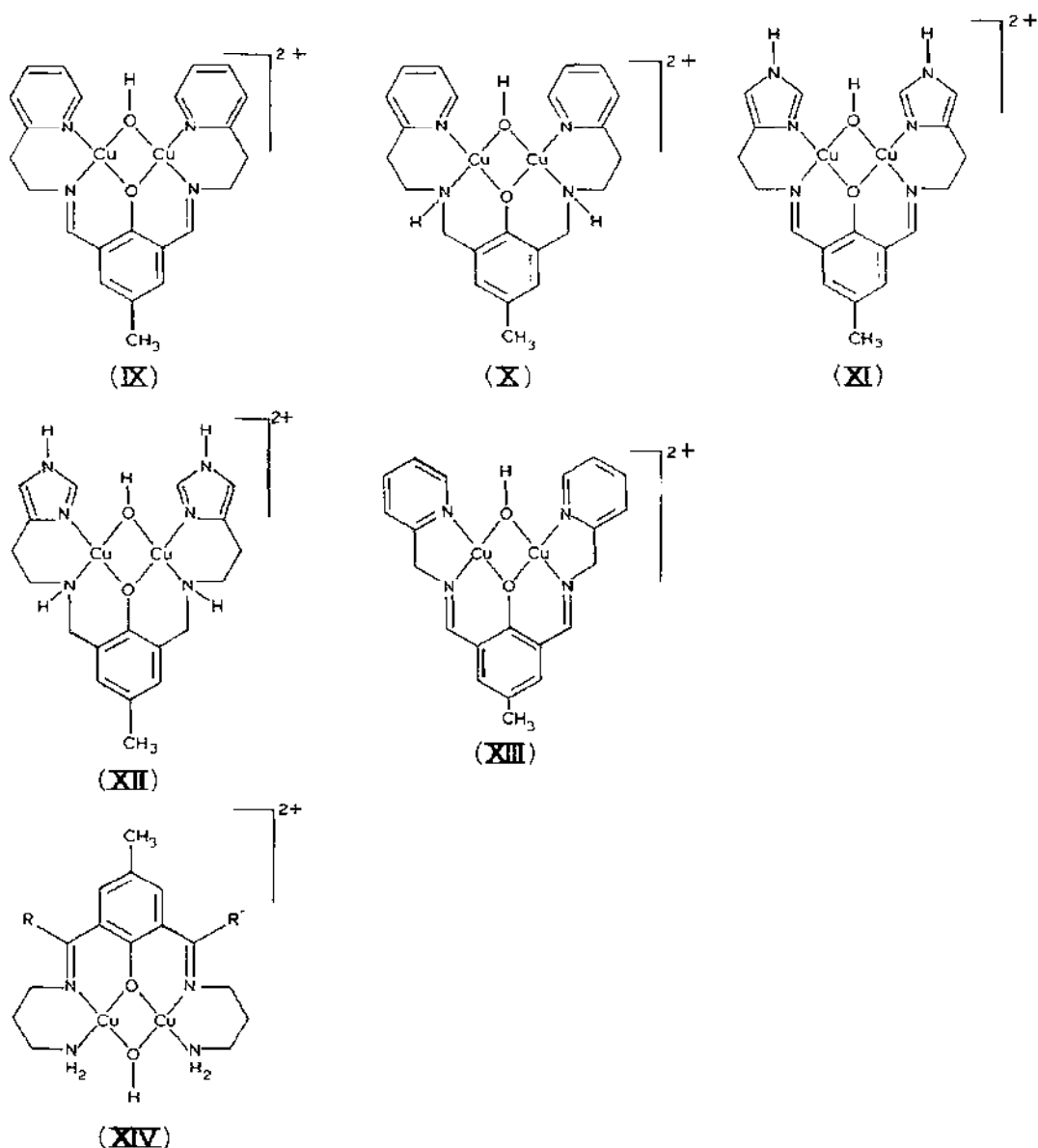
Compound	<i>n</i>	<i>R</i>	Solvent	CH <sub>3</sub> OH		
			DMF	MeCN	CH <sub>3</sub> OH	
			$E_{\text{Cu}^{\text{II}}/\text{Cu}^{\text{I}}}^{\text{ox}}$	$E_{\text{Cu}^{\text{II}}/\text{Cu}^{\text{I}}}^{\text{ox}}$	$E_{\text{Cu}^{\text{II}}/\text{Cu}^{\text{I}}}^{\text{ox}}$	$E_{\text{Cu}^{\text{II}}/\text{Cu}^{\text{I}}}^{\text{ox}}$
VI	3	2 H	0.26	-0.32	-0.32	
	3	2 CH <sub>3</sub>	-0.07	0.00	-0.21	0.15
	3	2 C <sub>2</sub> H <sub>5</sub>	+0.03	+0.07	-0.12	
	3	3 H			0.41	-0.92
	2	3 C <sub>2</sub> H <sub>5</sub>			-0.29	-0.29
VII			-0.19			
VIII			0.06			

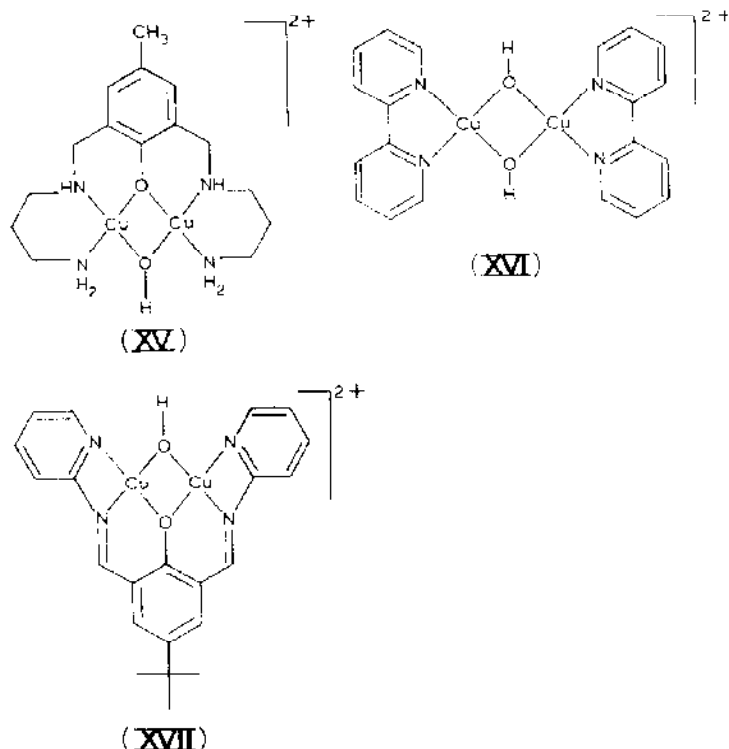
<sup>a</sup> From refs. 130-132.



single two-electron step into two very close one-electron steps. We neglect this aspect because it complicates the general picture, and does not affect the mean potential values; however, we point out another unexpected factor affecting the  $\text{Cu}^{\text{II}}\text{Cu}^{\text{II}}/\text{Cu}^{\text{I}}\text{Cu}^{\text{I}}$  reduction pathway. Examining Table 6, it is difficult to explain here (and as we shall see later in subsequent studies from these authors reported in D(iv) [130–132]) why R groups with increasing electron-donating ability facilitate the reduction steps.

A particular class of dicopper complexes coordinated to a  $\text{N}_2\text{--O}_2\text{--N}_2$  donor set is constituted by hydroxo-bridged complexes. The redox properties of compounds **IX**–**XVII** have been studied by electrochemical tech-





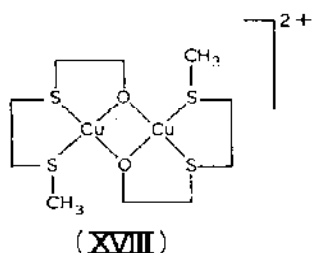
niques [77,78,87,133,134]. Generally these types of derivatives show irreversible, ill-defined cathodic reductions [77,78,87]. This behaviour has been attributed to the poor ability of the hydroxo-bridge to bind the electrogenerated copper(I) centres. In fact, in the presence of pyrazole, complexes **IX** and **XIII** display two separated well-defined one-electron reduction steps in the potential range from  $-0.1$  V to  $-0.5$  V, in DMF solution [77].

Compound **XVI** is however reduced in two distinct one-electron quasireversible charge transfers at  $+0.28$  V and  $-0.11$  V, respectively [133]. This easy reduction, comparable with that of compounds **II**, has been attributed to the high flexibility induced by the presence of two bridging hydroxyl groups, which support the likely tetrahedral rearrangement required to stabilize the electrogenerated copper(I) centres.

Even if this marked flexibility cannot be invoked in the case of compound **XVII**, it however reduces through two close one-electron quasireversible charge transfers at  $+0.39$  V and  $+0.22$  V, respectively [134]. There is indeed no structural reason accounting for the difference in redox behaviour between the notably similar compounds **IX** and **XVII**, but the solvents employed in the electrochemical studies (MeCN for **IX**, DMF for **XVII**).

### (iii) Adjacent $S_2-O_2-S_2$ donor set

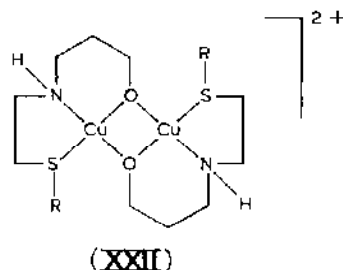
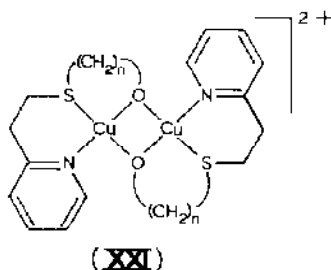
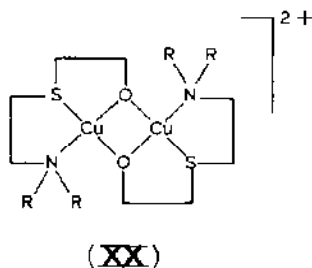
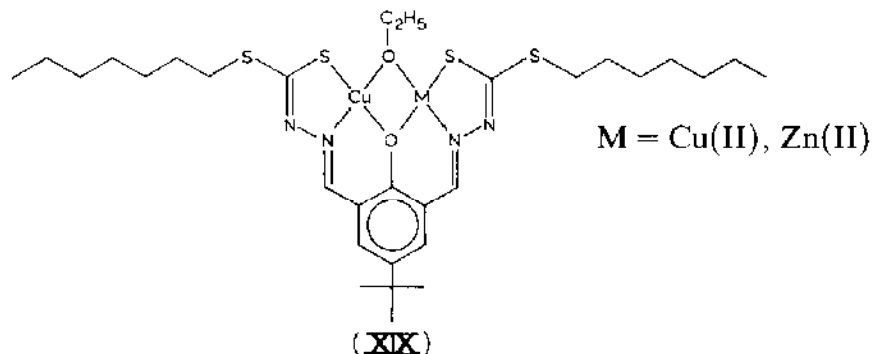
The alkoxo-bridged dicopper(II) compound **XVIII** containing thioether sulphur atoms, has been characterized electrochemically [130]. In DMF it



reduces to the corresponding  $\text{Cu}^{\text{I}}\text{Cu}^{\text{I}}$  species in a single two-electron step at +0.39 V, which in comparison with the related  $\text{N}_2\text{-O}_2\text{-N}_2$  **VI–VIII** derivatives, denotes that the substitution of sulphur for nitrogen makes the reduction notably easier.

(iv) *Adjacent NS–O<sub>2</sub>–SN donor set*

The redox properties of a series of dicopper(II) derivatives having mixed nitrogen–sulphur coordination of the type NS–O<sub>2</sub>–SN have been characterized [83,130].



The dicopper(II) complex **XIX** is reduced in two separate one-electron quasireversible steps, both in DMF and  $\text{CH}_2\text{Cl}_2$  solutions [83]. EPR data on the electrogenerated  $\text{Cu}^{\text{II}}\text{Cu}^{\text{I}}$  species prompted the authors to criticize conclusions on the extent of delocalization in mixed-valent species, when electrochemically evaluated through the above reported  $K_{\text{com}}$  [36,37], particularly in polar solvents, in which either variation of coordination number, or changes in geometry of the electroactive centres may occur.

The cathodic reduction of compounds **XXI** and **XXII** proceeds through a single two-electron step [130], while derivatives **XX** are reduced in two distinct one-electron steps. This difference in behaviour has been attributed to the fact that cationic compounds **XX**, prepared only with Cl<sup>-</sup> or Br<sup>-</sup> anions, are thought, on the basis of their conductivity, to have two inequivalent copper(II) moieties, i.e. a five coordinate high potential Cu(II) centre and a four-coordinate low-potential Cu(II) centre, according to

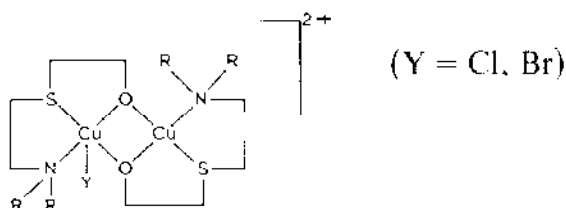


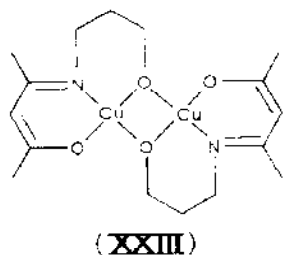
Table 7 summarizes potential data characterizing this type of compound coordinated to a NS·O<sub>2</sub>–NS donor set. The first reduction step of compound **XIX**, for homodinuclear copper(II) species is easier than that of the corresponding heterodinuclear species. As noted in Section D(i), electronic synergistic interactions have been invoked to account for this usual behaviour in bimetallomer redox chemistry.

The increased ability for thioetheralkoxo-bridged complexes to undergo a facile reduction with respect, not only to the 4-*t*-butyl-6-formylsalicylaldehyde derivative **XIX**, but also towards the N<sub>2</sub>–O<sub>2</sub>–N<sub>2</sub> homologues **VI**–**VIII**, is evidently due to the poor electron-donating ability of the sulphur atoms towards the copper centre, relative to nitrogen.

As discussed in D(ii), in alkoxo-bridged derivatives, electronic effects from substituents on redox potentials are difficult to rationalize.

(v) *Adjacent NO·O<sub>2</sub>–ON donor set*

A mixed nitrogen–oxygen donor set is present in the dicopper(II) complex **XXIII**, derived from condensation of 2,4-pentanedione with 3-amino-



1-propanol. This compound in CH<sub>3</sub>OH undergoes the two-electron Cu<sup>II</sup>Cu<sup>II</sup>/Cu<sup>I</sup>Cu<sup>I</sup> reduction in a single near-reversible step at  $E_{1/2} = -1.18$

TABLE 7  
Redox potentials (V) of the charge-transfers for compounds XIX–XXII<sup>a</sup>

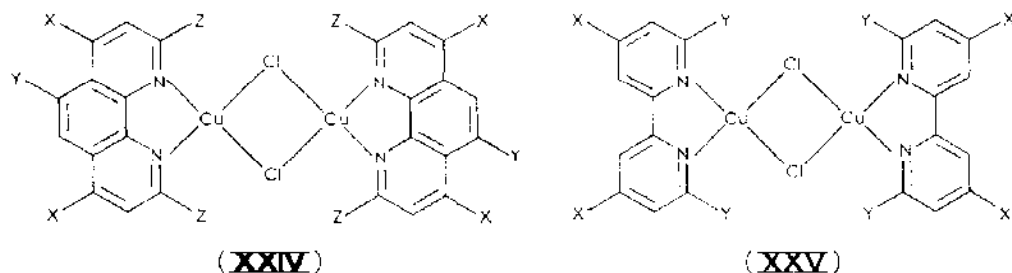
Compound	M	R	n	Y	$E_{(\text{Cu}^{\text{II}}/\text{Cu}^{\text{I}}\text{M}^{\text{II}})}^{0'}$	$E_{(\text{Cu}^{\text{II}}/\text{Cu}^{\text{I}}\text{M}^{\text{I}})}^{0'}$	Solvent	Ref.
<b>XIX</b>	Cu	n-C <sub>7</sub> H <sub>15</sub>			−0.70	−1.20	DMF	83
	Cu	n-C <sub>7</sub> H <sub>15</sub>			−0.66	−1.38	CH <sub>2</sub> Cl <sub>2</sub>	83
	Zn	n-C <sub>7</sub> H <sub>15</sub>			−0.93	–	DMF	83
<b>XX</b>	Cu	CH <sub>3</sub>		Cl	+0.44	−0.25	DMF	130
	Cu	C <sub>2</sub> H <sub>5</sub>		Cl	+0.37	−0.33	DMF	130
	Cu	n-C <sub>3</sub> H <sub>7</sub>		Cl	+0.45	−0.22	DMF	130
	Cu	n-C <sub>4</sub> H <sub>9</sub>		Cl	+0.36	−0.22	DMF	130
	Cu		2	ClO <sub>4</sub>	+0.18	+0.18	DMF	130
<b>XXI</b>	Cu		3	ClO <sub>4</sub>	+0.15	+0.15	DMF	130
	Cu							
<b>XXII</b>	Cu	CH <sub>3</sub>		ClO <sub>4</sub>	+0.05	+0.05	DMF	130
	Cu	C <sub>2</sub> H <sub>5</sub>		ClO <sub>4</sub>	+0.07	+0.07	DMF	130
	Cu	n-C <sub>3</sub> H <sub>7</sub>		ClO <sub>4</sub>	+0.10	+0.10	DMF	130
	Cu	i-C <sub>3</sub> H <sub>7</sub>		ClO <sub>4</sub>	+0.04	+0.04	DMF	130
	Cu	n-C <sub>4</sub> H <sub>9</sub>		ClO <sub>4</sub>	+0.08	+0.08	DMF	130

<sup>a</sup> In cationic compounds, Y denotes the counterion.

V [132]. While substitution of a nitrogen atom with a thio group favours access to the copper(I) centre, substitution with an oxygen atom stabilizes the copper(II) centres.

(vi) *Adjacent  $N_2$ - $Cl_2$ - $N_2$  donor set*

A few halogeno-bridged dicopper(I) complexes of the type **XXIV** and **XXV** have been prepared and characterized [135]. These dicopper(I) complexes undergo two quasireversible one-electron anodic charge-transfers  $Cu^I Cu^I / Cu^I Cu^{II}$  and  $Cu^I Cu^{II} / Cu^{II} Cu^{II}$  in  $Me_2CO$ .



In the case of two substituted derivatives (**XXIV**,  $Z = CH_3$ ; **XXV**,  $Y = CH_3$ ) a single step has indeed been displayed. This was interpreted as proof that the complexes are mononuclear [135]; however the data do not exclude the occurrence of the single-stepped  $Cu^I Cu^I / Cu^{II} Cu^{II}$  two-electron oxidation. Table 8 reports the redox potentials for these species. The high potential values for the redox changes of these compounds is noteworthy; in particular the high potential values for the  $Cu^{II} Cu^{II} / Cu^{II} Cu^I$  and  $Cu^{II} Cu^I / Cu^I Cu^I$  couples of **XXV** with respect to the corresponding hydroxo-bridged derivative **XVI**.

TABLE 8

Standard electrode potentials (V) for the anodic oxidation of dicopper(I) chloro-bridged complexes, in  $Me_2CO$ · $[NBu_4]ClO_4$  ( $0.1 \text{ mol dm}^{-3}$ ) solution [135]

Compound	X	Y	Z	$E_{(Cu^I/Cu^I/Cu^{II}Cu^I)}$	$E_{(Cu^{II}Cu^{II}/Cu^{II}Cu^I)}$
<b>XXIV</b>	H	H	Cl	+ 0.61	+ 0.96
	H	H	H	+ 0.57	+ 0.93
	H	$CH_3$	H	+ 0.55	+ 0.91
	$CH_3$	H	H	+ 0.50	+ 0.90
	$C_6H_5$	H	H	+ 0.56	+ 0.91
	H	H	$CH_3$	+ 0.90 <sup>a</sup>	+ 0.90 <sup>a</sup>
<b>XXV</b>	H	H	-	+ 0.55	+ 0.98
	$CH_3$	H	-	+ 0.50	+ 0.94
	H	$CH_3$	-	+ 0.93 <sup>a</sup>	+ 0.93 <sup>a</sup>

<sup>a</sup> Assuming a single two-electron oxidation step.

(vii) Adjacent  $N_3-O_2-N_3$  and  $N_2S-O_2-SN_2$  donor sets

The electrochemical behaviour of some homo- and heterodinuclear complexes having five-coordinate metal centres of the type **XXVI** has recently been reported [136].

$M = Cu(II), UO_2(VI)$

$X = NH, S$

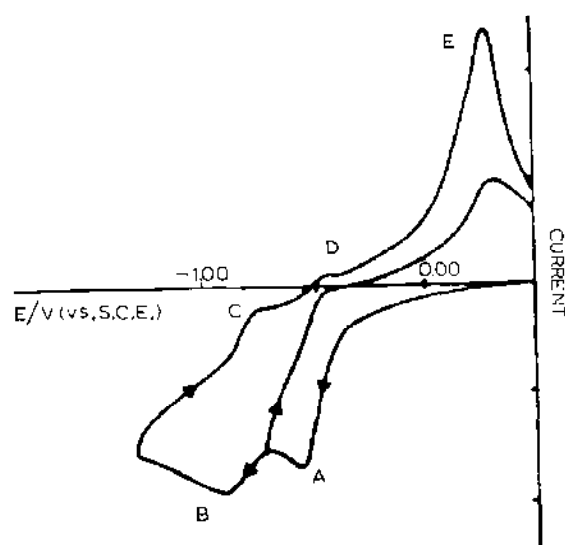
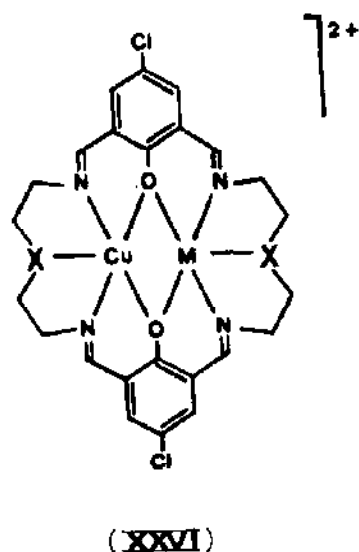


Fig. 66. Cyclic voltammetric response recorded at platinum electrode on a DMSO solution of the Cu-UO<sub>2</sub> complex **XXVI**. 0.1 M [NEt<sub>4</sub>]ClO<sub>4</sub> supporting electrolyte. Scan rate 0.2 V s<sup>-1</sup> [136].

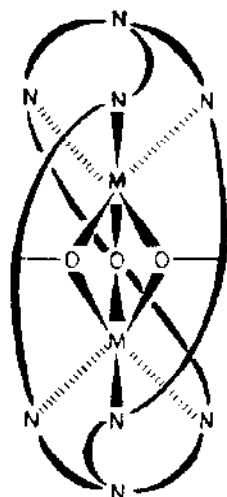
Figure 66 shows the cyclic voltammogram recorded on the heterodinuclear complex in DMSO solution. This behaviour is representative of electro-generated labile copper(I) complexes. In fact the features of the peak system A/D, due to the  $U^{VI}Cu^{II}/U^{VI}Cu^I$  couple, clearly indicate the occurrence of the decomplexation of the electrogenerated copper(I), which is reoxidized at peak E. The anodic-to-cathodic current ratio of the peak system B/C, due in its turn to the  $U^{VI}Cu^I/U^VCu^I$  couple, also manifests the instability of the electrogenerated uranyl(V) copper(I) moiety.

The corresponding homodinuclear copper(II) complexes ( $X = NH, S$ ) are reduced at a platinum electrode in two very close sequential one-electron steps. The lability of the electrogenerated copper(I) complexes is so high, or alternatively the charge transfers are totally irreversible, that reoxidation peaks could not be revealed even at the scan rate of  $50 \text{ V s}^{-1}$ .

Table 9 summarizes the redox potentials for these complexes. The kinetic complications do not allow accurate standard potential values to be obtained. It seems that structural constraints imposed by the fifth coordination labilize the electrogenerated copper(I) centres, with respect to the simple  $N_2-O_2 \cdot N_2$  four coordination.

(viii) *Adjacent  $N_2-O_3-N_2$  donor set*

The electrochemistry of the dicopper(II) clathrochelate **XXVII** has not yet been reported [46].



(**XXVII**)



TABLE 9

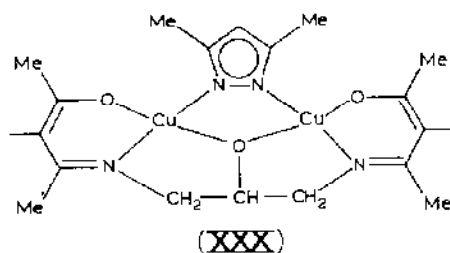
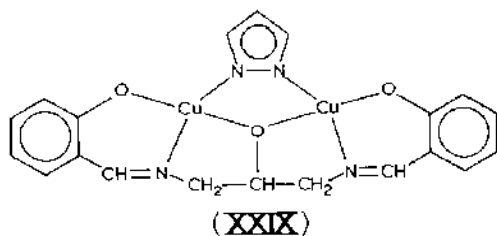
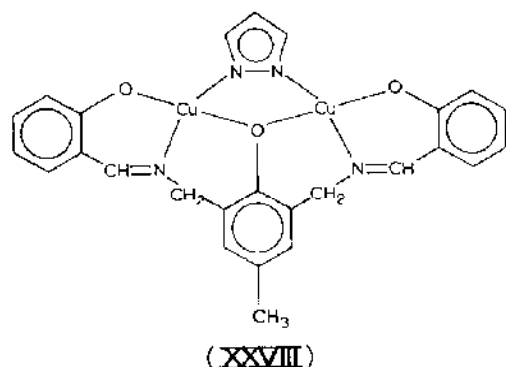
(Approximate) formal electrode potentials (V) for complexes of type XXVI in DMSO- $[\text{NEt}_4]\text{ClO}_4$  (0.1 mol dm<sup>-3</sup>) solution [136]

M	X	$E_{(\text{Cu}^{\text{II}}\text{M}^{\text{II}}/\text{Cu}^{\text{I}}\text{M}^{\text{I}})}^{0'}$	$E_{(\text{Cu}^{\text{I}}\text{M}^{\text{II}}/\text{Cu}^{\text{I}}\text{M}^{\text{I}})}^{0'}$
Cu	NH	-0.69 <sup>a</sup>	-0.69 <sup>a</sup>
Cu	S	-0.79 <sup>a</sup>	-0.79 <sup>a</sup>
UO <sub>2</sub>	S	-0.27	-0.60

<sup>a</sup> Peak potential values at 0.2 V s<sup>-1</sup>.

(ix) *Adjacent NON-O-NON donor set*

The series of complexes XXVIII-XXX, having an endogenous oxo or phenoxo bridge and an exogenous pyrazolato bridge, has recently been characterized electrochemically [95,137]. Apparently, all these compounds



reduce in DMF in two one-electron steps at different potentials (Figure 67). However both the dependence of the standard electrode potentials on the electrode materials, and an unexpected dependence of the second charge

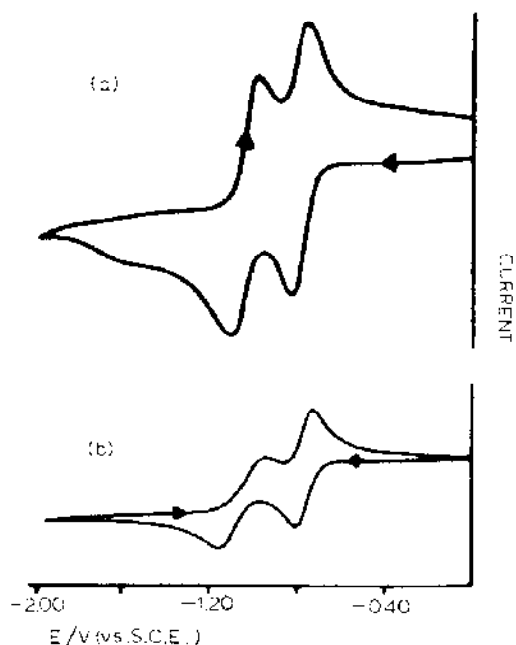


Fig. 67. Cyclic voltammograms recorded on **XXVIII** in DMF solution containing  $[\text{NEt}_4]\text{ClO}_4$  ( $0.1 \text{ mol dm}^{-3}$ ): (a) hanging mercury drop electrode; (b) platinum electrode. Scan rate  $0.02 \text{ V s}^{-1}$ . Temperature  $20^\circ\text{C}$  [95].

transfer on the temperature (the charge transfer is faster at low temperatures than at high temperatures) prompted the authors to search for electrode mechanisms more complicated than the often invoked simple quasireversible charge transfers [95,137]. A mechanism has been proposed involving simultaneous equilibria among stereochemical isomers, generated by the flexibility of the ligand. These electrogenerated isomers are too labile to be identified.

Table 10 summarizes the formal electrode potentials for these compounds. The electronic effects on the formal potentials are easily understood by considering that the endogenous phenoxo bridge is more electron-withdrawing than the oxo bridge; in addition the presence of electron-donat-

TABLE 10

Formal electrode potentials (V) for compounds **XXVIII**–**XXX**, measured in DMF– $[\text{NEt}_4]\text{ClO}_4$  ( $0.1 \text{ mol dm}^{-3}$ ) solution

Compound	$E_{\text{Cu}^{\text{II}}/\text{Cu}^{\text{I}}/2\text{Cu}^{\text{II}}/\text{Cu}^{\text{I}}}$	$E_{\text{Cu}^{\text{II}}/\text{Cu}^{\text{I}}/\text{Cu}^{\text{I}}/\text{Cu}^{\text{I}}}$	Ref.
<b>XXVIII</b>	–0.55	–0.80	95
<b>XXIX</b>	–0.76	–0.96 <sup>a</sup>	137
<b>XXX</b>	–0.86	1.09 <sup>a</sup>	137

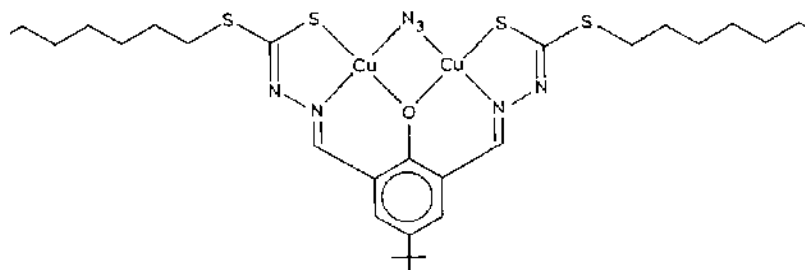
<sup>a</sup> Value from DC polarography; process irreversible in cyclic voltammetry.

ing methyl groups on both exogenous bridge and side chains disfavors the reduction process.

The redox potentials for these compounds lie in the same range as those relevant to  $N_2-O_2-N_2$  type **III** compounds, but are notably more cathodic than those of  $N_2-O_2-N_2$  alkoxo-bridged derivatives **VI–VIII**.

(x) *Adjacent NSN–O–NSN donor set*

The previously cited **XIX** has also been prepared with a terminal azido-bridging group, **XXXI**. While in DMF, the azido group is displaced by the solvent; in  $CH_2Cl_2$  the dicopper(II) compound maintains its composition

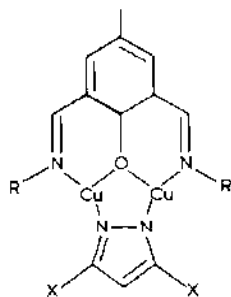


(**XXXI**)

and is reduced in two one-electron quasireversible charge transfers at the following formal potentials:  $E_{(Cu^{II}Cu^{II}/Cu^{II}Cu^I)}^{0'} = -0.33$  V;  $E_{(Cu^{II}Cu^I/Cu^I Cu^I)}^{0'} \cong -0.88$  V. The poorer electron-donating ability of azide with respect to ethoxide is evident, by comparison with potential data for compound **XIX** [83]. In addition comparison with **XXVIII**, having a NON–O–NON donor set, again suggests that the substitution of a “hard” oxygen atom with a “soft” sulphur atom favours the reduction of copper(II) centres.

(xi) *Adjacent  $N_2-O-N_2$  donor set*

A wide range of dicopper(I) complexes, **XXXII**, in which each copper centre is three-coordinate, has been prepared by condensation of dialdehydes with primary amines and bridging bidentate ligands, and has been electrochemically characterized [77]. All these compounds in DMF solutions



(**XXXII**)

TABLE 11

Formal electrode potentials (V) for the redox changes observed in DMF-[NBu<sub>4</sub>]ClO<sub>4</sub> (0.1 mol dm<sup>-3</sup>) solution of **XXXII**<sup>a</sup>

R	X	$E_{(Cu^I/Cu^I; Cu^{II}/Cu^I)}$	$E_{(Cu^{II}/Cu^I; Cu^{III}/Cu^{II})}$
	H	-0.21	-0.45
	CH <sub>3</sub>	0.19	-0.37
	H	-0.11	-0.34
	CH <sub>3</sub>	-0.11	-0.27
	H	+0.15	-0.08
	CH <sub>3</sub>	+0.21	0.00
	H	+0.13	-0.08
	CH <sub>3</sub>	+0.20	+0.01
n-C <sub>3</sub> H-	H	+0.15	-0.08
i-C <sub>3</sub> H-	H	+0.19	0.00
t-C <sub>3</sub> H-	H	+0.24	+0.05
t-C <sub>3</sub> H-	CH <sub>3</sub>	+0.24	+0.08
	H	-0.14	0.03
	H	+0.15	0.05
	H	-0.15	+0.01

<sup>a</sup> From ref. 77.

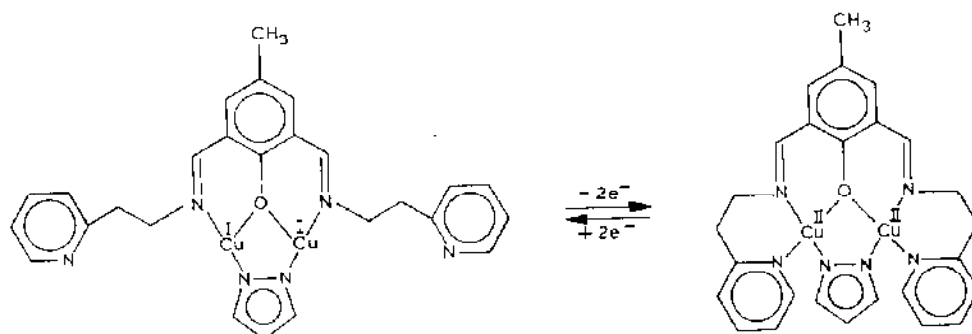
undergo two stepwise one-electron quasireversible anodic charge transfers  $Cu^I/Cu^{II}$  and  $Cu^{II}/Cu^{III}$ . Table 11 summarizes the formal electrode potentials for these sequential steps.

Two points deserve some comment:

(i) Electronic effects from the substituents are generally reversed with respect to those expected (electron-donating groups are expected to favour electron removal). This has been attributed to steric effects inhibiting the binding of electrogenerated copper(II) centres to a fourth donor atom (from the solvent or side arm coordinating groups), required for a square planar copper(II) geometry.

(ii) Pyridine-substituted derivatives are more easily oxidized than phenyl or alkyl substituted analogues.

This facile access to dicopper(II) derivatives is attributed to the following overall structural change subsequent to charge transfer:

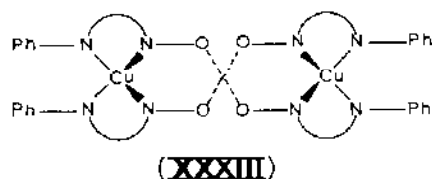


It is evident that the overall electrode process involves an ECEC or EEC mechanism, rather than a simple EE mechanism.

In spite of the slight resemblance of these species, particularly for pyridine substituted species, with dicopper(II) compound **XXVIII**, the  $\text{Cu}^{\text{II}}\text{Cu}^{\text{II}}/\text{Cu}^{\text{II}}\text{Cu}^{\text{I}}$  and  $\text{Cu}^{\text{II}}\text{Cu}^{\text{I}}/\text{Cu}^{\text{I}}\text{Cu}^{\text{II}}$  formal potentials for **XXXII** are higher. It seems that in mimicking "Type 3" copper centres, at least with respect to the redox potentials, a good strategy could involve starting from stereochemically favoured three-coordinate dicopper(I) molecules.

(xii) Remote  $N_4$  donor sets

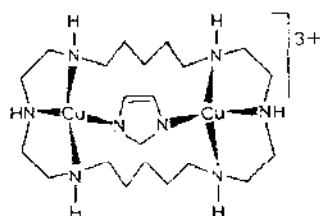
The electrochemical behaviour of the dicopper(I) phenylazo-oximate **XXXIII** has recently been reported [138]. In  $\text{CH}_2\text{Cl}_2$  solutions, at a glassy-



carbon electrode, this compound is oxidized to the mixed valent species  $\text{Cu}^{\text{I}}\text{Cu}^{\text{II}}$ . The one-electron step is however followed by rapid decomposition

of the  $\text{Cu}^{\text{I}}\text{Cu}^{\text{II}}$  species, preventing any reliable calculation of the formal potential for the redox change. The peak potential value of  $+1.09\text{ V}$  (at  $0.2\text{ V s}^{-1}$ ), testifies however for the notably high potential  $\text{Cu}^{\text{II}}/\text{Cu}^{\text{I}}$  redox couple present in this compound.

The electrochemistry of the dicopper(II) complex **XXXIV**, having two remote  $\text{N}_4$  chambers, has also been studied [139]. In this derivative the dicopper(II)–imidazolato complex is encapsulated in the cavity of a rather flexible macrocycle. In MeCN solution this complex reduces at a glassy-

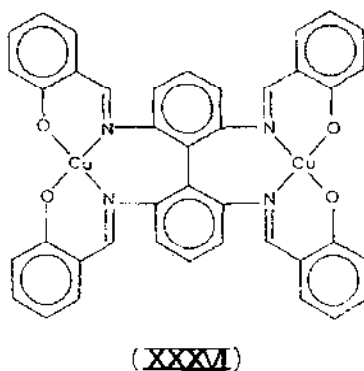
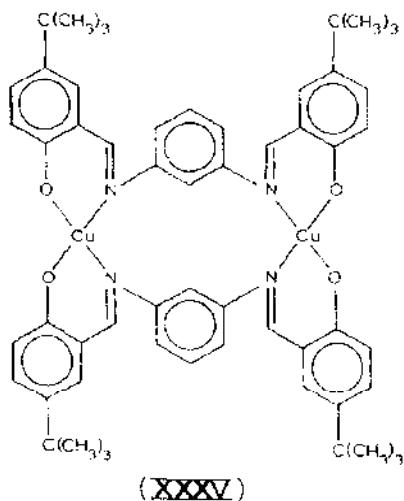


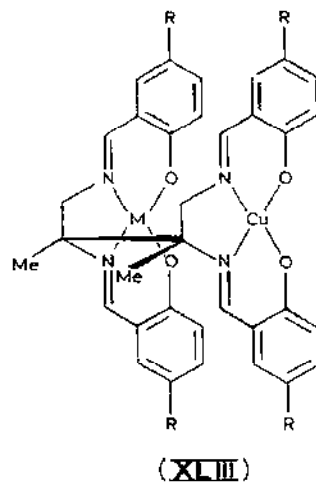
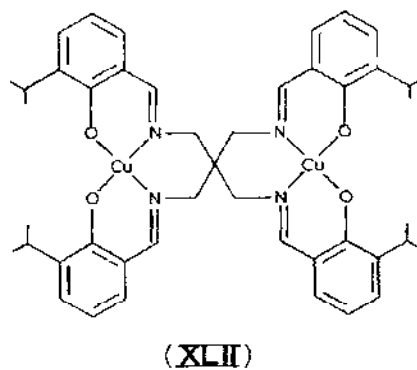
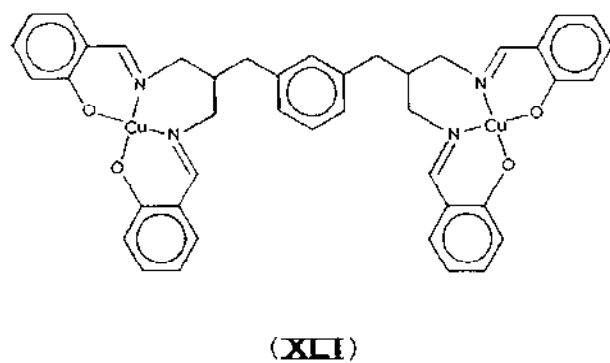
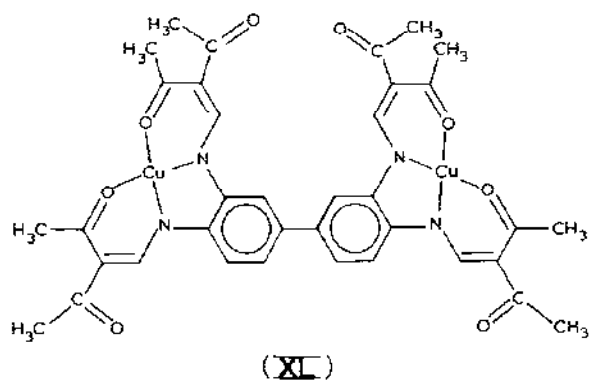
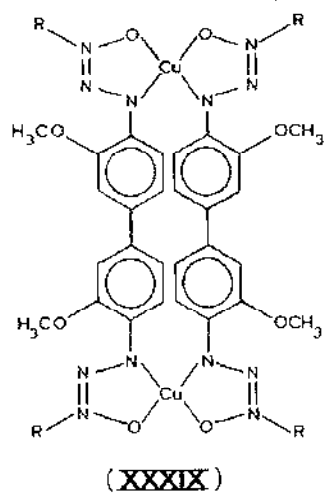
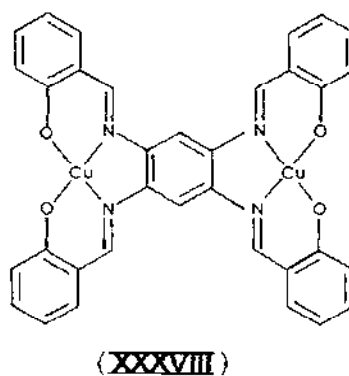
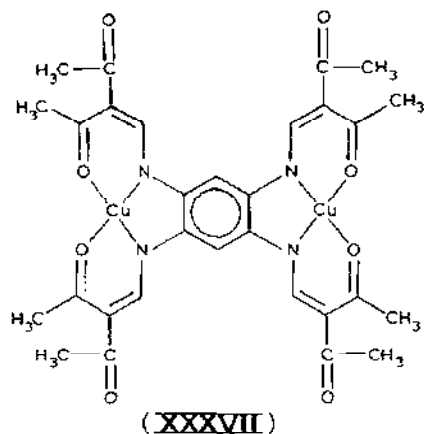
**XXXIV**

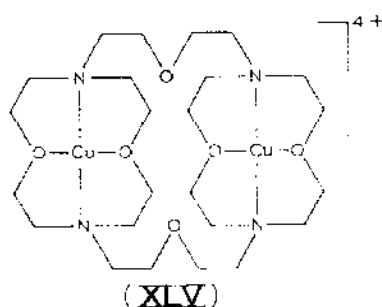
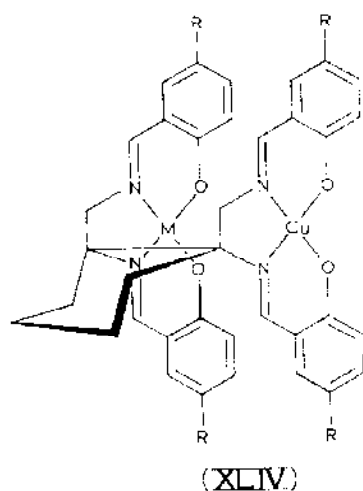
carbon electrode in two distinct irreversible one-electron charge transfers located at the following peak potential values:  $E_{\text{p}(\text{Cu}^{\text{II}}\text{Cu}^{\text{II}}/\text{Cu}^{\text{II}}\text{Cu}^{\text{I}})} = -0.48\text{ V}$ ;  $E_{\text{p}(\text{Cu}^{\text{II}}\text{Cu}^{\text{I}}/\text{Cu}^{\text{I}}\text{Cu}^{\text{I}})} = -0.59\text{ V}$ . The redox behaviour of complexes **XXXIII** and **XXXIV** shows the difficulty in preparing dicopper complexes with two separated  $\text{N}_4$  chambers, able to support the stereochemical rearrangements imposed by the  $\text{Cu}^{\text{II}} \rightleftharpoons \text{Cu}^{\text{I}}$  redox changes.

(xiii) Remote  $\text{N}_2\text{O}_2$  donor sets

A wide range of dicopper(II) compounds, in which each remote copper(II) centre is surrounded by a  $\text{N}_2\text{O}_2$  donor set, has been studied electrochemically [140–147].







A further subdivision can be attempted between those complexes in which the two chambers are linked by substantially rigid bridging systems, **XXXV-XXXVIII**, and those linked by more flexible bridging systems, **XXXIX-XLIV**. Generally, as can be deduced from Table 12, complexes of these types are reduced from  $\text{Cu}^{\text{II}}\text{Cu}^{\text{II}}$  to  $\text{Cu}^{\text{I}}\text{Cu}^{\text{I}}$ , in two sequential one-electron steps at the same (**XXXV**, **XXXVIII**, **XXXIX**, **XL**, **XLI**, **XLII**) or nearly the same potential; in the case of **XXXIX** and **XLI** this cathodic step is irreversible in character.

Complexes **XXXIX** allow access to the corresponding unusual dicopper(III) species through two distinct one-electron quasireversible anodic steps at surprisingly low potentials. Figure 68 shows the typical cyclic voltammetric response recorded in the anodic region for **XXXIX** ( $\text{R} = \text{Me}$ ).

Coupled ESR-electrolysis tests proved both the electrogenerated  $\text{Cu}^{\text{II}}\text{Cu}^{\text{III}}$  and  $\text{Cu}^{\text{III}}\text{Cu}^{\text{III}}$  species to be non-transient. Comparison with other complexes of this class shows that the effect of the triazene ring in the coordination of the copper(II) centre stabilizes the  $3+$  oxidation state, and destabilizes the  $1+$  oxidation state.

Attention must furthermore be focused on complexes **XLIII** and **XLIV**. As can be seen in Table 13, they are reduced in some cases in a single



TABLE 12  
Formal electrode potentials (V) for the redox changes observed in solution of compounds XXXV–XLII and XLV

Compound	R	$E_{(\text{Cu}^{\text{II}}\text{Cu}^{\text{II}}/\text{Cu}^{\text{II}}\text{Cu}^{\text{I}})}^{0'}$	$E_{(\text{Cu}^{\text{II}}\text{Cu}^{\text{I}}/\text{Cu}^{\text{I}}\text{Cu}^{\text{I}})}^{0'}$	$E_{(\text{Cu}^{\text{II}}\text{Cu}^{\text{II}}/\text{Cu}^{\text{II}}\text{Cu}^{\text{I}})}^{0'}$	$E_{(\text{Cu}^{\text{II}}\text{Cu}^{\text{II}}/\text{Cu}^{\text{II}}\text{Cu}^{\text{III}})}^{0'}$	Solvent	Ref.
XXXV	—	−0.46	−0.46	—	—	DMF	140, 141
XXXVI	—	−0.47	−0.59	—	—	DMF	140, 141
XXXVII	—	−0.81	−0.88	—	—	DMSO	141
XXXVIII	—	−1.28	−1.28	—	—	DMF	142
XXXIX	CH <sub>3</sub>	~ −0.8 <sup>a</sup>	~ −0.8 <sup>a</sup>	+0.77	+0.99	MeCN	143
	C <sub>2</sub> H <sub>5</sub>	~ −0.8 <sup>a</sup>	~ −0.8 <sup>a</sup>	+0.73	+0.98	MeCN	143
	n-C <sub>3</sub> H <sub>7</sub>	~ −0.8 <sup>a</sup>	~ −0.8 <sup>a</sup>	+0.74	+1.00	MeCN	143
	i-C <sub>3</sub> H <sub>7</sub>	~ −0.8 <sup>a</sup>	~ −0.8 <sup>a</sup>	+0.70	+0.96	MeCN	143
XL	—	−0.80	−0.80	—	—	DMSO	141
XLI	—	−1.16 <sup>a</sup>	−1.16 <sup>a</sup>	—	—	DMSO	144
XLII	—	−1.08	−1.08	—	—	DMF	142
XLV	—	+0.52	+0.46	—	—	PC <sup>b</sup>	145

<sup>a</sup> Peak potential values for irreversible processes. <sup>b</sup> PC, propylene carbonate.

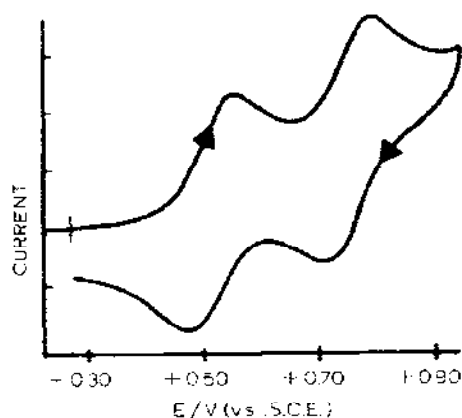


Fig. 68. Cyclic voltammogram recorded at a platinum electrode on a MeCN solution of **XXXIX** ( $R = \text{Me}$ ), containing  $[\text{NEt}_3]\text{ClO}_4$  ( $0.1 \text{ mol dm}^{-3}$ ) as supporting electrolyte. Scan rate  $0.2 \text{ V s}^{-1}$  [143].

$\text{Cu}^{\text{II}}\text{Cu}^{\text{II}}/\text{Cu}^{\text{I}}\text{Cu}^{\text{I}}$  two-electron step, and in other cases in two separate steps.

The appearance of two distinct cathodic processes was attributed [130,146,147] to the occurrence of an equilibrium between stacked and non-stacked species, the first cathodic process being due to the  $\text{Cu}^{\text{II}}\text{Cu}^{\text{II}}/\text{Cu}^{\text{II}}\text{Cu}^{\text{I}}$  step of the stacked species, and the second step due to the  $\text{Cu}^{\text{II}}\text{Cu}^{\text{II}}/\text{Cu}^{\text{I}}\text{Cu}^{\text{I}}$  non-stacked species.

TABLE 13

Formal electrode potentials (V) for the redox changes observed in  $\text{CH}_2\text{Cl}_2$ - $[\text{NBu}_4]\text{ClO}_4$  ( $0.1 \text{ mol dm}^{-3}$ ) solutions of homo- and heterodinuclear complexes **XLIII** and **XLIV**

Compound	R	M	$E_{(\text{Cu}^{\text{II}}\text{M}^{\text{II}}/\text{Cu}^{\text{I}}\text{M}^{\text{II}})}^{\text{a}}$	$E_{(\text{Cu}^{\text{II}}\text{M}^{\text{II}}/\text{Cu}^{\text{I}}\text{M}^{\text{I}})}^{\text{b}}$	Ref.
<b>XLIII</b>	H	Cu	-1.12	-1.29	130, 146
	$\text{CH}_3$	Cu	-1.42	-1.42	130, 146
	$t\text{-C}_4\text{H}_9$	Cu	1.45	-1.45	130, 146
	H	Ni	-0.86	-1.38	130, 147
	$\text{CH}_3$	Ni	-0.91	1.41	130, 147
	Br	Ni	-0.87	-1.24	130, 147
<b>XLIV</b>	H	Cu	-1.09	-1.40	130, 146
	$\text{CH}_3$	Cu	-1.09	1.40	130, 146
	$t\text{-C}_4\text{H}_9$	Cu	1.40	-1.40	130, 146
	H	Ni	-0.89	-1.42	130, 147
	$\text{CH}_3$	Ni	-0.94	1.41	130, 147
	Br	Ni	0.90	1.26	130, 147

<sup>a</sup> Authors quoted in the relevant references assign this step to the  $\text{Cu}^{\text{II}}\text{M}^{\text{II}}/\text{Cu}^{\text{I}}\text{M}^{\text{II}}$  redox change in the stacked species; see text. <sup>b</sup> Authors quoted in the relevant references assign this step to the  $\text{Cu}^{\text{II}}\text{M}^{\text{II}}/\text{Cu}^{\text{I}}\text{M}^{\text{II}}$  redox change in non-stacked heterodinuclear species, and to  $\text{Cu}^{\text{II}}\text{C}^{\text{II}}/\text{Cu}^{\text{I}}\text{M}^{\text{I}}$  in non-stacked homodinuclear species; see text.

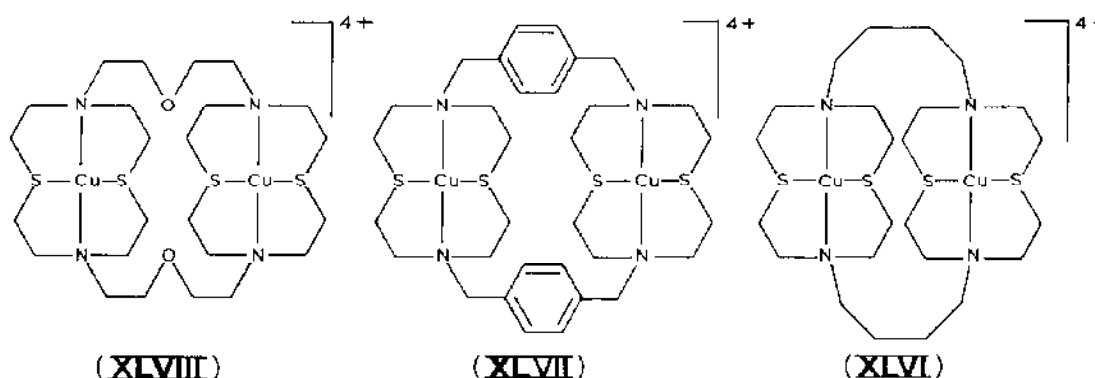
Indeed on the basis of the electrochemical measurements, this assumption, even if highly stimulating, is as plausible as the more simple one which assumes the occurrence of two distinct  $\text{Cu}^{\text{II}}\text{Cu}^{\text{II}}/\text{Cu}^{\text{II}}\text{Cu}^{\text{I}}$  and  $\text{Cu}^{\text{II}}\text{Cu}^{\text{I}}/\text{Cu}^{\text{I}}\text{Cu}^{\text{I}}$  steps. The same argument is true for the corresponding heterodinuclear complex, if one considers that Ni(II) in heterobimetallochromes is usually electroactive [21,127,128]. Hence in Table 13 both hypotheses have been taken into account.

Finally note that the cathodic reduction of the macrocyclic complex **XLV** not only proceeds through partially overlapping  $\text{Cu}^{\text{II}}\text{Cu}^{\text{II}}/\text{Cu}^{\text{II}}\text{Cu}^{\text{I}}$  and  $\text{Cu}^{\text{II}}\text{Cu}^{\text{I}}/\text{Cu}^{\text{I}}\text{Cu}^{\text{I}}$  redox changes centred at +0.49 V, but also gives rise to a further cathodic step at  $E^{0'} = -0.51$  V, due to reduction of cuprous centers to copper metal, followed by decomplexation from the ligand. The interest in these high-potential multisite receptors as models for biological functions is well documented [148].

An examination of Table 12 directed to the understanding of the role of the bridging system between the two metal chambers, seems to indicate that the flexibility of this system is unimportant with respect to the stereochemical changes favoring the copper(I) lodging, largely dominated by the flexibility of the chamber itself, as indicated by redox data for compound **XLV**.

(xiv) Remote  $\text{N}_2\text{S}_2$  donor sets

A series of macrocyclic dicopper(II) complexes, **XLVI**–**XLVIII**, containing two remote chambers of  $\text{N}_2\text{S}_2$  donor set, has been prepared and

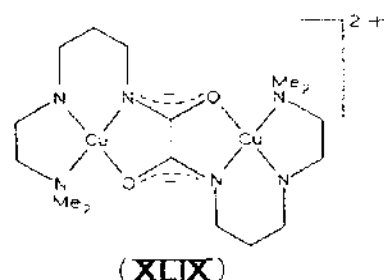


electrochemically characterized [145]. In propylene carbonate solution, all three complexes are reduced in a single quasireversible two-electron step, corresponding to the  $\text{Cu}^{\text{II}}\text{Cu}^{\text{II}}/\text{Cu}^{\text{I}}\text{Cu}^{\text{I}}$  redox change. The electrogenerated dicopper(I) species are quite stable in solution. Table 14 reports redox potentials for these types of copper(II) complexes. The great ability of these

dicopper(II) complexes to act as high-potential two-electron exchangers, so mimicking the redox properties of copper proteins, must be recognised.

(xv) Remote  $N_3O$  donor sets

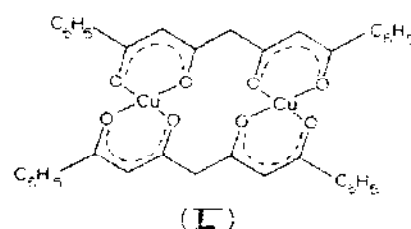
Only the dicopper(II) compound **XLIX**, having two remote  $N_3O$  chambers, has been briefly electrochemically investigated [132]. In  $CH_3OH$  this compound undergoes two distinct redox changes  $Cu^{II}Cu^{II}/Cu^{II}Cu^I$  and



$Cu^{II}Cu^I/Cu^ICu^I$  reversibly at potentials of  $-0.45$  V and  $-0.82$  V, respectively.

(xvi) Remote  $O_2O_2$  donor sets

The only electrochemically studied dicopper(II) compound **L**, having two remote  $O_2O_2$  donor sets, belongs to the 1,3,5,7-tetraketonate complexes.



At variance with the 1,3,5-triketonato analogue, which in DMF is reversibly reduced in one two-electron step, **L** in DMF undergoes irreversible

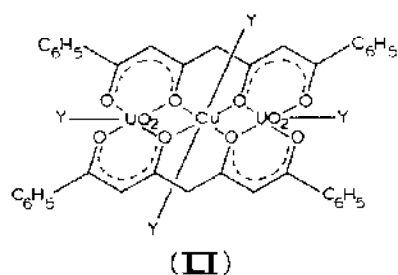
TABLE 14

Formal electrode potentials (V) for the two-electron cathodic reduction of complexes **XLVI**–**XLVIII** in  $PC-[NEt_4]ClO_4$  ( $0.1 \text{ mol dm}^{-3}$ ) solution <sup>a</sup>

Compound	$E_{(Cu^{II}Cu^{II}/Cu^ICu^I)}^{0'}$
<b>XLVI</b>	+0.46
<b>XLVII</b>	+0.72
<b>XLVIII</b>	+0.51

<sup>a</sup> From ref. 145.

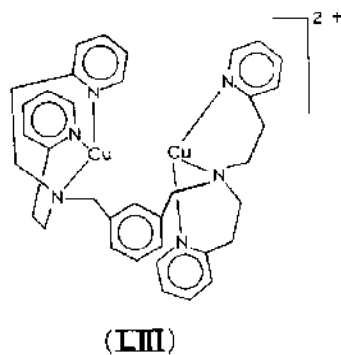
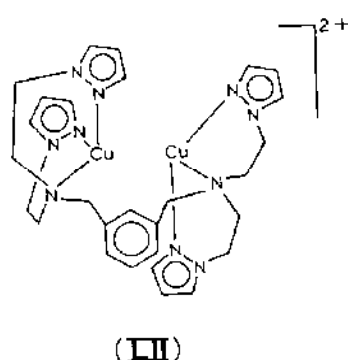
reduction [20]. The stabilizing effect of adjacent  $O_2O_2$  chambers on copper(I) centers is further shown by the fact that in the trinuclear-tetraketone **LI**, both the copper(II) and uranyl(VI) centers undergo separate near-reversible one-electron cathodic processes ( $E_{1/2 Cu^{II}UO_2^{VI}UO_2^{VI}/Cu^I UO_2^{VI}UO_2^{VI}} = -0.25$  V, in DMF) [149].



Y = pyridine

(xvii) Remote  $N_3$  donor sets

In recent years the chemistry of complexes of types **LII**, **LIII**, has been extensively investigated [150,151]. In order to test their ability to act as



models for some copper proteins, their redox properties have also been probed by electrochemical techniques. As seen in Fig. 69, both compounds display a similar oxidation pathway. They undergo a two-electron anodic change  $Cu^I Cu^I / Cu^{II} Cu^{II}$  in a single quasireversible process [151]. However, since the exhaustive two-electron electrolysis of **LII** in methanol leads to the corresponding di- $\mu$ -methoxo-bridged copper(II) complex, the anodic process must be followed by chemical steps, so that the electrode process should involve an EEC or ECEC mechanism in the overall reaction:

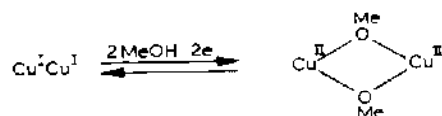


Table 15 summarizes redox data for these two similar dicopper(I) compounds.

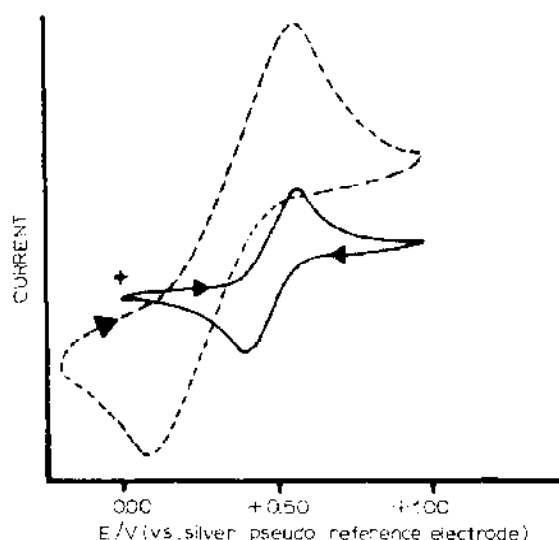


Fig. 69. Cyclic voltammograms recorded at a platinum electrode in MeOH solution containing  $[\text{NBu}_4]\text{BF}_4$  ( $0.1 \text{ mol dm}^{-3}$ ) (—) **LII**; (·····) **LIII** [151].

Two dicopper(II) compounds, **LIV** and **LV**, having the  $\text{N}_3$  donor set around each copper center, have been prepared from macrocyclic ligands, and electrochemically characterized. Despite their similarity, compound **LIV** is reduced in a single quasireversible two-electron step, generating the quite stable  $\text{Cu}^{\text{I}}\text{Cu}^{\text{I}}$  species [145], while compound **LV** is reduced in two distinct

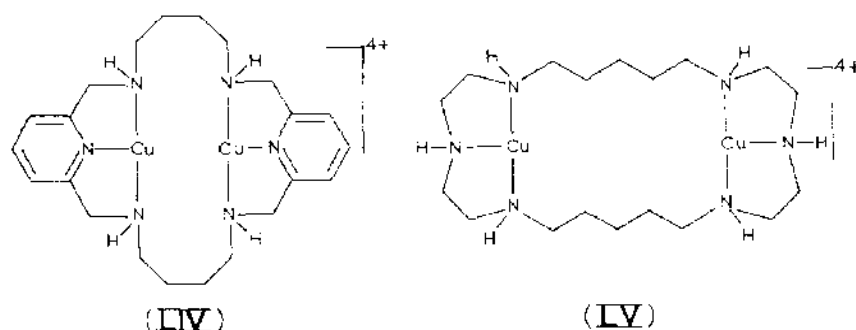


TABLE 15

Standard electrode potentials (V) for the two-electron anodic oxidation of compounds **LII** and **LIII**

Compound	$E_{(\text{Cu}^{\text{I}}\text{Cu}^{\text{I}}/\text{Cu}^{\text{II}}\text{Cu}^{\text{II}})}$	Solvent	Ref.
<b>LII</b>	+ 0.52	$\text{CH}_3\text{OH}$	151 <sup>a</sup>
<b>LIII</b>	+ 0.37	$\text{CH}_3\text{OH}$	151 <sup>a</sup>
	+ 0.16	DMF	105

<sup>a</sup> In ref. 151 potential values are reported vs. a silver wire pseudo-reference electrode. In our laboratory such a reference electrode shows a potential value of  $\pm 0.04 \text{ V}$  vs. N.H.E.

TABLE 16

Formal electrode potentials (V) for the cathodic processes of compounds **LIV** and **LV**

Compound	$E_{(\text{Cu}^{\text{II}}\text{Cu}^{\text{II}}/\text{Cu}^{\text{I}}\text{Cu}^{\text{I}})}^0$	$E_{(\text{Cu}^{\text{II}}\text{Cu}^{\text{I}}/\text{Cu}^{\text{I}}\text{Cu}^{\text{I}})}^0$	Solvent	Ref.
<b>LIV</b>	+0.04	+0.04	PC	145
<b>LV</b>	-0.30 <sup>a</sup>	-0.50 <sup>a</sup>	MeCN	139

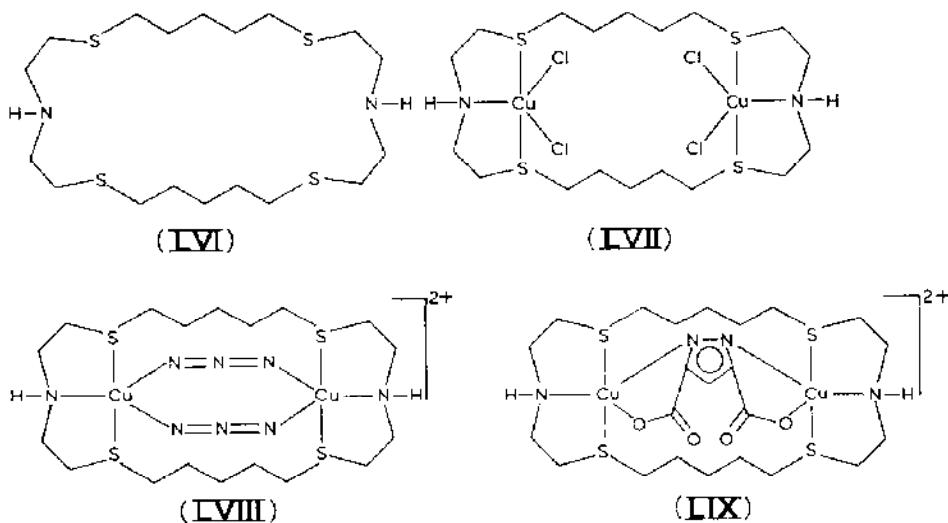
<sup>a</sup> Peak potential value for irreversible process.

one-electron irreversible steps [139]. Even if in the latter case the electrochemistry has only been briefly studied, it is likely that the irreversibility of the process is associated with fast chemical reactions involving the electro-generated copper(I) center rather than to an extremely low heterogeneous charge-transfer rate.

Compound **LIV** can in fact be reduced to the stable  $\text{Cu}^{\text{I}}\text{Cu}^{\text{I}}$  congener because of the presence of the pyridine ring, which stabilizes the two copper(I) centers. Table 16 summarizes the electrode potentials for the reduction processes of compounds **LIV** and **LV**.

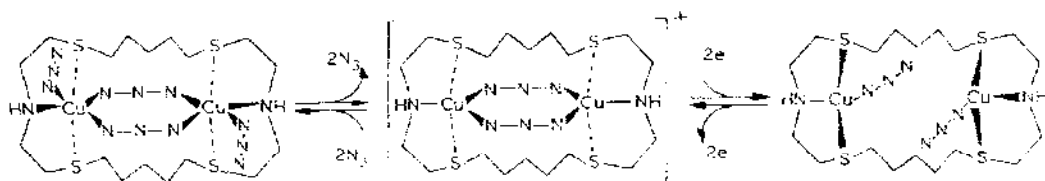
(xviii) Remote  $\text{NS}_2\text{Cl}_2$ ,  $\text{N}_3\text{S}_2$  and  $\text{N}_2\text{S}_2\text{O}$  donor sets

The compounds **LVII**–**LIX** have been grouped in a unique class, though with different remote donor atom sets, because all are inclusion complexes of the macrocyclic ligand 1,13-diaza-,4,10,16,22-tetrathiacyclotetracosane (24-ane- $\text{N}_2\text{S}_4$ ), **LVI**.



Both the chloro and azido derivatives are reduced from the  $\text{Cu}^{\text{II}}\text{Cu}^{\text{II}}$  to the  $\text{Cu}^{\text{I}}\text{Cu}^{\text{I}}$  form in a single two-electron step, resulting from two merging sequential one-electron charge-transfers ( $E_1^0 - E_2^0 < 100$  mV) [152].

Compound **LVIII** comes from the tetraazido derivative, which in DMSO releases two azides according to the scheme proposed.

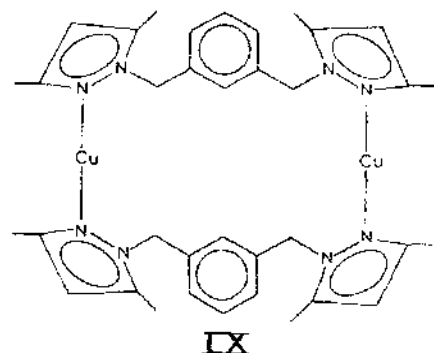


This scheme also shows the ability of this derivative to support the conformational changes induced by the redox activity.

The redox behaviour of compound **LIX** has not yet been definitively ascertained because the  $\text{Cu}^{\text{II}}\text{Cu}^{\text{II}}/\text{Cu}^{\text{I}}\text{Cu}^{\text{I}}$  step occurs at potentials very close to the likely reduction of pyrazole dicarboxylate groups to carboxaldehyde. The redox potential data for these inclusion dicopper(II) complexes are reported in Table 17.

(xix) Remote  $\text{N}_3$  donor sets

In the briefly represented class of two-coordinated copper complexes only the dicopper(I) compound **LX** has been studied electrochemically [153]. In



MeCN this compound shows, at a glassy-carbon electrode, an irreversible two-electron anodic process located at the notably high peak potential value

TABLE 17

Formal electrode potentials (V) for the dicopper(II) inclusion complexes **LVII-LIX**

Compound	$E_{(\text{Cu}^{\text{II}}\text{Cu}^{\text{II}}/\text{Cu}^{\text{I}}\text{Cu}^{\text{I}})}^0$	Solvent	Ref.
<b>LVII</b>	+ 0.49	DMSO	152
<b>LVIII</b>	+ 0.31	DMSO	152
<b>LIX</b>	0.06 <sup>a</sup>	DMSO	148

<sup>a</sup> Complicated by the closeness of the reduction of carboxylate groups to carboxaldehyde.

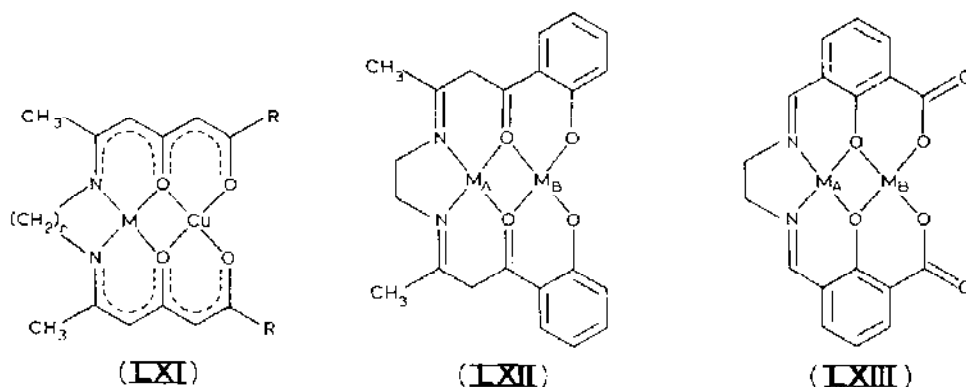


of  $E_{p(\text{Cu}^I\text{Cu}^I/\text{Cu}^{II}\text{Cu}^{II})} = +1.51$  V. The irreversibility of the redox change is associated with the lack of stabilizing donor atoms toward the electrogenerated copper(II) centers.

#### E. ELECTROCHEMISTRY OF BINUCLEAR COMPLEXES WITH SITES HAVING DIFFERENT DONOR ATOM SETS

##### (i) *Adjacent N<sub>2</sub>-O<sub>2</sub>-O<sub>2</sub> donor set*

A wide range of binuclear copper(II) complexes, **LXI-LXIII**, showing the adjacent N<sub>2</sub>O<sub>2</sub>O<sub>2</sub> donor set, has been studied.



$M = \text{Cu(II)}, \text{Ni(II)}$

$M_A = \text{Cu(II)}$

$M_A = \text{Cu(II)}, \text{Ni(II)}$

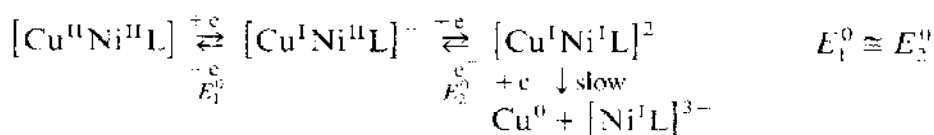
$M_B = \text{Cu(II)}, \text{UO}_2(\text{VI})$

$M_B = \text{Cu(II)}, \text{Ni(II)}, \text{UO}_2(\text{VI})$

The cathodic behaviour of homo- and heterodinuclear complexes of **LXI** may be "complicated" by the above cited (see Section D(i)) complexation with  $\text{Na}^+$  ions [47,49]. In the absence of  $\text{Na}^+$  ions, the homodinuclear complex **LXI** reduces in a single-stepped  $\text{Cu}^{II}\text{Cu}^{II}/\text{Cu}^I\text{Cu}^I$  quasireversible process. In the presence of  $\text{Na}^+$  ions the same process becomes reversible, and is shifted about 0.3 V towards less negative potentials, because of the stabilizing effect of  $\text{Na}^+$  ion-pairing towards electrogenerated anions.

The stereochemical changes accompanying the reduction should at least affect the rate of charge-transfer in the presence of complexing  $\text{Na}^+$  ions. In addition, we, and others [37], are surprised that two metal centers differing in their coordinating donor atom sets reduce at the same potential value, at least in the absence of  $\text{Na}^+$  ions. Also without considering that the occurrence of a two-electron reduction is disputed [37], we remark that, when dealing with dicopper(II) complexes, the consumption of two electrons per molecule of bimetallomer does not necessarily mean the formation of the

relevant  $\text{Cu}^{\text{I}}\text{Cu}^{\text{I}}$  species, unless this is proved by chemical, or electrochemical (for instance a CV test showing the presence of the reduced species of the starting complex) evidence. In fact the consumption of two electrons may arise from the frequently occurring  $\text{Cu}^{\text{II}}/\text{Cu}^0$  overall reduction, centered on only one metal moiety. Curiously in controlled potential electrolysis tests it is noted that two electrons per molecule are spent in a first step, resulting in a Cu/Hg amalgam, as well as a further two electrons per molecule in a second step at more negative potentials [49]. Only in the case of the compound with  $\text{R} = \text{t-C}_4\text{H}_9$  and  $n = 3$ , are four electrons ( $\text{Cu}^{\text{II}}\text{Cu}^{\text{II}}/\text{Cu}^0\text{Cu}^0$ ) per molecule involved at the potential of a single step. Only in this case, the sequential  $\text{Cu}^{\text{II}}\text{Cu}^{\text{II}}/\text{Cu}^{\text{II}}\text{Cu}^{\text{I}}$ , and  $\text{Cu}^{\text{II}}\text{Cu}^{\text{I}}/\text{Cu}^{\text{I}}\text{Cu}^{\text{I}}$  changes occur at the same potential in the cyclic voltammetric timescale. In this connection the same authors [49] maintain that in the heterodinuclear  $\text{Cu}^{\text{II}}\text{Ni}^{\text{II}}$  complex **LX**, both metal centers are one-electron reduced at the same potential. Further they noted that coulometric experiments provided the consumption of two electrons per molecule, with concomitant formation of copper metal. Assuming a reduction pathway of the type



the consumption of three electrons per molecule of complex would be expected.

Furthermore other authors have found that one of the homodinuclear compounds **LXI**, undergoes two distinct near reversible  $\text{Cu}^{\text{II}}\text{Cu}^{\text{II}}/\text{Cu}^{\text{II}}\text{Cu}^{\text{I}}$  and  $\text{Cu}^{\text{II}}\text{Cu}^{\text{I}}/\text{Cu}^{\text{I}}\text{Cu}^{\text{I}}$  reduction steps [132].

It is evident that the reduction pathway of this type of compound has not yet been unequivocally determined. The redox potentials for complexes **LXI** are reported in Table 18.

The electrochemistry of the copper(II) complexes **LXII** and **LXIII**, is characterized by the fact that the one-electron reduction of the metal centers is generally followed by decomplexation steps (EC mechanisms). For example, Fig. 70 shows the cathodic behaviour of both the homodinuclear complexes in DMSO solution. The CuCu complex **LXII** is reduced in two distinct sequential one-electron steps, irreversible in character. The CuCu complex, **LXIII** shows first a quasireversible  $\text{Cu}^{\text{II}}\text{Cu}^{\text{II}}/\text{Cu}^{\text{II}}\text{Cu}^{\text{I}}$  step (kinetically complicated by the decomplexation of the Cu(I) center), followed by the subsequent irreversible  $\text{Cu}^{\text{II}}\text{Cu}^{\text{I}}/\text{Cu}^{\text{I}}\text{Cu}^{\text{I}}$  step.

The appearance of the reoxidation peak at  $\approx +0.1$  V, due to  $\text{Cu}_{(\text{free})}^{\cdot-} \rightarrow \text{Cu}_{(\text{free})}^2$ , is indicative of the decomplexation reaction following charge transfer. We suggest the irreversibility of the charge transfer is a consequence of

TABLE 18

Formal electrode potentials (V) for the redox changes observed in the cathodic reduction of homo- and heterodinuclear compounds **LXI** in DMF solution; values in parentheses refer to the presence of Na<sup>+</sup> ions

R	n	M	$E_{(\text{Cu}^{\text{II}}\text{M}^{\text{II}}/\text{Cu}^{\text{I}}\text{M}^{\text{II}})}^{0'}$	$E_{(\text{Cu}^{\text{I}}\text{M}^{\text{II}}/\text{Cu}^{\text{I}}\text{M}^{\text{I}})}^{0'}$	Ref.
CH <sub>3</sub>	2	Cu	-0.78	-1.66	132
C <sub>6</sub> H <sub>5</sub>	2	Cu	-0.68 <sup>a</sup> (-0.32)	-1.68 <sup>a</sup> (-0.32)	47
t-C <sub>4</sub> H <sub>9</sub>	2	Cu	-0.78 (-0.45)	-0.78 (-0.45)	49
t-C <sub>4</sub> H <sub>9</sub>	2	Cu	-0.99	-	37
C <sub>6</sub> H <sub>5</sub>	3	Cu	-0.86 (-0.50)	0.86 (-0.50)	49
t-C <sub>4</sub> H <sub>9</sub>	3	Cu	-0.92	-0.92	49
C <sub>6</sub> H <sub>5</sub>	2	Ni	-0.66 (-0.36)	-0.66 (-0.36)	48

<sup>a</sup> Peak potential value for irreversible process.

the speed of the chemical reactions coupled to the reduction steps. According to this assumption, compound **LXII** displays much lower ability to bind the Cu(I) centres than **LXIII**. Only in the case of uranyl(VI) complexes, is the electrogeneration of uranyl(V) not complicated by decomplexation.

Table 19 summarizes the redox potentials for complexes **LXII** and **LXIII**.

In EC electrode processes, formal redox potentials must be derived from voltammograms recorded at potential scan rates sufficiently fast to overcome the occurrence of the chemical reactions following the charge transfer, i.e. in a cathodic process, for instance,  $(i_p)^a/(i_p)^c = 1$ . When, owing to the quasireversibility of the  $n$ -electron charge transfer, high scan rates cause  $\Delta E_p$  values to become higher than the theoretical  $59/n$  (mV) values, and

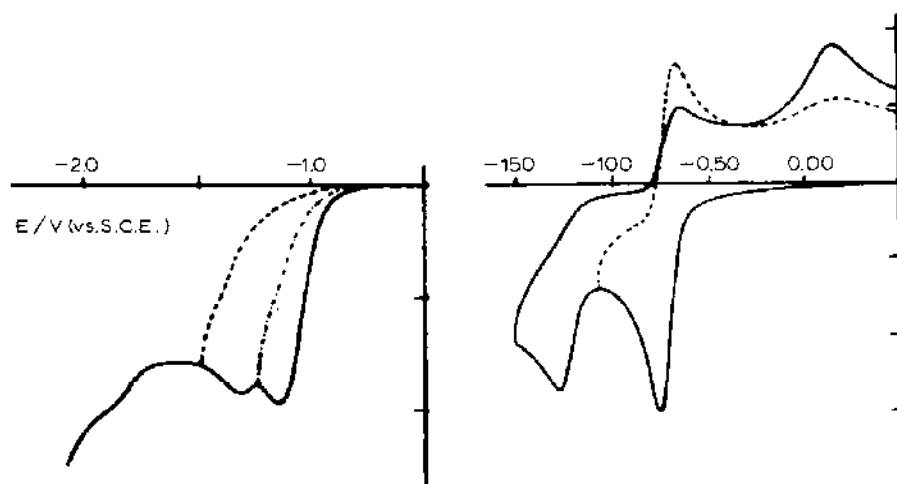


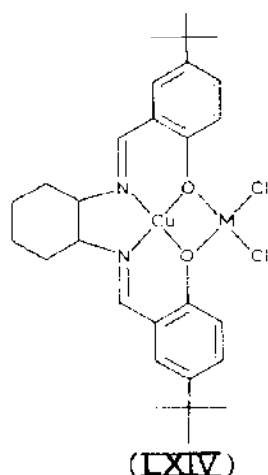
Fig. 70. Cyclic voltammetric responses recorded in DMSO solution (0.1 M in [NEt<sub>4</sub>]ClO<sub>4</sub>) of (a) **LXII** (M = Cu), (b) **LXIII** (M<sub>A</sub> = Cu; M<sub>B</sub> = Cu). Scan rate 0.2 V s<sup>-1</sup> [154,155].

where one can assume that the transfer coefficient  $\alpha$  is not very different from 0.5 (as usually happens), the cathodic shift of the reduction peak and the anodic shift of the directly associated reoxidation peak are substantially symmetric with respect to the formal potential.

It has been also reported that the dicopper complex **LXII** in DMF gives no distinct reduction steps [132].

(ii) *Adjacent N<sub>2</sub>-O<sub>2</sub>-Cl<sub>2</sub> donor sets*

Only the compound **LXIV**, showing the N<sub>2</sub>O<sub>2</sub>Cl<sub>2</sub> adjacent donor set, has been reported to undergo cathodic processes [157].



M = Cu(II), Zn(II), Hg(II)

The homodinuclear copper(II) complex undergoes two well-separated quasi-reversible one-electron reduction steps, with the more facile Cu<sup>II</sup>Cu<sup>II</sup>/Cu<sup>II</sup>Cu<sup>I</sup> step assigned to the O<sub>2</sub>Cl<sub>2</sub> coordinated copper center which can

TABLE 19

Formal electrode potentials (V) for the redox changes of each site observed in DMSO-[NEt<sub>4</sub>][ClO<sub>4</sub>] (0.1 mol dm<sup>-3</sup>) solutions of homo- and heterodinuclear complexes **LXII** and **LXIII**

Compound	M <sub>A</sub>	M <sub>B</sub>	$E_{(M_A^{II}, M_A^I)}^{0/}$	$E_{(M_B^{II}, M_B^I)}^{0/}$	Ref.
<b>LXII</b>	Cu	Cu	-1.09 <sup>a</sup>	-0.92 <sup>a</sup>	154
	Cu	UO <sub>2</sub>	-1.32	0.90	155
<b>LXIII</b>	Cu	Cu	-0.42	0.99 <sup>a</sup>	156
	Cu	Ni	0.73	1.48	156
	Cu	UO <sub>2</sub>	-0.53	0.53	156
	Ni	Cu	1.36	-0.73	156

<sup>a</sup> Peak potential value at 0.2 V s<sup>-1</sup> for irreversible process.

TABLE 20

Formal electrode potentials (V) for the redox changes of each metal site observed in  $\text{CH}_2\text{Cl}_2$  solutions of **LXIV**<sup>a</sup>

M	$E_{(\text{Cu}^{II}/\text{Cu}^I)}^{0'}$	$E_{(\text{M}^{II}/\text{M}^I)}^{0'}$
Cu	-1.40	+0.76
Hg	-1.43	-0.20
Zn	-1.43	-

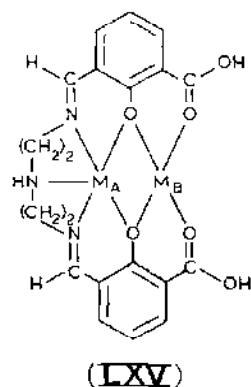
<sup>a</sup> From ref. 157.

easily rearrange to copper(I) in a tetrahedral configuration. The same behaviour is true for the heterodinuclear CuHg complex.

Table 20 summarizes the redox potentials of these complexes, and shows how much the different coordination in two close metal centres may affect the relevant redox properties.

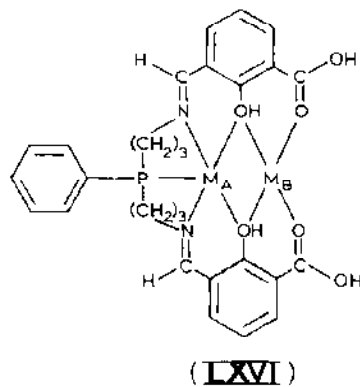
(iii) *Adjacent  $\text{N}_2\text{Y}-\text{O}_2-\text{O}_2$  ( $\text{Y} = \text{N}, \text{P}$ ) donor sets*

Two similar acyclic derivatives, **LXV** and **LXVI**, having a five-coordinate inner chamber and a four-coordinate outer chamber, have been electrochemically investigated [68,69].



$\text{M}_A = \text{Cu(II)}, \text{Ni(II)}$

$\text{M}_B = \text{Cu(II)}, \text{Ni(II)}, \text{UO}_2(\text{VI})$



$\text{M}_A = \text{Cu(II)}, \text{Ni(II)}$

$\text{M}_B = \text{Cu(II)}, \text{UO}_2(\text{VI})$

Unfortunately the electrochemical behaviour of such compounds is not straightforward, because of some interference from cathodic processes of the ligand itself and the irreversibility of most of the redox couples. However the potential data do roughly allow one to evaluate whether structural changes with respect to the  $\text{N}_2\text{O}_2\text{O}_2$  coordination stabilize low-valent centers. As in

TABLE 21

Formal electrode potentials (V) for the redox changes occurring at each center of dinuclear complexes **LXV** and **LXVI** in DMSO- $[\text{NEt}_4]\text{ClO}_4$  ( $0.1 \text{ mol dm}^{-3}$ ) solutions at a platinum electrode

Compound	$M_A$	$M_B$	$E_{(M_A^{II}/M_A^I)}$	$E_{(M_B^{II}/M_B^I)}$	Ref.
<b>LXV</b>	Cu	Cu	-0.54 <sup>a</sup>	-1.65	69
	Cu	Ni	-1.11 <sup>a</sup>	-1.80 <sup>a</sup>	69
	Cu	UO <sub>2</sub>	-0.41 <sup>a</sup>	-1.33	69
	Ni	Cu	-1.38 <sup>a</sup>	-0.45 <sup>a</sup>	69
<b>LXVI</b>	Cu	Cu	-1.04 <sup>a</sup>	-1.74 <sup>a</sup>	68
	Cu	UO <sub>2</sub>	-0.86 <sup>a</sup>	-1.74	68
	Ni	Cu	-1.74	-0.46 <sup>b</sup>	68

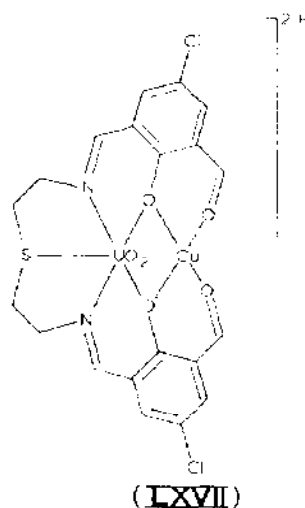
<sup>a</sup> Peak potential value at  $0.2 \text{ V s}^{-1}$  for irreversible process. <sup>b</sup> Mercury electrode.

the case of the precursor compound **LXIII**, kinetic complications following the charge transfers are also present.

Table 21 reports the redox potentials for these compounds. No significant improvement is reached with respect to the  $\text{N}_2\text{-O}_2\text{-O}_2$  assembly regarding thermodynamic access to reduced species; their kinetic lability is greatly increased. Finally, as expected,  $\text{N}_2\text{PO}_2$  coordination makes reduction of metal ions more difficult with respect to  $\text{N}_3\text{O}_2$  coordination, phenylphosphine groups being better electron donors than amino nitrogen atoms.

(iv) *Adjacent  $\text{N}_2\text{S-O}_2\text{-O}_2$  donor sets*

The electrochemical behaviour of the heterodinuclear compound **LXVII**, having two differently coordinated ( $\text{O}_2\text{O}_2$  and  $\text{N}_2\text{SO}_2$ ) adjacent chambers,

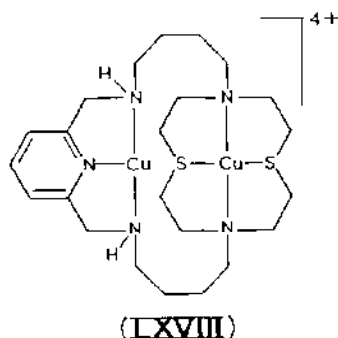


has recently been reported [136]. In DMSO solution, this complex gives rise to two close one-electron quasireversible cathodic processes, complicated by coupled decomplexation steps. The use of high scan rates in order to prevent these complications causes the merging of the two processes ( $\text{Cu}^{\text{II}}\text{UO}_2^{\text{VI}}/\text{Cu}^{\text{I}}\text{UO}_2^{\text{VI}}$ ,  $\text{Cu}^{\text{I}}\text{UO}_2^{\text{VI}}/\text{Cu}^{\text{I}}\text{UO}_2^{\text{V}}$ , respectively), so that only one formal electrode potential can be attributed to them at  $-0.34$  V.

(v)  $N_3$  remote-linked to  $N_2S_2$  donor sets

Dinuclear complexes containing two remote chambers having different donor atom sets are very rare. The only report containing electrochemical data deals with the compound **LXVIII** [145].

In propylene carbonate, each copper(II) center is reduced to the 1 + oxidation state at different potentials, because of the difference in coordina-



tion set. The  $\text{Cu}^{\text{II}}_{\text{N}_2\text{S}_2}/\text{Cu}^{\text{I}}_{\text{N}_2\text{S}_2}$  step occurs at  $+0.55$  V, whereas the  $\text{Cu}^{\text{II}}_{\text{N}_3}/\text{Cu}^{\text{I}}_{\text{N}_3}$  step occurs at  $+0.07$  V. The further reductions to  $\text{Cu}^0$ , concomitant with decomplexation, occur at potentials more negative than  $-0.37$  V.

## F. CONCLUSIONS

In the electrochemistry of dinuclear copper compounds both thermodynamic and kinetic aspects have to be considered.

The thermodynamic interest lies in the redox chemistry and is directed towards characterizing the  $\text{Cu}^{\text{II}}\text{Cu}^{\text{II}}/\text{Cu}^{\text{II}}\text{Cu}^{\text{I}}$  and  $\text{Cu}^{\text{II}}\text{Cu}^{\text{I}}/\text{Cu}^{\text{I}}\text{Cu}^{\text{I}}$  couples. First of all, one is interested in being able to determine if these redox changes proceed in a single two-electron step and secondly whether these redox changes occur at high or low potentials.

Although there have been attempts to rationalize the pathway of these cathodic processes on the basis of the interactions between the two copper centers [37,141,144], the great variety of electrode mechanisms we have reported, together with their occasional dependence on solvents and in some

cases, even on the supporting electrolyte, highlight the complexity involved in making predictions about the occurrence of a single step or two separated steps.

Regarding the synthesis of dicopper derivatives displaying high potential  $\text{Cu}^{\text{II}}/\text{Cu}^{\text{I}}$  redox couples, some strategies can be suggested:

(i) The preparation of dicopper(II) complexes having a tetrahedral assembly in the copper(II) coordination sphere. This is the case for the complexes **II**, derived from (acyl/benzoyl) phenolates; but consider also the hydroxo-bridged complexes **XVI** and **XVII**, thioalkoxo-bridged complexes **XVIII**, **XX**, **XXII**, halogeno-bridged complexes **XXIV**, **XXV**, arylazo-oximate **XXXIII**, macrotricyclic complexes **XLV**–**XLVIII**, and macrocyclic inclusion complexes, **LVII**–**LIX**, all of which favor the access to copper(I) centres because of their marked flexibility able to support tetrahedral coordination rearrangements.

(ii) The preparation of stereochemically stable three-coordinate dicopper(I) complexes, such as **XXXII**, **I,II**, **I,III**.

(iii) (Apparently) the preparation of two-coordinate dicopper(I) complexes. Really these derivatives are very rare, the only one being compound **LX**.

The kinetic aspect of the  $\text{Cu}^{\text{II}}\text{Cu}^{\text{II}}/\text{Cu}^{\text{I}}\text{Cu}^{\text{I}}$  overall reduction refers to the degree of stability of the electrogenerated  $\text{Cu}^{\text{II}}\text{Cu}^{\text{I}}$  and/or  $\text{Cu}^{\text{I}}\text{Cu}^{\text{I}}$  complexes. Indeed this aspect is in many cases neglected, not only in the short timescale of voltammetric studies, but also concerning characterization of the products from macroelectrolysis tests. Obviously this aspect is also connected to ligand structural design and to the difficulty of determining solvent effects. For instance it has been shown that the presence of five-coordinate copper(II) centers always causes fast decomplexation of generated copper(I) centers. From this point of view, the electrochemical behaviour of dinuclear copper complexes is still almost unexplored.

## REFERENCES

- 1 D.E. Fenton, U. Casellato, P.A. Vigato and M. Vidali, *Inorg. Chim. Acta*, 95 (1984) 187.
- 2 D.E. Fenton, U. Casellato, P.A. Vigato and M. Vidali, *Inorg. Chim. Acta*, 62 (1982) 57.
- 3 R.D. Willett, D. Gatteschi and O. Kahn, *Magneto-structural Correlations in Exchange Coupled Systems*, Nato ASI Series, D. Reidel Publishing Co., Dordrecht, Holland, 1983.
- 4 U. Casellato, P.A. Vigato, D.E. Fenton and M. Vidali, *Coord. Chem. Rev.*, 8 (1979) 199.
- 5 S.E. Groh, *Isr. J. Chem.*, 15 (1976/1977) 277.
- 6 F.L. Urbach, in H. Siegel (Ed.), *Metal Ions in Biological Systems*, Vol. 13, Dekker, New York and Basel, 1981, p. 73 and references therein.
- 7 E.I. Solomon, Binuclear copper active site, in T.G. Spiro (Ed.), *Copper Proteins*, Wiley-Interscience, New York, 1981, Chap. 2.
- 8 D.M. Dooley, R.A. Scott, E. Ellinghaus, E.I. Solomon and H.B. Gray, *Proc. Natl. Acad. Sci. U.S.A.*, 75 (1978) 3019.



- 9 D.J. Spira, M.E. Winkler and E.I. Solomon, *Biochem. Biophys. Res. Commun.*, 107 (1982) 721.
- 10 C.D. LuBien, M.E. Winkler, T.J. Thamann, R.A. Scott, M.S. Co, K.O. Hodgson and E.I. Solomon, *J. Am. Chem. Soc.*, 103 (1981) 7014.
- 11 M.E. Winkler, D.J. Spira, C.D. LuBien, T.J. Thamann and E.I. Solomon, *Biochem. Biophys. Res. Commun.*, 107 (1982) 727.
- 12 J.A. Fee and R.G. Briggs, *Biochim. Biophys. Acta*, 400 (1975) 439.
- 13 J.A. Fee, *J. Biol. Chem.*, 248 (1973) 4229.
- 14 L. Calabrese, D. Cocco and A. Desideri, *FEBS Lett.*, 106 (1979) 142.
- 15 E.L. Muttarties, T.N. Rhodin, E. Band, G.F. Brucker and W.R. Pretzer, *Chem. Rev.*, 79 (1979) 91.
- 16 D.E. Fenton, in A.G. Sykes (Ed.), *Advances in Inorganic and Bioinorganic Mechanism*, Vol. 2, Academic Press, London, 1983, p. 187.
- 17 R. Robson, *Inorg. Nucl. Chem. Lett.*, 6 (1970) 125.
- 18 R. Robson, *Aust. J. Chem.*, 23 (1970) 2217.
- 19 D.E. Fenton and R.L. Lintvedt, *J. Am. Chem. Soc.*, 100 (1978) 1931.
- 20 D.E. Fenton and R.L. Lintvedt, *J. Am. Chem. Soc.*, 100 (1978) 6367.
- 21 S.K. Mandal and K. Nag, *Inorg. Chem.*, 22 (1983) 2567.
- 22 C.W. Dudley, T.N. Huckerby and C. Oldham, *J. Chem. Soc. A*, (1970) 2606.
- 23 F. Sagara, H. Kobayashi and K. Ueno, *Bull. Chem. Soc. Jpn.*, 45 (1972) 900.
- 24 M.I. Kobachnick, S.T. Joffe, E.M. Popov and K.V. Vasturo, *Tetrahedron*, 12 (1961) 76.
- 25 S.T. Joffe, E.M. Popov, K.V. Tulikova and M.I. Kobachnick, *Tetrahedron*, 18 (1962) 923.
- 26 G. Allen and R. Dwek, *J. Chem. Soc. B*, (1966) 161.
- 27 A.B. Blake and C.R. Fraser, *J. Chem. Soc. Dalton Trans.*, (1974) 2554.
- 28 M.J. Heeg, J.L. Mack, M.D. Glick and R.L. Lintvedt, *Inorg. Chem.*, 20 (1981) 833.
- 29 R.L. Lintvedt, M.D. Glick, B.K. Tomlonovic, D.P. Gavel and J.M. Kuznaj, *Inorg. Chem.*, 15 (1976) 1633.
- 30 J.W. Guthrie, R.L. Lintvedt and M.D. Glick, *Inorg. Chem.*, 19 (1980) 2949.
- 31 N.M. Pinkington and R.R. Robson, *Aust. J. Chem.*, 23 (1970) 225.
- 32 W.D. Carlisle, D.E. Fenton, P.B. Roberts, U. Casellato, P.A. Vigato and R. Graziani, *Transition Met. Chem.*, 11 (1986) 292.
- 33 B.F. Hoskins, N.J. Meheod and H.A. Schaap, *Aust. J. Chem.*, 29 (1976) 515.
- 34 B.F. Hoskins and G.A. Williams, *Aust. J. Chem.*, 28 (1975) 2607.
- 35 S.L. Lambert and D.H. Hendrickson, *Inorg. Chem.*, 18 (1979) 2683.
- 36 R.R. Gagné, C.A. Koval and T.J. Smith, *J. Am. Chem. Soc.*, 99 (1977) 8367.
- 37 R.R. Gagné, C.A. Koval, T.J. Smith and M.C. Cimolino, *J. Am. Chem. Soc.*, 101 (1979) 4571.
- 38 R.R. Gagné, L.M. Henling and T.J. Kistenmacher, *Inorg. Chem.*, 19 (1980) 1226.
- 39 A.W. Addison, *Inorg. Nucl. Chem. Lett.*, 12 (1976) 899.
- 40 R.C. Long and D.N. Hendrickson, *J. Am. Chem. Soc.*, 105 (1983) 1513.
- 41 V. Casellato, D. Fregona, S. Sitran, S. Tamburini, P.A. Vigato and D.E. Fenton, *Inorg. Chim. Acta*, 110 (1985) 181.
- 42 U. Casellato, P. Guerriero, S. Tamburini, P.A. Vigato and R. Graziani, *Inorg. Chim. Acta*, 119 (1986) 215.
- 43 N.A. Bailey, D.E. Fenton, I.T. Jackson, R. Moody and C. Rodriguez de Barbarin, *J. Chem. Soc., Chem. Commun.*, (1983) 1463.
- 44 V. McKee and J. Smith, *J. Chem. Soc. Chem. Commun.*, (1983) 1465.
- 45 O. Kahn, *Inorg. Chim. Acta*, 62 (1982) 3.

- 46 M.D. Timken, W.A. Marrit, D.N. Hendrickson, R.R. Gagné and E. Sinn, *Inorg. Chem.*, 24 (1985) 4202.
- 47 R.L. Lintvedt and L.S. Kramer, *Inorg. Chem.*, 22 (1983) 796.
- 48 R.L. Lintvedt, L.S. Kramer, G. Ranger, F.W. Corfield and M.D. Glick, *Inorg. Chem.*, 22 (1983) 3580.
- 49 R.L. Lintvedt, G. Ranger and B.A. Schoenfelner, *Inorg. Chem.*, 23 (1984) 688.
- 50 H. Adams, M.A. Bailey, D.E. Fenton, M.S. Leal Gonzales and C.A. Phillips, *J. Chem. Soc., Dalton Trans.*, (1983) 371.
- 51 R.L. Lintvedt, L. Stecher Kramer, G. Ranger, P.W. Corfield and M.D. Glick, *Inorg. Chem.*, 22 (1983) 3580.
- 52 E.E. Ednok and C.J. O'Connor, *Inorg. Chim. Acta*, 88 (1984) 224.
- 53 J.F. Wishart, C. Ceccarelli, R.L. Lintvedt, J.M. Berg, D.P. Foley, J.E. Hahn, K.O. Hodgson and R. Weis, *Inorg. Chem.*, 22 (1983) 1667.
- 54 F.M. Herberstein in J.D. Dunitz and A.J. Ibers (Eds.), *Perspectives in Structural Chemistry*, Vol. 4, Wiley, New York, 1971, p. 166.
- 55 G. Wittig, *Ann. Chem.*, 446 (1926) 173.
- 56 D.E. Fenton, S. Gayda, U. Casellato, P.A. Vigato and M. Vidali, *Inorg. Chim. Acta*, 27 (1978) 9.
- 57 R. Graziani, M. Vidali, U. Casellato and P.A. Vigato, *Transition Met. Chem.*, 3 (1978) 239.
- 58 R. Graziani, M. Vidali, U. Casellato and P.A. Vigato, *Transition Met. Chem.*, 3 (1978) 138.
- 59 R. Graziani, M. Vidali, G. Rizzardi, U. Casellato and P.A. Vigato, *Inorg. Chim. Acta*, 36 (1979) 145.
- 60 J. Galy, J. Jaud, O. Kahn and P. Tola, *Inorg. Chim. Acta*, 36 (1979) 229.
- 61 O. Kahn, J. Galy, Y. Journaux, J. Jaud and T. Morgenstern-Badarau, *J. Am. Chem. Soc.*, 104 (1982) 2165.
- 62 M. Mikuriya, H. Okawa, S. Kida and I. Veda, *Bull. Chem. Soc. Jpn.*, 51 (1978) 2920.
- 63 J. Galy, J. Jaud, O. Kahn and P. Tola, *Inorg. Chem.*, 19 (1980) 2945.
- 64 I. Morgenstern-Badarau, M. Rerat, O. Kahn, J. Jaud and J. Galy, *Inorg. Chem.*, 21 (1982) 3050.
- 65 J.P. Beale, J.A. Cunningham and D.J. Phillips, *Inorg. Chim. Acta*, 33 (1979) 113.
- 66 Y. Journaux, O. Kahn and H. Condanne, *Angew. Chem. Int. Ed. Engl.*, 21 (1982) 624.
- 67 R. Coombes, D.E. Fenton, P.A. Vigato, U. Casellato and M. Vidali, *Inorg. Chim. Acta*, 54 (1981) L155.
- 68 U. Casellato, D. Fregona, S. Sitran, S. Tamburini, P.A. Vigato and P. Zanello, *Inorg. Chim. Acta*, 95 (1984) 279.
- 69 U. Casellato, D. Fregona, S. Sitran, S. Tamburini, P.A. Vigato and P. Zanello, *Inorg. Chim. Acta*, 95 (1964) 309.
- 70 H. Okawa, I. Ando and S. Kida, *Bull. Chem. Soc. Jpn.*, 47 (1974) 3041.
- 71 W.D. McFadyen and R. Robson, *J. Coord. Chem.*, 5 (1976) 49.
- 72 H. Okawa and S. Kida, *Bull. Chem. Soc. Jpn.*, 14 (1974) 1172.
- 73 H. Okawa, S. Kida, Y. Muto and T. Tokii, *Bull. Chem. Soc. Jpn.*, 45 (1972) 2480.
- 74 H. Okawa, T. Tokii, Y. Nonaka, Y. Muto and S. Kida, *Bull. Chem. Soc. Jpn.*, 46 (1973) 1462.
- 75 T. Ichinose, Y. Nishida, H. Okawa and S. Kida, *Bull. Chem. Soc. Jpn.*, 47 (1974) 3045.
- 76 I. Dickson and R. Robson, *Inorg. Chem.*, 13 (1974) 1301.
- 77 R.R. Gagné, R.P. Kreh and J.A. Dodge, *J. Am. Chem. Soc.*, 101 (1979) 6917.
- 78 J.J. Grzybowski, F.H. Merrell and F.L. Urbach, *Inorg. Chem.*, 17 (1978) 3078.

- 79 B.F. Hopkins, R. Robson and H.A. Schoap, *Inorg. Nucl. Chem. Lett.*, 8 (1975) 21.
- 80 J.G. Hughes and R. Robson, *Inorg. Chim. Acta*, 36 (1979) 237.
- 81 M. Loney, P.D. Nichols and R. Robson, *Inorg. Chim. Acta*, 47 (1980) 87.
- 82 R. Robson, *Inorg. Chim. Acta*, 57 (1982) 71.
- 83 R.S. Drago, M.J. Desmond, B.B. Corden and K.A. Miller, *J. Am. Chem. Soc.*, 105 (1983) 2287.
- 84 J.R. Majeste, C.L. Klein and E.D. Stevens, *Acta Crystallogr., Sect. C* 39 (1983) 52.
- 85 R.R. Gagné, M.W. McCool and R.E. Marsh, *Acta Crystallogr., Sect. B* 36 (1980) 2420.
- 86 J. Lorosch, H. Paulus and W. Haase, *Inorg. Chim. Acta*, 106 (1985) 101.
- 87 S.K. Mandal and K. Mag, *J. Chem. Soc., Dalton Trans.*, (1984) 2141.
- 88 S.K. Mandal and K. Nag, *J. Chem. Soc., Dalton Trans.*, (1983) 2429.
- 89 J. Lorosch and W. Haase, *Inorg. Chim. Acta*, 108 (1985) 35.
- 90 W. Mazurek, K.J. Berry, K.S. Murray, M.J. O'Connor, M.R. Snow and A.G. Wedd, *Inorg. Chem.*, 21 (1982) 3071.
- 91 W. Mazurek, B.J. Kennedy, K.S. Murray, M.J. O'Connor, J.R. Rodgers, M.R. Snow, A.G. Wedd and P.R. Zwack, *Inorg. Chem.*, 24 (1985) 3258.
- 92 Y. Nishida, M. Takeuchi, K. Takahashi and S. Kida, *Chem. Lett.*, (1982) 1915.
- 93 G.D. Fallon, S.K. Murray, W. Mazurek and M.J. O'Connor, *Inorg. Chim. Acta*, 96 (1985) L53.
- 94 Y. Nishida, M. Takeuchi, K. Takahashi and S. Kida, *Chem. Lett.*, (1985) 631.
- 95 W. Mazurek, H.M. Bond, K.S. Murray, M.J. O'Connor and A.G. Wedd, *Inorg. Chem.*, 24 (1985) 2484.
- 96 V. McKee, J.V. Dagdigian, R. Bau and C.A. Reed, *J. Am. Chem. Soc.*, 103 (1981) 7000.
- 97 V. McKee, M. Zvagulis, J.V. Dagdigian, M.G. Patch and C.A. Reed, *J. Am. Chem. Soc.*, 106 (1984) 4765.
- 98 C.Y. Ng, A.E. Martell and R.J. Motekaitis, *J. Coord. Chem.*, 9 (1979) 255.
- 99 C.H. Ng, R.J. Motekaitis and A.E. Martell, *Inorg. Chem.*, 18 (1979) 2982.
- 100 K.D. Karlin, P.L. Dahlstrom, L.T. Dipierro, R.A. Simon and J. Zubieta, *J. Coord. Chem.*, 11 (1981) 61.
- 101 K.D. Karlin, J.R. Hyde and J. Zubieta, *Inorg. Chim. Acta*, 66 (1982) L23.
- 102 M.M. Taqui Khan and A.E. Martell, *Inorg. Chem.*, 14 (1975) 676.
- 103 M.M. Taqui Khan, A.E. Martell, R. Mohinddin and R. Ahmed, *J. Coord. Chem.*, 10 (1980) 1.
- 104 K.D. Karlin, P.L. Dahlstrom, S.N. Cozzette, P.M. Scensney and J. Zubieta, *J. Chem. Soc., Chem. Commun.*, (1981) 881.
- 105 K.D. Karlin, Y. Gultneh, J.P. Hutchinson and J. Zubieta, *J. Am. Chem. Soc.*, 104 (1982) 5240.
- 106 K.D. Karlin, J.C. Hayes, Y. Gultneh, R.W. Cruse, J.W. McKown, J.P. Hutchinson and J. Zubieta, *J. Am. Chem. Soc.*, 106 (1984) 2121.
- 107 K.D. Karlin, R.W. Cruse, Y. Gultneh, J.C. Hayes and J. Zubieta, *J. Am. Chem. Soc.*, 106 (1984) 3372.
- 108 M.E. Winkler, K. Lerch and E.I. Solomon, *J. Am. Chem. Soc.*, 103 (1981) 7001.
- 109 K. Karlin, Y. Gultneh, T. Nicholson and J. Zubieta, *Inorg. Chem.*, 24 (1985) 3725.
- 110 T.R. Demmin, M.D. Swerdloff and M.M. Rogic, *J. Am. Chem. Soc.*, 103 (1981) 5795.
- 111 M.M. Rogic, M.D. Swerdloff and T.R. Demmin, in K.D. Karlin and J. Zubieta (Eds.), *Copper Coordination Chemistry: Biochemical and Inorganic Perspectives*, Adenine Press, New York, 1983, p. 259.
- 112 D.G. Brown and W.J.Z. Hughes, *Naturforsch., Teil B*, 36 (1983) 5693.
- 113 Y. Nishida, H. Shimo, H. Maehara and S. Kida, *J. Chem. Soc., Dalton Trans.*, (1985) 1945.

- 114 T.N. Sorrell, D.L. Jameson and C. O'Connor, *Inorg. Chem.*, 23 (1984) 190.
- 115 V.H. Crawford, H.W. Richardson, J.R. Wasson, D.J. Hodgson and W.E. Hatfield, *Inorg. Chem.*, 15 (1976) 2107.
- 116 D.J. Hodgson, *Prog. Inorg. Chem.*, 19 (1975) 173.
- 117 M. Suzuki, H. Kanatomi and I. Murase, *Bull. Chem. Soc. Jpn.*, 57 (1984) 36.
- 118 M. Suzuki and A. Uehara, *Inorg. Chim. Acta*, 87 (1984) L29.
- 119 H.P. Berends and D.W. Stephan, *Inorg. Chim. Acta*, 99 (1985) L53.
- 120 J.A. Fee, *Struct. Bonding (Berlin)*, 23 (1975) 1.
- 121 K.D. Karlin and J. Zubieta (Eds.), *Copper Coordination Chemistry: Biochemical and Inorganic Perspectives*, Adenine Press, New York, 1983.
- 122 A.J. Bard and L.R. Faulkner, *Electrochemical Methods*, J. Wiley, New York, 1980.
- 123 D. Bauer and M. Breant, *Electroanal. Chem.*, 8 (1975) 281.
- 124 B. Tulyathan and W.E. Geiger, *J. Am. Chem. Soc.*, 107 (1985) 5960.
- 125 R.L. Lintvedt, in K.D. Karlin and J. Zubieta (Eds.), *Copper Coordination Chemistry: Biochemical and Inorganic Perspectives*, Adenine Press, New York, 1983, pp. 129–156.
- 126 B. Aldhikary, A.K. Biswas, K. Nag, P. Zanello and A. Cinquantini, *Polyhedron*, in press.
- 127 R.R. Gagné and C.L. Spiro, *J. Am. Chem. Soc.*, 102 (1980) 1443.
- 128 R.R. Gagné, C.L. Spiro, T.J. Smith, C.A. Hamann, W.R. Thies and A.K. Shienke, *J. Am. Chem. Soc.*, 103 (1981) 4073.
- 129 M.B. Robin and P. Day, *Adv. Inorg. Chem. Radiochem.*, 10 (1967) 247.
- 130 S. Kida, H. Owaka and Y. Nishida, in K.D. Karlin and J. Zubieta (Eds.), *Copper Coordination Chemistry: Biochemical and Inorganic Press*, New York, 1983, pp. 425–444.
- 131 M. Aihara, Y. Kubo, Y. Nishida and S. Kida, *Bull. Chem. Soc. Jpn.*, 54 (1981) 3207.
- 132 Y. Nishida, N.A. Oishi, H. Kuramoto and S. Kida, *Inorg. Chim. Acta*, 57 (1982) 253.
- 133 C. Lapinte, L. Nadjo and G. Meyer, *XII Int. Conf. Organometallic Chemistry*, Vienna, IUPAC, September, 1985, p. 446.
- 134 J.M. Latour, D. Limosin and S.S. Tandon, *Inorg. Chim. Acta*, 107 (1985) L1.
- 135 S. Kitagawa, M. Munakata and N. Niyaji, *Bull. Chem. Soc. Jpn.*, 56 (1983) 2258.
- 136 P. Zanello, A. Cinquantini, P. Guerriero, S. Tamburini and P.A. Vigato, *Inorg. Chim. Acta*, 117 (1986) 91.
- 137 W. Mazurek, A.M. Bond, M.J. O'Connor and A.J. Wedd, *Inorg. Chem.*, 25 (1986) 906.
- 138 S. Pal, D. Bandyopadhyay, D. Datta and A. Chakravorty, *J. Chem. Soc., Dalton Trans.*, (1985) 159.
- 139 P.K. Coughlin and S.J. Lippard, *Inorg. Chem.*, 23 (1984) 1446.
- 140 G.S. Patterson and R.H. Holm, *Bioinorg. Chem.*, 4 (1975) 257.
- 141 E.F. Hasty, L.J. Wilson and D.N. Hendrickson, *Inorg. Chem.*, 17 (1978) 1834.
- 142 H. Doine, F.S. Stephens and R.D. Cannon, *Inorg. Chim. Acta*, 75 (1983) 155.
- 143 P.S. Zacharias and A. Ramachandraiah, *Polyhedron*, 4 (1985) 1013.
- 144 B.C. Whitmore and R. Eisenberg, *Inorg. Chem.*, 22 (1983) 1.
- 145 J.P. Gisselbrecht and M. Gross, *Adv. Chem. Ser.*, 201 (1982) 109.
- 146 T. Izumitani, M. Nakamura, H. Okawa and S. Kida, *Bull. Chem. Soc. Jpn.*, 55 (1982) 2122.
- 147 H. Okawa, M. Kakimoto, T. Izumitani, M. Nakamura and S. Kida, *Bull. Chem. Soc. Jpn.*, 56 (1983) 149.
- 148 Y.L. Agnus, in K.D. Karlin and J. Zubieta (Eds.), *Copper Coordination Chemistry: Biochemical and Inorganic Perspectives*, Adenine Press, New York, 1983, pp. 371–394.
- 149 R.L. Lintvedt, B.A. Schoenfelner, C. Ceccarelli and M.D. Glick, *Inorg. Chem.*, 23 (1984) 2867.
- 150 K.D. Karlin, J.C. Hayes and J. Zubieta, in K.D. Karlin and J. Zubieta (Eds.), *Copper*

Coordination Chemistry: Biochemical and Inorganic Perspectives, Adenine Press, New York, 1983, pp. 456-472.

- 151 T.N. Sorrell, M.R. Malachowski and D.J. Jameson, *Inorg. Chem.*, 21 (1982) 93.
- 152 Y. Agnus, R. Louis, J.P. Gisselbrecht and R. Weiss, *J. Am. Chem. Soc.*, 106 (1984) 93.
- 153 T.N. Sorrell and D.L. Jameson, *J. Am. Chem. Soc.*, 104 (1982) 2053.
- 154 P. Zanello, P.A. Vigato and G.A. Mazzocchin, *Transition Met. Chem.*, 7 (1982) 291.
- 155 P. Zanello, P.A. Vigato, U. Casellato, S. Tamburini and G.A. Mazzocchin, *Transition Met. Chem.*, 8 (1983) 294.
- 156 P. Zanello, S. Tamburini, P.A. Vigato and G.A. Mazzocchin, *Transition Met. Chem.*, 9 (1984) 176.
- 157 M. Nakamura, H. Okawa and S. Kida, *Inorg. Chim. Acta*, 62 (1982) 201.